厚生労働科学研究委託費

難治性疾患等克服研究事業

（難治性疾患等実用化研究事業(難治性疾患実用化研究事業)）

「遺伝性ミオパチーの次世代型統合的診断拠点形成」

平成２６年度　委託業務成果報告書

業務主任者　西野　一三

平成２７（２０１５）年　3月

目　　次

厚生労働科学研究委託費
（難治性疾患等実用化研究事業（難治性疾患実用化研究事業））

委託業務成果報告（総括）

遺伝性ミオパチーの次世代型統合的診断拠点形成

業務主任者　　西野　一三　　疾病研究第一部　部長

研究要旨

国立精神・神経医療研究センターは過去35年以上に亘り、筋病理を中心とする筋疾患診断サービスを提供してきた。その結果、本邦筋生検例の約8割の検体がNCNPに集積している。本研究では、従来の方法では遺伝学的診断が未確定であった遺伝性ミオパチー例（ミトコンドリア病を含む）を対象として、次世代解析装置による網羅的遺伝子解析を行い、すでに世界最高峰レベルにある筋疾患病理診断と組み合わせることで、国内は元より海外までを視野に入れた、より高度な次元の統合的診断拠点へと飛躍させることを目指し、１．既知遺伝子のハイスループット解析、２．全エクソーム解析、３．新規原因遺伝子変異の病原性証明と疾患分子病態解明、４．病理・画像所見解析、５．国内外の連携を柱として研究を進めている。

ハイスループット解析については、既知筋疾患原因遺伝子を網羅する4つのパネルを作成し、ターゲットリシークエンス法により既知遺伝子変異をスクリーニングする方法を確立した。今年度研究開始後380例について解析を行い、発端者88例で原因を同定することができた。ミトコンドリア病については、ECHS1変異例を見いだした。

全エクソーム解析は350例で解析が終了している。現在までに60症例で原因遺伝子変異を同定している。この中には、tubular aggregate myopathyの原因遺伝子ORAI1の同定、世界第2例目のDAG1変異例同定、ネマリンミオパチーの新規原因遺伝子LMOD3同定などの他、本邦初となるMEGF10やANO5変異例の同定などの成果を上げた。

病原性証明研究としては、α-dystroglycanopathyとtubular aggregate myopathyに焦点を当て、全エクソーム解析から得られた変異候補の絞り込みと病原性証明を行う系を立ち上げた。前者については、HAP1細胞を用いた病原性証明の系を確立し、後者については変異を導入したHEK293細胞および患者由来筋管細胞において、細胞内カルシウム動態を評価することで、ORAI1優性変異による恒常的SOCE活性化が、Tubular aggregate形成および骨格筋障害の原因であることを明らかにした。

画像・病理所見については、レポジトリーのシステムを構築し、情報蓄積を開始した。また、早期呼吸障害を伴う遺伝性ミオパチーの筋病理所見の再評価を行い、necklace cytoplasmic bodyが感度・特異度ともに高い優れた病理学的マーカーであることが判明した。

国内外の連携については、2014年に提供した筋病理診断は国際的に最高水準と思われる827件であった。凍結筋の総検体数は2014年末で15140検体となり、世界有数の筋レポジトリーとなっている。諸外国との連携については、7月より、タイ人医師2名を、9月より中国人医師1名を、更に3月か

らは韓国人医師2名を受け入れて、筋疾患診断に関する研修ならびに研究に携わっている。また、アウトリーチ活動としては、インドネシア、タイ、マレーシア、台湾、エジプトなどにおいて、臨床病理カンファレンスを開催するとともに、講義や患者診察などを行った。今後このような診断支援活動を継続するには、研究費とは別の形の財政的支援が必要である。

１．既知遺伝子のハイスループット解析（三橋里美・国立精神・神経医療研究センター神経研究所疾病研究第一部　室長、後藤雄一・国立精神・神経医療研究センター神経研究所疾病研究第二部　部長）

２．全エクソーム解析（西野一三・国立精神・神経医療研究センター神経研究所疾病研究第一部　部長）

３．新規原因遺伝子変異の病原性証明と疾患分子病態解明（野口悟・国立精神・神経医療研究センター神経研究所疾病研究第一部　室長）

４．病理・画像所見解析（石山昭彦・国立精神・神経医療研究センター病院小児神経科医師、西野一三・国立精神・神経医療研究センター神経研究所疾病研究第一部　部長）

５．国内外の連携（西野一三・国立精神・神経医療研究センター神経研究所疾病研究第一部　部長）

A.研究目的

国立精神・神経医療研究センター（NCNP）は1978年以来過去35年以上に亘り、筋病理を中心とする筋疾患診断サービスを提供してきた。その結果、本邦筋生検例の約8割の検体がNCNPに集積している。原因遺伝子解析についても診断サービスを提供してきたが、これまでは技術的な制限からスポット的なサンガー法による遺伝子診断に終始していた。本申請研究では、従来の方法では遺伝学的診断が未確定であった遺伝性ミオパチー例（ミトコンドリア病を含む）を対象として、次世代解析装置による網羅的遺伝子解析を行い、すでに世界最高峰レベルにある筋疾患病理診断と組み合わせることで、国内は元より海外までを視野に入れた、より高度な次元の統合的診断拠点へと飛躍させることを目指す。

歴史的に、筋疾患は病理所見に基づいて分類・診断がなされてきたが、今後は、遺伝子型による疾患分類が進み疾患概念自体のパラダイムシフトが起こると予想される。我々は、次世代遺伝子解析によって得られる遺伝子型と、これまでに蓄積された筋病理、さらには、現在蓄積しつつある画像所見を組み合わせて、遺伝子型・表現型相関の統合的理解を進めて新たな概念の確立に寄与する。国内の連携は元より、海外諸国との連携を視野に入れていく必要性は明らかである。アジア諸国との連携を深めて、国際拠点となるべく基盤形成を進める。

B.研究方法

１．国立精神・神経医療研究センターに筋病理診断および、遺伝子解析の依頼された検体のうち、遺伝的に未診断の遺伝性筋疾患例に対して、既知の全筋疾患遺伝子を網羅する4種類の筋疾患遺伝子パネル（筋ジストロフィー(65遺伝子)、先天性ミオパチー(42遺伝子)、代謝性ミオパチー(45遺伝子)、異常タンパク質の凝集や縁取り空胞を特徴とするミオパチー(36遺伝子)）を作成し、次世代シークエンサーIonPGMを用いて既知遺伝子変異ターゲットリシークエンス解析を行った。対象となる症例を、筋病理診断および臨床診断によって、いずれかのカテゴリーに分類し、解析を行った。

ミトコンドリア病については、これまで患者で報告のある200近くの遺伝子に加えて、800近くのミトコンドリア関連遺伝子を調べる目的で、総計7368領域をキャプチャーできるように設計したHaloplex®によって関心領域をキャプチャーした上で、次世代シークエンサーMiSeqによりターゲットリシークエンスを行った。特にミトコンドリア呼吸鎖複合体の活性を測定する生化学検査において複数の呼吸鎖酵素活性低下及びミトコンドリアDNA由来タンパク質の翻訳活性の低下している2検体を選定し解析した。患者1は1歳9ヶ月の男児でLeigh症候群を呈し、患者2は1歳5ヶ月の女児

で高乳酸血症を呈している。いずれの患者の両親も血族婚ではなかった。

２．全エクソーム解析

国立精神・神経医療研究センターに診断依頼された検体のうちで既知遺伝子変異ハイスループット解析を行ってもなお原因遺伝子不明であった 83 例および、遺伝子診断未知でいずれのカテゴリーにも属さず新規原因遺伝子が疑われる症例を含めた 192 例を対象とした。全エクソームキャプチャーキットを用い HiSeq1000 にてゲノム情報を取得した。既に構築済みの解析パイプラインを通して、候補遺伝子を絞り込み、候補遺伝子変異は、サンガー法で確認した。さらに、これまでに解析を行った 400 例についても、引き続き原因遺伝子の同定を進めている。

３．新規原因遺伝子変異の病原性証明と疾患分子病態解明

α-dystroglycanopathy 患者 20 名を対象に全エクソーム解析を行い見いだされた変異候補の α-dystroglycan 糖鎖への影響を評価すべく、HAP1 細胞（野生型、POMGNT2-KO）（Netherlands Cancer Institute の Dr. Brummelkamp より供与）を用いた測定系を構築した。野生型および変異ヒト POMGNT2 cDNA は、レンチウイルスベクター用いて HAP1 細胞にトランスフェクトさせた。α-dystroglycan の糖鎖エピトープに対する抗体 IIH6 にて HAP1 生細胞を染色し、当該遺伝子変異の α-dystroglycan 糖鎖への影響を評価した。また、ヒト野生型および変異 myc−POMGNT2 cDNA を Hele 細胞に導入・発現させ、myc 標識タンパク質の細胞内局在を解析した。

Tubular aggregate myopathy については、見出した ORAI1 変異(Gly98Ser, Leu138Phe)の SOCE への影響を確認するため、罹患者由来の筋管細胞及び上記変異を有する ORAI1 を過剰発現させた HEK293 細胞を用いて、細胞外 Ca2+濃度変化に伴う細胞内 Ca2+濃度変化を測定した。また、細胞内 Ca2+濃度変化が細胞外からの Ca2+流入によるものなのか、SR をはじめとする細胞内 Ca2+貯蔵器官から放出されたものなのかを見極めるために、Mn2+ quenching 実験を行った。

４．病理・画像所見解析

骨格筋および脳画像の管理については、国立精神・神経医療研究センター脳病態統合イメージングセンター（IBIC; Integrative Brain Imaging Center）で開発した Web 上での画像登録、閲覧が可能なシステム（IBISS; Integrative Brain Imaging Support System）を用いた。これは IBIC が独自に開発した臨床放射線画像登録に特化したオンラインサポートシステムで、厳重なセキュリティーのもと、研究に必要な画像情報、臨床情報を共有できるオンライン上の仮想空間である。IBISS 内での遺伝性ミオパチー画像登録フォームを作成し、2005 年 1 月以降に当センターで精査を行った症例で、遺伝学的未確定なミオパチー症例の骨格筋画像、ミトコンドリアミオパチーの脳画像の登録を行った。

また、本プロジェクトの中で同定された早期呼吸障害を伴う遺伝性ミオパチー（Hereditary myopathy with early respiratory failure: HMERF）14 家系 17 例の筋病理所見の再検討を行った。

５．国内外の連携

国内に向けては、従来より提供している筋疾患診断サービスの提供を継続する。国外に向けては、アジアを中心とする諸外国からの研修医師・技師を受け入れ、筋疾患学の基礎とともに筋疾患研究の最先端を経験させることで、帰国後に当該地域で診断サービスを提供することができる様にするとともに、筋疾患分野で指導的な立場に立てるように支援する。また、専門家がおらず必要とされる地域に積極的に出向くアウトリーチ型の活動も加えることで、国際連携の基盤を形成する。

（倫理面への配慮）

本研究において使用するヒト試料は、共同研究施設である NCNP 倫理委員会で承認された所定の承諾書を用いて、患者あるいはその親権者から遺伝子解析を含む研究利

用に対する検体の使用許可を得たものを用いた。

C.研究結果

１．既知遺伝子のハイスループット解析

IonPGMを用いて、380検体の解析を行った。88症例で、病気の原因の可能性がある遺伝子変異を同定した。この中には、新規の変異や、日本人で初めて疾患を同定した症例、報告症例数が非常にまれな症例も含まれていた。原因遺伝子が不明例83症例を含む、192例をHiSeq1000シークエンサーでエクソーム解析中である。

ミトコンドリア病については、患者1でECHS1の、患者2で遺伝子Xの複合ヘテロ接合型変異を見いだした。患者1由来の筋芽細胞では、HCHS1蛋白質の発現が低下していた。患者2では蛋白質Xの発現に変化は見られなかったが、蛋白質X葉酸代謝に関与しており、ミトコンドリアのtRNAの修飾に関する基質の代謝に寄与することから、その基質の不足によってmtDNAの翻訳異常が引き起こされる可能性がある。

２．全エクソーム解析

これまでにエクソーム解析を行った475例中350例で、解析が終了している。このうち、60の症例で病気の原因である可能性のある遺伝子変異を見出すことができた。この中には、1.tubular aggregate myopathyの新規の変異遺伝子*ORAI1*の同定、2．α-dystroglycanopathyと病理学的に確定された例の中から世界第2例目となる*DAGI*変異例を同定、3．*LMOD3*変異がネマリンミオパチーの新たな原因であることを同定、4.*TK2*変異による筋線維未熟性を伴う先天性ミオパチーの同定、5. 中心核ミオパチーの新規原因遺伝子Xの同定（海外の研究者との共同研究のため遺伝子名は未公表）、6.*LMNA*変異による核内ロッドを伴う先天性ミオパチーの同定、7. 本邦初の*MEGF10*先天性ミオパチーの同定、8. 本邦初の*ANO5*変異の同定、などの成果が含まれ、さらに病因解析を進めている。

解析ソフトウェアを更新し、より信頼性の高い結果が得られることが期待されるGATKv.3.1を用いた解析パイプラインを構築した。解析の省力・省時間化を目指し、GATKv.3.1へのアップデートに加えて、これまでに解析したNCNP内のエクソームデータベースを構築し横断的に解析するシステムを構築した。

３．新規原因遺伝子変異の病原性証明と疾患分子病態解明

α-dystroglycanopathy3 名に POMGNT2 変異 c.494T>C(p.M165T) 及び c.785C>T (p.P253L)複合ヘテロ接合変異(1 名)、c.785C>T (p.P253L)ホモ接合変異(2 名)を見出した。両方の変異は、ともにミスセンス変異であると推定された。また、両変異ともにグリコシルトランストランスフェラーゼ様ドメインに存在していた。

野生型 HAP1 細胞は、ラミニン上で培養することで、α-dystroglycan は集積し、IIH6 抗体で染色された。一方、POMGNT2-KO 細胞では IIH6 抗体での染色は見られなかった。POMGNT2-KO 細胞への野生型 POMGNT2cDNA の導入により IIH6 抗体陽性となった。一方、p．M165T 及び p.P253L 変異 POMGNT2 cDNA の導入では、IIH6 抗体陰性であった。Hela 細胞に導入された p．M165T 及び p.P253L 変異 POMGNT2 は、野生型 POMGNT2 と同様に、小胞体での局在が見られた。しかしながら、HEK293 細胞で発現させた p.M165T 及び p.P253L 変異 POMGNT2 は、野生型 POMGNT2 に比べ、10%以下の比活性しか検出されなかった。

Tubular aggregate myopathy については、細胞外に Ca2+を加えることで、変異 ORAI1 をもつ細胞では有意に細胞内 Ca2+濃度が上昇し、ORAI1 チャネルの特異的阻害剤により抑制されること見出した。またこの細胞内 Ca2+濃度上昇は、細胞内 Ca2+貯蔵器官から放出されたものではなく、細胞外から細胞内へ Ca2+が異常流入していることによるものであることを明らかにした。以上の結果より、ORAI1 優性変異による恒常的 SOCE 活性化が、Tubular aggregate 形成および骨格筋障害の原因であることが示された。

４．病理・画像所見解析
遺伝性ミオパチーでの IBISS 画像登録にあたっての倫理申請を行い承認を得て、遺伝性ミオパチー画像登録フォームを作成した。今年度は遺伝学的未診断例の遺伝性ミオパチー47 例の骨格筋画像と、ミトコンドリアミオパチー12 例の脳画像の集積を行った。今後は、次世代遺伝子解析で得られた遺伝子情報をもとに、表現型評価ツールとして筋病理とあわせて骨格筋画像や脳画像所見との相関を解析する。

HMERF については、筋病理所見を再検討した結果、cytoplasmic body が筋線維内でネックレス状に配列する所見（necklace cytoplasmic body と命名）が感度 82%、特異度 99%と極めて優れた筋病理学的マーカーであることが明らかとなった。

５．国内外の連携

2014年には827件の筋病理診断を行った。諸外国の筋疾患診断拠点では殆どが年間検体数500件程度であり、国際的に最高水準にある筋疾患診断拠点であることが確認された。本邦における年間筋生検数は1000件を超える程度と予想されることから、約8割の検体が国立精神・神経医療研究センターに集まっていることが確認された。診断後の検体はレポジトリーとして蓄積されているが、凍結筋の総検体数は2014年末で15140検体となり、世界有数の筋レポジトリーとなっている。

諸外国との連携については、7月より、タイ人医師2名を、9月より中国人医師1名を、更に3月からは韓国人医師2名を受け入れて、筋疾患診断に関する研修ならびに研究に携わっている。アウトリーチ活動としては、8月にこれまで筋疾患専門医のいなかったインドネシアを訪問し、ジャカルタのCipto Mangunkusumo 病院において、講義、患者診察、筋生検等を現地神経内科医とともに行った。これが契機となり、3月末には日本神経学会およびインドネシア神経学会の共催でワークショップが開催されることになっている。また、その他、タイ・バンコクのSiriraj病院およびBhumibol Adulyadej病院、マレーシア・クアラルンプールのマラヤ大学、台湾・高雄市の高雄医学大学において、臨床病理カンファレンスを開催するとともに、講義や患者診察などを行った。さらに、筋疾患専門医が殆どいないエジプトに出向き、カイロのEgyptair病院で、現地医師とともに筋疾患患者約150名を2度の訪問で診察し、更に筋生検を行った。加えて、これら地域からの診断支援要請に応えて、筋病理を初めとする筋疾患診断支援を行った。

D.考察

１．既知遺伝子のハイスループット解析
遺伝子診断が未知の遺伝性筋疾患に対して、筋疾患遺伝子パネルによる、次世代シークエンサーIonPGMを活用することにより、効率のよい遺伝子診断が可能である。しかし、網羅的変異解析にもかかわらず、未だ70%の症例で、原因遺伝子が判明していない。この原因として、ターゲット領域以外の変異、もしくはリピート、欠失や挿入などの検出が難しい変異である可能性や、遺伝性疾患という臨床診断が間違っている可能性もあるが、新規の筋疾患原因遺伝子による疾患である可能性が高いと考えている。これらの症例に対しては、エクソームシークエンスによる、遺伝情報の蓄積を行うことで、新規の筋疾患原因が明らかとなると考えられる。

ミトコンドリア病については、1例で病因確定を行い投稿論文として報告した。今後ECHS1の欠損とミトコンドリアの翻訳異常、呼吸鎖複合体の活性低下の関連について更に解析を行う予定である。

２．全エクソーム解析
遺伝子診断が未知の遺伝性筋疾患に対して、筋疾患遺伝子パネルによる、次世代シークエンサーIonPGMによるスクリーニングを行った後、診断未知の筋疾患に対してエクソームシークエンスを行うことで、新規疾患原因遺伝子を見出す方法は、省コスト、省時間を考える上でも有効であると思われる。今後は、変異の病原性についての解析が必要であり、同じ変異を持った症例の蓄積が病原性の証明には大切であることから、今

後さらにエクソームシークエンスによる、遺伝情報の蓄積を行い、新規の筋疾患原因が明らかにしていくことが必要である

３．新規原因遺伝子変異の病原性証明と疾患分子病態解明

HAP1 細胞を用いた変異の病因性の証明方法は、他の遺伝子変異を原因とする□-dystroglycanopathy まで、広く利用することができることが示された。今後は、変異遺伝子補完実験で、HAP1 細胞が発現する□-dystroglycan とラミニンとの結合実験など生化学的解析を行うことで、この方法の有効性を示していきたいと考えている。

これまでORAI1遺伝子の劣性変異により重症複合型免疫不全症が引き起こされることは知られていたが、今回優性変異により骨格筋疾患を来すという新たな知見を得た。また、ORAI1 と複合体を形成する STIM1 の優性変異でも同様に、SOCE が活性化され Tubular aggregate myopathy を発症することが報告されており、SOCE 活性による細胞内 Ca2+濃度変化が骨格筋障害に関与していると推察された。以上の知見は、新規の筋疾患概念を提唱するものであり、細胞内 Ca2+動態と骨格筋障害の関連を解明する端緒となり得る。また、Tubular aggregate myopathy の病態が ORAI1 チャネルの機能獲得型変異であることを明らかにし、その特異的阻害剤が有効であるという in vitro での実験結果を得たことから、治療法への応用が期待される。

４．病理・画像所見解析

遺伝性ミオパチーの骨格筋画像では、遺伝子型と表現型が明らかな例のなかで、疾患特異性の高い筋罹患分布の特徴が知られており、骨格筋画像における筋選択性として知られている。今後このような遺伝子型・表現型相関を確立するためにはさらに多くの画像登録が必要であり、加えて、他施設からの筋病理診断例のレポジトリ―蓄積にあわせた画像登録が望まれる。画像登録を単施設から複数施設への登録システムへ発展し、筋レポジトリ―と関連付けられる画像集積を行うには、撮像条件等の統一などを検討していく必要がある。

HMERFについては、過去の筋病理標本の再検討の結果、極めて優れた筋病理学的マーカーを同定することができた。筋病理所見は数多くあるものの、高度の疾患特異性を有する所見は数えるほどしかなく、今回の同定は極めて有意義であると考える。

５．国内外の連携

国内では筋生検検体の約8割の検体を集めて筋病理診断を中心とする筋疾患診断サービスを行った。診断件数においても診断内容においても世界最高水準のものであることが確認された。

この診断サービスに係る費用は研究の一環として研究費で賄われているが、実態は診療支援である。特に「難病の患者に対する医療等に関する法律」が施行され医療費助成の対象となる疾患が増えてその診断基準が整理されていく中で、多くの筋疾患の診断基準において、商業的サービスのない遺伝子診断や筋病理解析が必須条件となっている現実は、事実上、研究者が無償で提供しているサービスが医療制度の根幹を担っていることを明白に示している。加えて、このようなサービス提供は、研究者が夜間や休日などの時間を削って提供しているのが実情であるが、その専門的な知識と技術、労働に対する対価は全く支払われていないのが現実である。このような診断サービスが日本の医療制度を維持するのに必須であることは明白であり、このようないわば「日本の隠れた医療費」に対する早急な財政的対策が求められる。

諸外国との連携については、順調にネットワークを拡大しつつある。特にこれまで専門家が全くいなかったインドネシアとの接点ができたことは今後の発展に大きく寄与すると期待される。しかし、依然としてアジア域では、筋疾患専門医が存在しない地域があり、今後そのような地域へのアプローチも積極的に行い、筋疾患学分野での先進国である本邦の責務を果たすことが求められる。

E.結論

4 つの既知筋疾患原因遺伝子パネルによるスクリーニング方法を開発し、その有用性を明らかにした。診断未知の筋疾患患者にたいする全エクソーム解析によって、新規遺伝子の発見につながる結果を示した。α-dystroglycanopathy での変異病原性評価システムとして HAP1 細胞を用いる方法を確立した。病理・画像所見のレポジトリーを構築するとともに HMERF では necklace cytoplasmic body が感度・特異度ともに高い優れた病理学的マーカーを示した。国内外の連携を推進し、ネットワーク拡大の基盤を形成した。

F.健康危険情報

特になし

G.研究発表

１．論文発表

Endo Y, Noguchi S, Hara Y, Hayashi YK, Motomura K, Miyatake S, Murakami N, Tanaka S, Yamashita S, Kizu R, Bamba M, Goto YI, Matsumoto N, Nonaka I, Nishino I: Dominant mutations in *ORAI1* cause tubular aggregate myopathy with hypocalcemia via constitutive activation of store-operated Ca^{2+} channels. Hum Mol Genet. 2015 Feb 1; 24(3): 637-48.

Dong M, Noguchi S, Endo Y, Hayashi YK, Yoshida S, Nonaka I, Nishino I: DAG1 mutations associated with asymptomatic hyperCKemia and hypoglycosylation of α-dystroglycan. Neurology. 2015 Jan 20; 84(3): 273-9.

Yuen M, Sandaradura SA, Dowling JJ, Kostyukova AS, Moroz N, Quinlan KG, Lehtokari VL, Ravenscroft G, Todd EJ, Ceyhan-Birsoy O, Gokhin DS, Maluenda J, Lek M, Nolent F, Pappas CT, Novak SM, D'Amico A, Malfatti E, Thomas BP, Gabriel SB, Gupta N, Daly MJ, Ilkovski B, Houweling PJ, Davidson AE, Swanson LC, Brownstein CA, Gupta VA, Medne L, Shannon P, Martin N, Bick DP, Flisberg A, Holmberg E, Van den Bergh P, Lapunzina P, Waddell LB, Sloboda DD, Bertini E, Chitayat D, Telfer WR, Laquerrière A, Gregorio CC, Ottenheijm CA, Bönnemann CG, Pelin K, Beggs AH, Hayashi YK, Romero NB, Laing NG, Nishino I, Wallgren-Pettersson C, Melki J, Fowler VM, MacArthur DG, North KN, Clarke NF: Leiomodin-3 dysfunction results in thin filament disorganization and nemaline myopathy. J Clin Invest. 2014 Nov; 124(11): 4693-708.

Miyatake S, Koshimizu E, Hayashi YK, Miya K, Shiina M, Nakashima M, Tsurusaki Y, Miyake N, Saitsu H, Ogata K, Nishino I, Matsumoto N: Deep sequencing detects very-low-grade somatic mosaicism in the unaffected mother of siblings with nemaline myopathy. Neuromuscul Disord. 2014 Jul; 24(7): 642-7.

Kawase K, Nishino I, Sugimoto M, Togawa T, Sugiura T, Kouwaki M, Kibe T, Koyama N, Yokochi K: Nemaline myopathy with *KLHL40* mutation presenting as congenital totally locked-in state. Brain Dev. [Epub Feb 2015] ahead of print

Puppo F, Dionnet E, Gaillard MC, Gaildrat P, Castro C, Vovan C, Karine B, Bernard R, Attarian S, Goto K, Nishino I, Hayashi YK, Magdinier F, Krahn M, Helmbacher F, Bartoli M, Levy N: Identification of variants in the 4q35 gene FAT1 in patients with a Facioscapulohumeral dystrophy (FSHD)-like phenotype. Hum Mutat. [Epub Jan 2015] ahead of print

Montassir H, Maegaki Y, Murayama K, Yamazaki T, Kohda M, Ohtake A, Iwasa H,

Yatsuka Y, Okazaki Y, Sugiura C, Nagata I, Toyoshima M, Saito Y, Itoh M, Nishino I, Ohno K: Myocerebrohepatopathy spectrum disorder due to POLG mutations: A clinicopathological report. Brain Dev. [Epub Nov 2014] ahead of print

Uruha A, Hayashi YK, Oya Y, Mori-Yoshimura M, Kanai M, Murata M, Kawamura M, Ogata K, Matsumura T, Suzuki S, Takahashi Y, Kondo T, Kawarabayashi T, Ishii Y, Kokubun N, Yokoi S, Yasuda R, Kira JI, Mitsuhashi S, Noguchi S, Nonaka I, Nishino I: Necklace cytoplasmic bodies in hereditary myopathy with early respiratory failure. J Neurol Neurosurg Psychiatry. [Epub Sep 2014] ahead of print

Sanmaneechai O, Likasitwattanakul S, Sangruchi T, Nishino I: Ophthalmoplegia in congenital neuromuscular disease with uniform type 1 fiber. Brain Dev. [Epub Aug 2014] ahead of print

Yonekawa T, Nishino I: Ullrich congenital muscular dystrophy: clinicopathological features, natural history and pathomechanism(s). J Neurol Neurosurg Psychiatry. 86(3): 280-287, Mar 2015

Wang CH, Liang WC, Minami N, Nishino I, Jong YJ: Limb-girdle Muscular Dystrophy Type 2A with Mutation in *CAPN3*: The First Report in Taiwan. Pediatr Neonatol. 56(1): 62-65, Feb, 2015

Tanboon J, Hayashi YK, Nishino I, Sangruchi T: Kyphoscoliosis and easy fatigability in a 14-year-old boy. Neuropathology. 35(1): 91-93, Feb 2015

Kawase K, Nishino I, Sugimoto M, Kouwaki M, Koyama N, Yokochi K: Hypoxic ischemic encephalopathy in a case of intranuclear rod myopathy without any prenatal sentinel event. Brain Dev. 37(2): 265-269, Feb, 2015

Falcone S, Roman W, Hnia K, Gache V, Didier N, Laine J, Aurade F, Marty I, Nishino I, Charlet-Berguerand N, Romero NB, Marazzi G, Sassoon D, Laporte J, Gomes ER: N-WASP is required for Amphiphysin-2/BIN1-dependent nuclear positioning and triad organization in skeletal muscle and is involved in the pathophysiology of centronuclear myopathy. EMBO Mol Med. 6(11): 1455-1475, Nov, 2014

Saitsu H, Tohyama J, Walsh T, Kato M, Kobayashi Y, Lee M, Tsurusaki Y, Miyake N, Goto YI, Nishino I, Ohtake A, King MC, Matsumoto N: A girl with West syndrome and autistic features harboring a de novo TBL1XR1 mutation. J Hum Genet. 59(10): 581-583, Oct, 2014

Fujii T, Hayashi S, Kawamura N, Higuchi MA, Tsugawa J, Ohyagi Y, Hayashi YK, Nishino I, Kira JI: A case of adult-onset reducing body myopathy presenting a novel clinical feature, asymmetrical involvement of the sternocleidomastoid and trapezius muscles. J Neurol Sci. 343(1-2): 206-210, Aug, 2014

Cho A, Hayashi YK, Monma K, Oya Y, Noguchi S, Nonaka I, Nishino I: Mutation profile of the *GNE* gene in Japanese patients with distal myopathy with rimmed vacuoles (GNE myopathy). J Neurol Neurosurg Psychiatry. 85(8): 912-915, Aug, 2014

Mukai M, Sugaya K, Ozawa T, Goto Y, Yanagishita A, Matsubara S, Bokuda K, Miyakoshi A, Nakao I. Isolated mitochondrial stroke-like episodes in an elderly patient with MT-ND3 gene mu-

tation. Neurol Cli Neurosci (in press)

Sakai C, Yamaguchi S, Sasaki M, Miyamoto Y, Matsushima Y, Goto Y.
ECHS1 mutations cause combined respiratory chain deficiency resulting in Leigh syndrome. Hum Mut 36: 232-239, 2015

Ohnuki Y, Takahashi K, Iijima E, Takahashi W, Suzuki S, Ozaki Y, Kitao R, Mihara M, Ishihara T, Nakamura M, Sawano Y, Goto Y, Izumi S, Kulski J-K, Shiina T, Takizawa S. Multiple deletions in mitochondrial DNA in a
patient with progressive external ophthaloplegia, leukoencephalopathy and hypogonadism. Inter Med 53: 1365-1369, 2014

Miyatake S, Koshimizu E, Hayashi YK, Miya K, Shiina M, Nakashima M, Tsurusaki Y, Miyake N, Saitsu H, Ogata K, Nishino I, Matsumoto N: Deep sequencing detects very-low-grade somatic mosaicism in the unaffected mother of siblings with nemaline myopathy. Neuromuscul Disord. 24(7): 642-647, Jul, 2014

２．学会発表

Endo Y, Noguchi S, Hara Y, Hayashi YK, Motomura K, Murakami N, Tanaka S, Yamashita S, Kizu R, Bamba M, Goto Y, Miyatake S, Matsumoto N, Nonaka I, Nishino I: Dominant mutations in ORAI1 cause tubular aggregate myopathy with hypocalcemia via constitutive activation of store-operated Ca^{2+} channels. 19th International Congress of the World Muscle Society, Berlin, Germany (Langenbeck-Virchow-Haus), 10.8, 2014 (10.7-10.11)

Wen-Chen Liang, Wenhua Zhu, Satomi Mitsuhashi, Ichizo Nishino, Yuh-Jyh Jong, An 8-year-old girl with congenital cataracts and motor development delay, 14th AOMC ANNUAL SCIENTIFIC MEETING 2015, バンコク, 3.4.2015

Wenhua Zhu, Jantima Tanboo, Takashi Ito Satomi Mitsuhashi, Ichizo Nishino, A 35-year-old man with distal muscle weakness, contractures, and persistent hyperCKemia, 14th AOMC ANNUAL SCIENTIFIC MEETING 2015, バンコク, 3.4.2015

Wen-Chen Liang, Wenhua Zhu, Satomi Mitsuhashi, Satoru Noguchi, Ichizo Nishino, A case report of TRAPPC11 disease: a wider clinical spectrum with multiple systemic involvement. The 4th Oriental Congress of Neurology, 上海, 3.28.2015

Sakai C, Matsushima Y, Sasaki M, Miyamoto Y, Goto Y: Targeted exome sequencing identified a novel genetic disorder in mitochondrial fatty acid β-oxidation. Euromit 2014, Tampere, Finland, 6.16, 2014

Matsushima Y, Hatakeyama H, Takeshita E, Kitamura T, Kobayashi K, Yoshinaga H, Goto Y. Leigh-like syndrome associated with calcification of the bilateral basal ganglia caused by compound heterozygous mutations in mitochondrial poly(A) polymerase. Euromit 2014, Tampere, Finland, 6.16, 2014

Goto Y: Mitochondrial Disease. Asian & Oceanian Epilepsy Congress 2014. Singapore, 8.7, 2014

H. 知的財産権の出願・登録状況（予定を含む）

１．特許取得
なし

２．実用新案登録
なし

３．その他

なし

厚生労働科学研究委託費
（難治性疾患等実用化研究事業（難治性疾患実用化研究事業））

委託業務報告書（業務項目）

遺伝性ミオパチーの次世代型統合的診断拠点形成
１．既知遺伝子のハイスループット解析

業務主任者　　三橋　里美　　疾病研究第一部　室長
後藤　雄一　　疾病研究第二部　部長

研究要旨

診断未知の筋疾患について、遺伝性筋疾患の原因となることが知られている遺伝子群を臨床病理学的特徴より4つのカテゴリーに分類した筋疾患遺伝子パネルを作成し、次世代シークエンサーIonPGMを用いて、網羅的にシークエンス解析を行った。約25%の症例で原因と考えられる遺伝子変異を同定することができた。これまで同定できた遺伝子変異は、本邦ではじめての報告となる遺伝子や、新規変異、または、臨床症状からは疑われていなかった疾患であることが判明したものなどがあり、網羅的解析の重要性が示された。診断が確定できなかった症例については、エクソームシークエンスを行い、さらなる解析を行う。

ミトコンドリア病については、約800のミトコンドリア関連タンパク質をコードする遺伝子配列を調べるために、7368箇所の領域をキャプチャーするHaloplex®を用いた解析を生化学的に複数の呼吸鎖酵素複合体の活性低下が認められる2症例に試みた。その結果、それぞれに病因の可能性の高い遺伝子変異が、コンパウンドヘテロ接合体で見いだされ、そのうち１例では表現系回復実験を行い病因と確定した。この方法の有用性が確認できた。今後はミトコンドリア機能異常が確定している症例についての解析を継続させるとともに、臨床診断への応用も視野に入れた活用法を追求する。

A.研究目的

遺伝性筋疾患の原因となる遺伝子は、報告されているだけでも 100 種類以上あり、巨大な遺伝子も多数存在する。これらの遺伝子を従来のサンガーシークエンス法でシークエンスすることは、コストも人員も時間もかかり、網羅的解析はほぼ不可能であった。よって、これまでの遺伝子変異解析は、スポット的な方法に限られていた。本研究では、近年の次世代シークエンサー技術の進歩を利用し、次世代シークエンサーIonPGM を用いて、効率的で網羅的な遺伝性筋疾患の遺伝子解析を目指す。

B.研究方法

国立精神・神経医療研究センターに筋病理診断および、遺伝子解析の依頼された検体のうち、遺伝的に未診断の遺伝性ミオパチーに対して、4 種類の筋疾患遺伝子パネルを使った、次世代シークエンサーIonPGM を用いて、既知遺伝子変異のターゲットリシークエンス解析を行った。このパネルは、これまでに遺伝性筋疾患の原因として報告されている遺伝子をほぼ全て含み、筋ジストロフィー(65 遺伝子)、先天性ミオパチー(42 遺伝子)、代謝性ミオパチー(45 遺伝子)、異常タンパク質の凝集や縁取り空胞を特徴とするミオパチー(36 遺伝子)の４種類に

分類してあり（括弧内は含まれる遺伝子数)、コーディング領域およびスプライス部位に対して、97%のカバー率を持っている。対象となる症例を、筋病理診断および臨床診断によって、いずれかのカテゴリーに分類し、解析を行った。

ミトコンドリア病については、これまで患者で報告のある 200 近くの遺伝子に加えて、800 近くのミトコンドリア関連遺伝子を調べる目的で、総計 7368 領域をキャプチャーできるように設計した Haloplex®によって関心領域をキャプチャーした上で、次世代シークエンサーMiSeq によりターゲットリシークエンスを行った。過去 30 年以上の期間に収集した mtDNA に病的変異を持たない患者骨格筋は、おおよそ 1000 検体を保有しており、その中で、ミトコンドリア呼吸鎖複合体の活性を測定する生化学検査において複数の呼吸鎖酵素活性低下及びミトコンドリア DNA 由来タンパク質の翻訳活性の低下している 2 検体を選定した。患者 1 は 1 歳 9 ヶ月の男児で Leigh 症候群を呈し、患者 2 は 1 歳 5 ヶ月の女児で高乳酸血症を呈している。いずれの患者の両親も血族婚ではなかった。翻訳活性に関しては、エメチンで各 DNA の翻訳活性を抑制した後に、35S メチオニンでラベルした 13 個のミトコンドリアタンパク質を PAGE で検出した。次世代シーケンサーは MiSeq（illumina 社）を用いた。

（倫理面への配慮）

本研究において使用するヒト試料は、共同研究施設である NCNP 倫理委員会で承認された所定の承諾書を用いて、患者あるいはその親権者から遺伝子解析を含む研究利用に対する検体の使用許可を得たものを用いた。

C.研究結果

IonPGMを用いて、380検体の解析を行った。88症例で、病気の原因の可能性がある遺伝子変異を同定することができた。この中には、α-dystroglycanopathyの原因遺伝子である*POMT2*，*POMGNT2*，*ISPD*の新規変異や、世界で報告が2例目となる*TRAPPC11*変異、報告が非常にまれな*MATR3*の新規変異などを同定し、学会報告した。また、呼吸不全などの特徴的な臨床像を示さず、確定診断が付かなかった症例において、既報告の*TTN*変異を見出し、HMERFという診断が得られたため、今後の臨床経過の予測に貢献することができた。また、原因遺伝子が不明であった症例のち、83症例を含む、192例をHiSeq1000シークエンサーでエクソーム解析中である。

ミトコンドリア病については、患者1でECHS1の、患者2で遺伝子Xの複合ヘテロ接合型変異を見いだした。患者1由来の筋芽細胞では、HCHS1蛋白質の発現が低下していた。患者2では蛋白質Xの発現に変化は見られなかったが、蛋白質X葉酸代謝に関与しており、ミトコンドリアのtRNAの修飾に関する基質の代謝に寄与することから、その基質の不足によってmtDNAの翻訳異常が引き起こされる可能性について今後解析を行う予定である。

D.考察

遺伝子診断が未知の遺伝性筋疾患に対して、筋疾患遺伝子パネルによる、次世代シークエンサーIonPGMを活用することにより、効率のよい遺伝子診断が可能である。しかし、網羅的変異解析にもかかわらず、未だ70%の症例で、原因遺伝子が判明していない。この原因として、ターゲット領域以外の変異、もしくはリピート、欠失や挿入などの検出が難しい変異である可能性や、遺伝性疾患という臨床診断が間違っている可能性もあるが、新規の筋疾患原因遺伝子による疾患である可能性が高いと考えている。これらの症例に対しては、エクソームシークエンスによる、遺伝情報の蓄積を行うことで、新規の筋疾患原因が明らかとなると考えられる。

ミトコンドリア病については、1例で病因確定を行い投稿論文として報告した。今後ECHS1の欠損とミトコンドリアの翻訳異常、呼吸鎖複合体の活性低下の関連について更に解析を行う予定である。

E.結論

IonPGM を用いて、既知の筋疾患原因遺伝子を網羅的に解析することが可能であるとともに、新規遺伝子の発見につながる結果を示した。今後は、さらに解析症例を増やし、診断未知の筋疾患エクソームデータベースを構築し、新規遺伝子発見と疾患病態解明に繋げて行くことが期待される。

ミトコンドリア病については、これまで病因変異の不明であったミトコンドリアミオパチー患者の核 DNA コードの原因遺伝子の同定を行うことに成功し、約 800 の遺伝子をターゲットしたターゲットリシークエンス解析の有用性を示した。今後は機能解析（機能回復実験）が可能な試料をもつ患者を中心に症例を重ねてその研究的意義を高めつつ、臨床の現場にどのように応用させるかについての研究も行うことが肝要と考える。

F.健康危険情報

特になし

G.研究発表

１．論文発表

Uruha A, Hayashi YK, Oya Y, Mori-Yoshimura M, Kanai M, Murata M, Kawamura M, Ogata K, Matsumura T, Suzuki S, Takahashi Y, Kondo T, Kawarabayashi T, Ishii Y, Kokubun N, Yokoi S, Yasuda R, Kira JI, Mitsuhashi S, Noguchi S, Nonaka I, Nishino I: Necklace cytoplasmic bodies in hereditary myopathy with early respiratory failure. J Neurol Neurosurg Psychiatry. [Epub ahead of print]

Kida H, Sano K, Yorita A, Miura S, Ayabe M, Hayashi Y, Nishino I, Taniwaki T. First Japanese case of muscular dystrophy caused by a mutation in the anoctamin 5 gene.
Neurol and Clin Neurosci. [Epub ahead of print]

Mukai M, Sugaya K, Ozawa T, Goto Y, Yanagishita A, Matsubara S, Bokuda K, Miyakoshi A, Nakao I. Isolated mitochondrial stroke-like episodes in an elderly patient with MT-ND3 gene mutation. Neurol Clin Neurosci. [Epub ahead of print]

Sakai C, Yamaguchi S, Sasaki M, Miyamoto Y, Matsushima Y, Goto Y.
ECHS1 mutations cause combined respiratory chain deficiency resulting in Leigh syndrome. Hum Mut 36: 232-239, 2015

Ohnuki Y, Takahashi K, Iijima E, Takahashi W, Suzuki S, Ozaki Y, Kitao R, Mihara M, Ishihara T, Nakamura M, Sawano Y, Goto Y, Izumi S, Kulski J-K, Shiina T, Takizawa S. Multiple deletions in mitochondrial DNA in a patient with progressive external ophthaloplegia, leukoencephalopathy and hypogonadism. Inter Med 53: 1365-1369, 2014

２．学会発表

三橋里美, 次世代シークエンサーを用いた筋疾患の遺伝子診断システムについて, 第三回骨格筋研究会, 3.7.2015

Wen-Chen Liang, Wenhua Zhu, Satomi Mitsuhashi, Ichizo Nishino, Yuh-Jyh Jong, An 8-year-old girl with congenital cataracts and motor development delay, 14th AOMC ANNUAL SCIENTIFIC MEETING 2015, バンコク, 3.4.2015

Wenhua Zhu, Jantima Tanboo, Takashi Ito Satomi Mitsuhashi, Ichizo Nishino, A 35-year-old man with distal muscle weakness, contractures, and persistent hyperCKemia, 14th AOMC ANNUAL SCIENTIFIC MEETING 2015, バンコク, 3.4.2015

Wen-Chen Liang, Wenhua Zhu, Satomi Mitsuhashi, Satoru Noguchi, Ichizo Nishino, A case report of TRAPPC11 disease: a wider clinical spectrum with

multiple systemic involvement. The 4th Oriental Congress of Neurology, 上海, 3.28.2015
Sakai C, Matsushima Y, Sasaki M, Miyamoto Y, Goto Y: Targeted exome sequencing identified a novel genetic disorder in mitochondrial fatty acid β-oxidation. Euromit 2014, Tampere, Finland, 6.16, 2014

Matsushima Y, Hatakeyama H, Takeshita E, Kitamura T, Kobayashi K, Yoshinaga H, Goto Y. Leigh-like syndrome associated with calcification of the bilateral basal ganglia caused by compound heterozygous mutations in mitochondrial poly(A) polymerase. Euromit 2014, Tampere, Finland, 6.16, 2014

Goto Y: Mitochondrial Disease. Asian & Oceanian Epilepsy Congress 2014. Singapore, 8.7, 2014

H. 知的財産権の出願・登録状況（予定を含む）

１． 特許取得
なし

２． 実用新案登録
なし

３． その他
なし

厚生労働科学研究委託費
（難治性疾患等実用化研究事業（難治性疾患実用化研究事業））

委託業務成果報告（業務項目）

遺伝性ミオパチーの次世代型統合的診断拠点形成
２．全エクソーム解析

業務主任者　西野一三　国立精神･神経医療研究センター神経研究所　**疾病研究第一部　部長**

研究要旨

診断未知の筋疾患について、遺伝性筋疾患の原因となることが知られている遺伝子に対して網羅的解析を行った結果、診断が確定できなかった症例について、エクソームシークエンスを行った。また、臨床病理学的所見から、既知遺伝子の変異では説明できない症例については、直接エクソーム解析を行った。Tubular aggregate myopathyの新規原因遺伝子*ORAI1*を見出した他、世界第2例目の*DAGI*変異例同定、新たなネマリンミオパチー原因遺伝子*LMOD3*の同定などの成果を上げた。この他にも多数の候補原因遺伝子を見出し、さらに病因解析を進めている。また、インフォマティクス解析パイプラインをGATKv.3.1を用いたものにアップデートするとともに、エクソーム解析のデータベースを横断的に解析するためのデータベースを構築した。今後、さらに効率よく原因遺伝子変異を見出すことが可能となることが期待される。

A.研究目的

遺伝性筋疾患の原因となる遺伝子は、報告されているだけでも 100 種類以上あるが、これらの遺伝子の網羅的解析によっても、原因となる遺伝子変異が確定できない症例が多数存在する。本研究では、これらの症例に対して、エクソーム解析を行い、原因となる遺伝子変異の同定を目指す。

B.研究方法

国立精神・神経医療研究センターに診断依頼された検体のうちで既知遺伝子変異ハイスループット解析を行ってもなお原因遺伝子不明であった 83 例および、遺伝子診断未知でいずれのカテゴリーにも属さず新規原因遺伝子が疑われる症例を含めた 192 例を対象とした。全エクソームキャプチャーキットを用いてライブラリーを作製し、HiSeq1000 にてゲノム情報を取得した。既に構築済みの解析パイプラインを通して、候補遺伝子を絞り込み、候補遺伝子変異は、サンガー法で確認した。バイオインフォマティクスおよび日本人多型の判断に関しては、横浜市立大学・松本直通教授（研究協力者）と連携して進めた。さらに、これまでに解析を行った 400 例についても、引き続き原因遺伝子の同定を進めている。

（倫理面への配慮）

本研究において使用するヒト試料は、共同研究施設である NCNP 倫理委員会で承認された所定の承諾書を用いて、患者あるいはその親権者から遺伝子解析を含む研究利用に対する検体の使用許可を得たものを用いた。

C.研究結果

これまでにエクソーム解析を行った475例中350例で、解析が終了している。このうち、60の症例で病気の原因である可能性のある遺伝子変異を見出すことができた。この中には、1.tubular aggregate myopathyの新規の変異遺伝子*ORAI1*の同定、2．α-dystroglycanopathyと病理学的に確定された例の中から世界第2例目となる*DAG1*変異例を同定、3．*LMOD3*変異がネマリンミオパチーの新たな原因であることを同定、4.*TK2*変異による筋線維未熟性を伴う先天性ミオパチーの同定、5. 中心核ミオパチーの新規原因遺伝子Xの同定（海外の研究者との共同研究のため遺伝子名は未公表）、6.*LMNA*変異による核内ロッドを伴う先天性ミオパチーの同定、7. 本邦初の*MEGF10*先天性ミオパチーの同定、8. 本邦初のANO5変異の同定、などの成果が含まれ、さらに病因解析を進めている。

Tubular aggregate myopathyでは、見いだされた変異をHEK293細胞に導入しFura-2を用いて細胞内カルシウム動態を評価した。その結果、野生型ORAI1を導入した細胞では細胞外カルシウ濃度にかかわらず細胞内カルシウム濃度がほぼ一定に保たれるのに対し、変異体導入細胞では、細胞内カルシウム濃度が順次上昇した。この上昇はストア作動性チャネル特異的阻害剤で正常化されたことから、ORAI1変異がORAI1チャネルをconstitute activeに変え、常に開口状態にしていることが示された。患者筋管細胞を用いた実験でも同様の結果を得た。

平成26年度は、解析ソフトウェアを更新し、より信頼性の高い結果が得られることが期待されるGATKv.3.1を用いた解析パイプラインを構築した。また解析の省力・省時間化を目指し、これまでに解析したNCNP内のエクソームデータベースを構築し、横断的に解析するシステムを構築した。これにより、同じ変異をもった症例を容易に見出すことや、病気の原因として疑わしい遺伝子に変異をもつ症例を抽出することが容易に可能となった。

D.考察

遺伝子診断が未知の遺伝性筋疾患に対して、筋疾患遺伝子パネルによる、次世代シークエンサーIonPGMによるスクリーニングを行った後、診断未知の筋疾患に対してエクソームシークエンスを行うことで、新規疾患原因遺伝子を見出す方法は、省コスト、省時間を考える上でも有効であると思われる。今後は、変異の病原性についての解析が必要であり、同じ変異を持った症例の蓄積が病原性の証明には大切であることから、今後さらにエクソームシークエンスによる、遺伝情報の蓄積を行い、新規の筋疾患原因が明らかにしていくことが必要である

E.結論

診断未知の筋疾患患者にたいするエクソーム解析によって、新規遺伝子の発見につながる結果を示した。今後は、さらに解析症例を増やし、エクソームデータベースを構築し、新規遺伝子発見と疾患病態解明に繋げて行く。

F.健康危険情報

特になし

G.研究発表

１．論文発表

Endo Y, Noguchi S, Hara Y, Hayashi YK, Motomura K, Miyatake S, Murakami N, Tanaka S, Yamashita S, Kizu R, Bamba M, Goto YI, Matsumoto N, Nonaka I, Nishino I: Dominant mutations in *ORAI1* cause tubular aggregate myopathy with hypocalcemia via constitutive activation of store-operated Ca^{2+} channels. Hum Mol Genet. 2015 Feb 1; 24(3): 637-48.

Dong M, Noguchi S, Endo Y, Hayashi YK, Yoshida S, Nonaka I, Nishino I: DAG1 mutations associated with asymptomatic hyperCKemia and hypoglycosylation of α-dystroglycan. Neurology. 2015 Jan 20; 84(3): 273-9.

Yuen M, Sandaradura SA, Dowling JJ,

Kostyukova AS, Moroz N, Quinlan KG, Lehtokari VL, Ravenscroft G, Todd EJ, Ceyhan-Birsoy O, Gokhin DS, Maluenda J, Lek M, Nolent F, Pappas CT, Novak SM, D'Amico A, Malfatti E, Thomas BP, Gabriel SB, Gupta N, Daly MJ, Ilkovski B, Houweling PJ, Davidson AE, Swanson LC, Brownstein CA, Gupta VA, Medne L, Shannon P, Martin N, Bick DP, Flisberg A, Holmberg E, Van den Bergh P, Lapunzina P, Waddell LB, Sloboda DD, Bertini E, Chitayat D, Telfer WR, Laquerrière A, Gregorio CC, Ottenheijm CA, Bönnemann CG, Pelin K, Beggs AH, Hayashi YK, Romero NB, Laing NG, Nishino I, Wallgren-Pettersson C, Melki J, Fowler VM, MacArthur DG, North KN, Clarke NF: Leiomodin-3 dysfunction results in thin filament disorganization and nemaline myopathy. J Clin Invest. 2014 Nov; 124(11): 4693-708.

Miyatake S, Koshimizu E, Hayashi YK, Miya K, Shiina M, Nakashima M, Tsurusaki Y, Miyake N, Saitsu H, Ogata K, Nishino I, Matsumoto N: Deep sequencing detects very-low-grade somatic mosaicism in the unaffected mother of siblings with nemaline myopathy. Neuromuscul Disord. 2014 Jul; 24(7): 642-7.

２．学会発表

Endo Y, Noguchi S, Hara Y, Hayashi YK, Motomura K, Murakami N, Tanaka S, Yamashita S, Kizu R, Bamba M, Goto Y, Miyatake S, Matsumoto N, Nonaka I, Nishino I: Dominant mutations in ORAI1 cause tubular aggregate myopathy with hypocalcemia via constitutive activation of store-operated Ca^{2+} channels. 19th International Congress of the World Muscle Society, Berlin, Germany (Langenbeck-Virchow-Haus), 10.8, 2014 (10.7-10.11)

H. 知的財産権の出願・登録状況（予定を含む）

１．特許取得

なし

２．実用新案登録

なし

３．その他

なし

厚生労働科学研究委託費
（難治性疾患等実用化研究事業（難治性疾患実用化研究事業））
委託業務成果報告書（業務項目）

遺伝性ミオパチーの次世代型統合的診断拠点形成
３．新規原因遺伝子変異の病原性証明と疾患分子病態解明

業務主任者　野口悟　国立精神･神経医療研究センター神経研究所　**室長**

研究要旨

孤発例の原因遺伝子解析では、次世代シークエンサーによって数十にも及ぶ遺伝子変異候補が見いだされるが、真の変異を探しだすこと、変異の病因性を証明することは、依然として難しい課題である。□-dystroglycanopathyおよびtubular aggregate myopathy患者を対象として行った全エクソーム解析から得られた変異候補を絞り込み、効率的に変異の病因性の証明をすることを目指した。□-dystroglycanopathyについては、*POMGNT2*遺伝子変異について解析した。*POMGNT2*遺伝子を欠失した半数体株化細胞HAP1に対して、変異または野生型POMGNT2 cDNAを導入することで、細胞の表現型が回復出来るのかを指標に、用いた遺伝子変異の病因性を判断した。さらに、変異POMGNT2の酵素活性の測定、細胞内局在の解析を行った。Tubular aggregate myopathyについては、見出したORAI1変異(Gly98Ser, Leu138Phe)のストア作動性カルシウム流入への影響を確認するため、罹患者由来の筋管細胞及び上記変異を有するORAI1を過剰発現させたHEK293細胞を用いて、細胞外Ca2+濃度変化に伴う細胞内Ca2+濃度変化を測定した。その結果、細胞外にCa2+を加えることで、変異ORAI1をもつ細胞では有意に細胞内Ca2+濃度が上昇し、ORAI1チャネルの特異的阻害剤により抑制されること見出した。このことは、ORAI1優性変異による恒常的SOCE活性化が、Tubular aggregate形成および骨格筋障害の原因であることを示している。

A.研究目的

次世代シークエンサー解析によって見いだされる各種変異候補の病原性証明と分子病態解明のために、機能解析の系を確立することを目的としている。今年度は、全エクソーム解析で見いだされたα-dystroglycanopathy および tubular aggregate myopathy の候補変異を評価する系を確立することを目的とした。

B.研究方法

α-dystroglycanopathy患者20名を対象とし、イルミナ社Hiseq1000にて全エクソーム解析を行お見いだされた変異候補のα-dystroglycan糖鎖への影響を評価すべく、HAP1細胞（野生型、*POMGNT2*-KO）の供与をNetherlands Cancer InstituteのDr. Brummelkampより受けた。ヒトPOMGNT2 cDNAは、ヒト

骨格筋cDNAプールからPCRにて増幅・クローニングした。PCRエラーにて生じた変異は、site-directed mutagenesisにて参照配列に矯正し、野生型cDNAを得た。変異の導入にはさらに、site-directed mutagenesisを用いた。野生型及び変異cDNAは、pLVSIN-IRES-ZsGreenにクローニングし、レンチウイルスベクタークローンを得た。レンチウイルスベクターの作製は定法を用いた。変異の病因性の評価は、HAP1生細胞をα-dystroglycanの糖鎖エピトープに対する抗体IIH6にて染色することで行った。今回用いた変異は劣性遺伝変異が予想されるため、もし、見いだされた変異が「真の変異」であり、変異タンパク質が機能を失っていた場合には、欠損細胞は変異遺伝子の導入で蛍光染色が陽性とならない。もし、変異が〝多型〟であって、依然として機能タンパク質が作られる場合には、蛍光染色が陽性となると考えられた。そこで、ZsGreen陽性にて遺伝子導入細胞を同定し、かつIIH6染色の回復の有無を調べることで、変異を評価した。ヒト野生型および変異myc−POMGNT2 cDNAをHele細胞に導入･発現させ、myc標識タンパク質の細胞内局在を解析した。ヒト野生型および変異myc−POMGNT2 cDNAをHEK293細胞に導入･発現させた。膜画分を調製した。1% TritonX-100にて抽出後、抽出物をMannose -α-4-MU及びUDP-GlcNAcと６時間反応させた。反応生成物GlcNAc-Man -α-4-MUをHPLCにて、Amide-80カラムにて分離定量した。同定した生成GlcNAc-Man -α-4-MUが、β-ヘキソサミニダーゼ消化により消失することを確認した。

Tubular aggregate myopathyを呈する18症例に対して行った全エクソーム解析により、罹患者6名のORAI1遺伝子にヘテロ接合性変異を見出した。骨格筋収縮は主に筋小胞体（SR）から放出されるCa2+濃度により制御されており、SR内のCa2+を一定に保つ機構としてストア作動性カルシウム流入（store-operated Ca2+ entry; SOCE） と呼ばれる細胞外から細胞内へのCa2+流入機構が存在する。このCa2+流入を担うのがストア作動性Ca2+チャネルであり、ORAI1はその主要構成成分である。見出したORAI1変異(Gly98Ser, Leu138Phe)のSOCEへの影響を確認するため、罹患者由来の筋管細胞及び上記変異を有するORAI1を過剰発現させたHEK293細胞を用いて、細胞外Ca2+濃度変化に伴う細胞内Ca2+濃度変化を測定した。また、細胞内Ca2+濃度変化が細胞外からのCa2+流入によるものなのか、SRをはじめとする細胞内Ca2+貯蔵器官から放出されたものなのかを見極めるために、Mn2+ quenching実験を行った。

（倫理面への配慮）

すべての組み換え DNA 実験は、カルタヘナ議定書に基づく「遺伝子組み換え生物等の使用等の規制による生物の多様性の確保に関する法律」と関係省令を遵守し、国立精神・神経センター神経研究所組み換え DNA 実験安全委員会の審査・承認(筋疾患関連遺伝子のクローニング: 26-01)を得ている。

C.研究結果

α-dystroglycanopathy3名に *POMGNT2*変異 c.494T>C(p.M165T) 及び c.785C>T (p.P253L)複合ヘテロ接合変異(1名)、c.785C>T (p.P253L)ホモ接合変異(2名)を見出した。両方の変異は、ともにミスセンス変異であると推定された。また、両変異ともにグリコシルトランストランスフェラーゼ様ドメインに存在していた。変異が見出された患者には、きわめて軽い筋ジストロフィーを認めた。筋病理についても、わずかな壊死・再生線

維を示す、ごく軽いものであった。また、脳の形成不全などは認められなかった。

野生型 HAP1 細胞は、ラミニン上で培養することで、α-dystroglycan は集積し、IIH6 抗体で染色された。一方、*POMGNT2*-KO 細胞では IIH6 抗体での染色は見られなかった。*POMGNT2*-KO 細胞への野生型 POMGNT2cDNA の導入により IIH6 抗体陽性となった。一方、p. M165T 及び p.P253L 変異 POMGNT2 cDNA の導入では、IIH6 抗体陰性であった。Hela 細胞に導入された p. M165T 及び p.P253L 変異 POMGNT2 は、野生型 POMGNT2 と同様に、小胞体での局在が見られた。しかしながら、HEK293 細胞で発現させた p.M165T 及び p.P253L 変異 POMGNT2 は、野生型 POMGNT2 に比べ、10%以下の比活性しか検出されなかった。

罹患者由来の筋管細胞及び変異 ORAI1 を過剰発現させた HEK293 細胞の液体培地を、Ca2+を含有していない培養液、生体内における細胞外 Ca2+濃度と同等の 2mM を含有する培養液、20mM 高濃度 Ca2+を含有する培養液に変換することで、細胞内 Ca2+濃度がどのように変化するのかを経時的に測定した。細胞外に Ca2+を加えることで、変異 ORAI1 をもつ細胞では有意に細胞内 Ca2+濃度が上昇し、ORAI1 チャネルの特異的阻害剤により抑制されること見出した。またこの細胞内 Ca2+濃度上昇は、細胞内 Ca2+貯蔵器官から放出されたものではなく、細胞外から細胞内へ Ca2+が異常流入していることによるものであることを明らかにした。以上の結果より、ORAI1 優性変異による恒常的 SOCE 活性化が、Tubular aggregate 形成および骨格筋障害の原因であることが示された。

D.考察

α-dystroglycanopathy の原因遺伝子は、現在 18 種類以上が同定されている。α-dystroglycanopathy の原因遺伝子は、糖鎖合成に関わる酵素をコードしているものが大半であり、患者で同定された変異の証明には変異遺伝子産物の酵素活性を測定する方法が一般的である。しかしながら、変異遺伝子毎に異なるアッセイ系を構築せねばならず、充分に証明されていないままに報告されることもある。また、機能が同定されていない遺伝子に関しては、証明の方法もないのが現状である。Jae らによって報告された HAP1 細胞を用いたα-dystroglycanopathy の候補遺伝子を予測、実証した方法は、理論上、すべての候補遺伝子、遺伝子変異を同じ方法にて検定しうるものである。今回、POMGNT2 変異に応用したが、変異 cDNA による機能回復は観察されず、当該変異が病因であることを証明することに成功した。

組み換え変異 POMGNT2 タンパク質は、活性の低下を示し、これらの変異が病因変異であることを再び強く支持した。これまで、*POMGNT2* 変異による α-dystroglycanopathy では、症状の重い WWS の報告がある。今回見出された患者は、非常に軽い肢帯型筋ジストロフィーであるが、興味深いことに、変異タンパク質活性は低下していたものの、まったく失われているわけではなく、少量の残存活性が検出された。この活性により、α-dystroglycan の糖鎖修飾が部分的に保持され、軽い症状を引き起こしているものと考えられた。また、遺伝子変異はグリコシルトランスフェラーゼドメインに存在したが、変異タンパク質の発現や細胞内分布には影響がなく、活性の低下のみが検出されたことと関係しているのかもしれない。以上の結果から、以前報告した *DAG1* 変異での

α-dystroglycanopathy と合わせて、HAP1 細胞を用いた変異の病因性の証明方法は、他の遺伝子変異を原因とする α-dystroglycanopathy まで、広く利用することができることが示された。今後は、変異遺伝子補完実験で、HAP1 細胞が発現するα-dystroglycan とラミニンとの結合実験など生化学的解析を行うことで、この方法の有効性を示していきたいと考えている。

これまで ORAI1 遺伝子の劣性変異により重症複合型免疫不全症が引き起こされることは知られていたが、今回優性変異により骨格筋疾患を来すという新たな知見を得た。また、ORAI1 と複合体を形成する STIM1 の優性変異でも同様に、SOCE が活性化され Tubular aggregate myopathy を発症することが報告されており、SOCE 活性による細胞内 Ca2+濃度変化が骨格筋障害に関与していると推察された。以上の知見は、新規の筋疾患概念を提唱するものであり、細胞内 Ca2+動態と骨格筋障害の関連を解明する端緒となり得る。また、Tubular aggregate myopathy の病態が ORAI1 チャネルの機能獲得型変異であることを明らかにし、その特異的阻害剤が有効であるという in vitro での実験結果を得たことから、治療法への応用が期待される。

E.結論

α-dystroglycanopathy および tubular aggregate myopathy を対象に、遺伝子変異の病因性の証明をおこなった。

F.健康危険情報

なし

G.研究発表

１．論文発表

Dong M, Noguchi S, Endo Y, Hayashi YK, Yoshida S, Nonaka I, Nishino I. *DAG1* mutations associated with asymptomatic hyperCKemia and hypoglycosylation of □-dystroglycan. Neurology, 84, 273-279. 2015.

Uruha A, Hayashi YK, Oya Y, Mori-Yoshimura M, Kanai M, Murata M, Kawamura M, Ogata K, Matsumura T, Suzuki S, Takahashi Y, Kondo T, Kawarabayashi T, Ishii Y, Kokubun N, Yokoi S, Yasuda R, Kira JI, Mitsuhashi S, Noguchi S, Nonaka I, Nishino I. Necklace cytoplasmic bodies in hereditary myopathy with early respiratory failure. J Neurol Neurosurg Psychiatry jnnp-2014-309009. 2014

Endo Y, Noguchi S, Hara Y, Hayashi YK, Motomura K, Miyatake S, Murakami N, Tanaka S, Yamashita S, Kizu R, Bamba M, Goto Y, Matsumoto N, Nonaka I, Nishino I. Dominant mutations in *ORAI1* cause tubular aggregate myopathy with hypocalcemia via constitutive activation of store-operated Ca^{2+} channels. Hum Mol Genet 24, 637-648, 2014.

２．学会発表

Endo Y, Noguchi S, Hara Y, Hayashi YK, Motomura K, Murakami N, Tanaka S, Yamashita S, Kizu R, Bamba M, Goto Y, Miyatake S, Matsumoto N, Nonaka I, Nishino I: Dominant mutations in ORAI1 cause tubular aggregate myopathy with hypocalcemia via constitutive activation of store-operated Ca^{2+} channels. 19th International Congress of the World Muscle Society, Berlin, Germany (Langenbeck-Virchow-Haus), 10.8, 2014 (10.7-10.11)

H. 知的財産権の出願・登録状況（予定を含む）

１．特許取得

なし

２．　実用新案登録
なし

３．　その他
なし

厚生労働科学研究委託費
難治性疾患等実用化研究事業(難治性疾患実用化研究事業)
委託業務成果報告

遺伝性ミオパチーの次世代型統合的診断拠点形成
４．病理・画像所見解析

業務主任者　石山 昭彦　国立精神・神経医療研究センター病院　小児神経診療部　医師
西野一三　国立精神・神経医療研究センター神経研究所　疾病研究第一部部長

研究要旨

遺伝性ミオパチーには多くの病型が存在する。遺伝学的に未診断の例は未だ多く存在するが次世代シークエンサーを用いた遺伝子解析技術の進歩により、これまで未診断だった例の遺伝子変異が同定されるようになってきた。新規遺伝子の変異では遺伝子型と表現型の妥当性を評価する必要性があるが、筋病理さらには骨格筋画像や脳画像所見は表現型として有用な情報となりうる。そのため臨床情報や筋レポジトリ―に加え、骨格筋画像や脳画像を統合的に蓄積し管理することは重要であり、これらを適切に評価することで新たな疾患概念の確立に寄与する可能性がある。今年度は画像登録にあたっての体制整備を行い、遺伝学的未診断例の遺伝性ミオパチー47 例の骨格筋画像、ミトコンドリアミオパチー12 例の脳画像の集積を行った。また、本プロジェクトの中で同定された早期呼吸障害を伴う遺伝性ミオパチー（Hereditary myopathy with early respiratory failure: HMERF）14 家系 17 例の筋病理所見の再検討を行い、necklace cytoplasmic body が感度・特異度ともに極めて高い優れた病理学的マーカーであることが分かった。

A. 研究目的

遺伝性ミオパチーには多様な病型が存在するが、これまでは主に筋病理所見にもとづいた診断がなされてきた。近年、次世代遺伝子解析の技術の進歩により、これまで遺伝学的に未診断だった例の変異が、既知あるいは新規を含め多く同定されるようになってきた。そのため現時点でも遺伝子型にもとづいた疾患名称が用いられるなど、疾患概念自体のパラダイムシフトが生じている。遺伝子型と表現型の相関を適切に評価することはその混乱を回避することのみならず、疾患名称や疾患概念の確立に重要な要素となる。

本研究では次世代遺伝子解析によって得られた遺伝子型と表現型の相関を評価するための表現型評価ツールとして、筋レポジトリ―とそれに伴う臨床情報に骨格筋ならびに脳画像を加え、画像情報の統合的な管理、評価を行う体制整備を構築する。また、遺伝子異常が明らかとなった疾患について筋病理所見ならびに画像所見を再検討することで、遺伝子型・表現型の相関を確立することを目的とする。

B. 研究方法

骨格筋および脳画像の管理については、(独)国立精神・神経医療研究センター脳病態統合イメージングセンター（IBIC; Integrative Brain Imaging Center）で開発した Web 上での画像登録、閲覧が可能なシステム（IBISS; Integrative Brain Imaging Support System）を用いた。こ

れは IBIC が独自に開発した臨床放射線画像登録に特化したオンラインサポートシステムで、厳重なセキュリティーのもと、研究に必要な画像情報、臨床情報を共有できるオンライン上の仮想空間である。これを用いることで将来的に多施設からの画像登録を視野に入れることが可能となる。

IBISS 内での遺伝性ミオパチー画像登録フォームを作成し、2005 年 1 月以降に当センターで精査を行った症例で、遺伝学的未確定なミオパチー症例の骨格筋画像、ミトコンドリアミオパチーの脳画像の登録を行った。

また、本プロジェクトの中で同定された早期呼吸障害を伴う遺伝性ミオパチー（Hereditary myopathy with early respiratory failure: HMERF）14 家系 17 例の筋病理所見の再検討を行った。

（倫理面への配慮）

本研究において使用するすべてのヒト検体から得られた情報はいずれも疾患の確定診断のために筋病理、生化学、免疫学的ならびに遺伝子レベルでの解析が必要でありかつ患者および家族もこれを希望し、患者および家族の了解を得た上で採取した組織（生検・剖検筋、皮膚、血球など）を用いて得られたものであり、かつ（独）国立精神・神経医療研究センター倫理委員会で承認された所定の承諾書を用いて、患者あるいはその親権者から遺伝子解析を含む研究使用に対する検体の使用許可（インフォームド・コンセント）を得たものである。遺伝子解析に関しては「ヒトゲノム解析研究に関する共通指針」を遵守した上で施行されたものである。これら情報を使用するに当たってはプライバシーを尊重し、匿名化した上で使用する。

また骨格筋画像において得られた情報も、「疫学調査研究に関する倫理指針」に準じて行われ、本研究では個別のインフォームド・コンセントを得ることは計画していないが、インフォームド・コンセントを得ずに本研究を実施可能とする根拠は、得られた検査所見は過去に診断や経過観察等診療のために得られた診療録情報の一部であり、本研究のために新たに資料や情報収集をすることはなく、疫学研究の倫理指針（平成 19 年 8 月 16 日全部改正）の「第 3　インフォームド・コンセント等 1. 研究対象者からインフォームド・コンセントを受ける手続等」の「(2) 観察研究を行う場合、[2] 人体から採取された資料を用いない場合 ｲ. 既存資料のみ用いる観察研究の場合」に該当することにあたり、同倫理委員会でも承認が得られている。

C. 研究結果

遺伝性ミオパチーでの IBISS 画像登録にあたっての倫理申請を行い承認を得て、遺伝性ミオパチー画像登録フォームを作成した。今年度は遺伝学的未診断例の遺伝性ミオパチー47 例の骨格筋画像と、ミトコンドリアミオパチー12 例の脳画像の集積を行った。今後は、次世代遺伝子解析で得られた遺伝子情報をもとに、表現型評価ツールとして筋病理とあわせて骨格筋画像や脳画像所見との相関を解析する。

HMERF については、筋病理所見を再検討した結果、cytoplasmic body が筋線維内でネックレス状に配列する所見（necklace cytoplasmic body と命名）が感度 82%、特異度 99%と極めて優れた筋病理学的マーカーであることが明らかとなった。

D. 考察

遺伝性ミオパチーの骨格筋画像では、遺伝子型と表現型が明らかな例のなかで、疾患特異性の高い筋罹患分布の特徴が知られており、骨格筋画像における筋選択性として知られている。とくに単一遺伝子が原因である病型では明瞭な筋選択性を認める。本研究では、次世代遺伝子解析によって得られた遺伝子型の表現型を確認する目的で、筋病理や画像所見を組み合わせて表現型との相関の統合的理解を深めることを第一の目的にしている。しかし遺伝学的に未診断例のなかの画像を見ると類似の所見を認める群があり、画像集積が進み症例蓄積が増え、データ管理が整うと、同様の所見を呈する表現型の一群の分類から候補遺伝子を絞り込める可能性が出てくる。そのためには多くの画像登録が必要であり、今後は他施設からの筋病理診断例のレポジトリ―蓄積にあわせた画像登録が望まれる。画像登録を単施設から複数施設への登録システムへ発展し、筋レポジトリ―と関連付けられる画像集積を行うには、撮像条件等の統一な

ど検討課題は残るものの今後、重要であると考える。

HMERF については、過去の筋病理標本の再検討の結果、極めて優れた筋病理学的マーカーを同定することができた。筋病理所見は数多くあるものの、高度の疾患特異性を有する所見は数えるほどしかなく、今回の同定は極めて有意義であると考える。

E. 結論

遺伝性ミオパチーでの骨格筋画像、脳画像登録システムを構築した。今後、次世代遺伝子解析で得られた遺伝子情報をもとに、遺伝子型と表現型相関について解析を行い新たな疾患概念の確立を目指す。また、筋レポジトリーとの関連付けを想定した他施設からの登録システムも課題である。

HMERF については、necklace cytoplasmic body が高度の疾患特異性を有する新たな病理学的マーカーであることを見いだした。

F. 健康危険情報

なし

G. 研究発表

1. 論文発表

Uruha A, Hayashi YK, Oya Y, Mori-Yoshimura M, Kanai M, Murata M, Kawamura M, Ogata K, Matsumura T, Suzuki S, Takahashi Y, Kondo T, Kawarabayashi T, Ishii Y, Kokubun N, Yokoi S, Yasuda R, Kira JI, Mitsuhashi S, Noguchi S, Nonaka I, Nishino I. Necklace cytoplasmic bodies in hereditary myopathy with early respiratory failure. J Neurol Neurosurg Psychiatry. [Epub ahead of print]

Kubota K, Saito Y, Ohba C, Saitsu H, Fukuyama T, Ishiyama A, Saito T, Komaki H, Nakagawa E, Sugai K, Sasaki M, Matsumoto N. Brain magnetic resonance imaging findings and auditory brainstem response in a child with spastic paraplegia 2 due to a PLP1 splice site mutation. Brain Dev. 37(1):158-162, 2015

Okubo M, Fujita A, Saito Y, Komaki H, Ishiyama A, Takeshita E, Kojima E, Koichihara R, Saito T, Nakagawa E, Sugai K, Yamazaki H, Kusaka K, Tanaka H, Miyake N, Matsumoto N, Sasaki M. A family of distal arthrogryposis type 5 due to a novel PIEZO2 mutation. Am J Med Genet A. [Epub ahead of print]

2. 学会発表

石山昭彦、湯浅正太、本橋裕子、竹下絵里、齋藤貴志、小牧宏文、中川栄二、須貝研司、佐々木征行：脊髄性筋萎縮症における臨床病型と F 波の多様性. 第 44 回日本臨床神経生理学会学術大会、福岡、11/19-11/21.2014

湯浅正太、石山昭彦、齊藤 祐子、齋藤貴志、斎藤義朗、小牧宏文、中川栄二、須貝研司、佐々木征行：多趾症を伴い、進行性運動障害を呈した 11 歳男性例. 第 55 回日本神経病理学会総会学術研究会、東京、6/5-6/7.2014

Mana Higashihara, Masahiro Sonoo, Akihiko Ishiyama, Yu Nagashima, Haruo Uesugi, Madoka Yoshimura Mori, Miho Murata, Shigeo Murayama, Hirofumi Komaki: Quantitative analysis of surface EMG for pediatric neuromuscular disorders. American association of neuromuscular & electrodiagnostic medicine 61st Annual Meeting, Savannah, October 29-November 1, 2014

Mariko Okubo, Akihiko Ishiyama, Hirofumi Komaki, Eri Takeshita, Takashi Saito, Yoshiaki Saito, Eiji Nakagawa, Kenji. Sugai, Yukiko K. Hayashi, Ichizo Nishino, Masayuki Sasaki: Selectivity patterns on lower limb skeletal muscle imaging in patients with nemaline myopathy. 19th international congress of the world muscle society, Berlin, Germany, October7- October 11, 2014

Shinpei Baba a, Satoko Takanoha, Aihiko Ishiyama, Hirofumi Komaki, Eri Takeshita, Hirofumi Imaizumi, Yuji Abe, Mariko Kobayashi, Yusuke Kumazawa, Masayuki Sasaki:

Association between resting energy expenditure and body weight change in patients with Duchenne muscular dystrophy. 19th international congress of the world muscle society, Berlin, Germany, October7-October 11, 2014

H. 知的財産権の出願・登録状況

1. 特許取得
   なし
2. 実用新案登録
   なし
3. その他
   なし

厚生労働科学研究委託費
（難治性疾患等実用化研究事業（難治性疾患実用化研究事業））

委託業務成果報告（業務項目）

遺伝性ミオパチーの次世代型統合的診断拠点形成
５．国内外の連携

業務主任者　　西野　一三　　疾病研究第一部　部長

研究要旨

国立精神・神経医療研究センター（NCNP）は1978年以来過去35年以上に亘り、筋病理を中心とする筋疾患診断サービスを提供してきた。その結果、全国の医療機関から、本邦筋生検例の約8割の検体がNCNPに集積するに至っている。この強力な国内ネットワークを更に国際的に発展させるべく、アジア諸国からの医師（タイ2名、中国1名）を研修目的で受け入れた。これに加えて、3月からは韓国人医師2名が来日し研修を開始している。また、インドネシア、マレーシア、タイ、台湾で臨床病理カンファレンスを開催して当該地域の筋疾患診療水準向上に寄与するとともに、エジプトでは筋疾患患者の診察を行うなど診療支援を行った。また、上記各国からの診断支援要請にも応え、将来的な国際的ネットワーク形成に向けた基板形成に努めた。筋疾患診断は現実的には本邦の医療の一部として組み込まれているにもかかわらず、その費用は研究費で賄われているのが現状であり、「隠れた医療費」となっている。このような診断サービスが本邦の医療にとって必要なことは明白であり、早急な財政的対策が求められる。

A.研究目的

国立精神・神経医療研究センター（NCNP）は 1978 年以来過去 35 年以上に亘り、筋病理を中心とする筋疾患診断サービスを提供してきた。その結果、全国の医療機関から、本邦筋生検例の約 8 割の検体が NCNP に集積するに至っている。この強力な国内ネットワークを活用して、国内医療機関への診断サービス提供を継続することは元より、さらに国際的にも発展させていく必要がある。特に筋疾患は希少であり、専門家も少ないことから、特にアジア域においては日本が学問的に指導的立場を取らざるを得ない。言い換えれば、本邦はそのような責務を担っていると言える。

B.研究方法

国内に向けては、従来より提供している筋疾患診断サービスの提供を継続する。国外に向けては、アジアを中心とする諸外国からの研修医師・技師を受け入れ、筋疾患学の基礎とともに筋疾患研究の最先端を経験させることで、帰国後に当該地域で診断サービスを提供することができる様にするとともに、筋疾患分野で指導的な立場に立てるように支援する。また、専門家がおらず必要とされる地域に積極的に出向くアウトリーチ型の活動も加えることで、国際連携の基盤を形成する。

（倫理面への配慮）

ネットワーク形成は研究倫理指針とは関連しないものである。診断サービス提供については、「神経・筋疾患研究資源レポジトリーの構築と運用」（倫理委員会承認番号

XXXX-116（20-9-7））において承認を受けている。

C.研究結果

2014年には827件の筋病理診断を行った。諸外国の筋疾患診断拠点では殆どが年間検体数500件程度であり、国際的に最高水準にある筋疾患診断拠点であることが確認された。本邦における年間筋生検数は1000件を超える程度と予想されることから、約8割の検体が国立精神・神経医療研究センターに集まっていることが確認された。診断後の検体はレポジトリーとして蓄積されているが、凍結筋の総検体数は2014年末で15140検体となり、世界有数の筋レポジトリーとなっている。

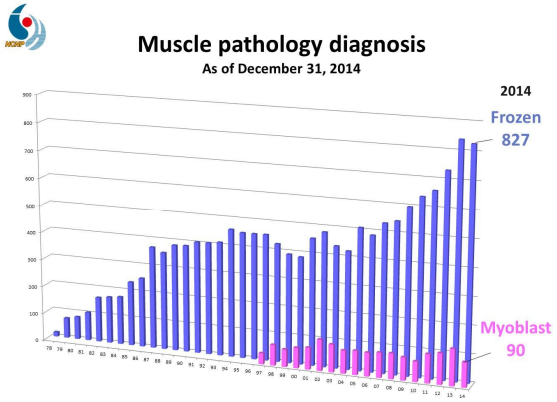

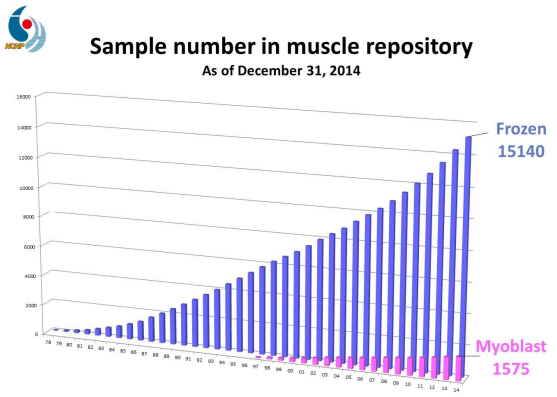

諸外国との連携については、7月より、タイ人医師2名を、9月より中国人医師1名を、更に3月からは韓国人医師2名を受け入れて、筋疾患診断に関する研修ならびに研究に携わっている。アウトリーチ活動としては、8月にこれまで筋疾患専門医のいなかったインドネシアを訪問し、ジャカルタのCipto Mangunkusumo 病院において、講義、患者診察、筋生検等を現地神経内科医とともに行った。これが契機となり、3月末には日本神経学会およびインドネシア神経学会の共催でワークショップが開催されることになっている。また、その他、タイ・バンコクのSiriraj病院およびBhumibol Adulyadej病院、マレーシア・クアラルンプールのマラヤ大学、台湾・高雄市の高雄医学大学において、臨床病理カンファレンスを開催するとともに、講義や患者診察などを行った。さらに、筋疾患専門医が殆どいないエジプトに出向き、カイロのEgyptair病院で、現地医師とともに筋疾患患者約150名を2度の訪問で診察し、更に筋生検を行った。加えて、これら地域からの診断支援要請に応えて、筋病理を初めとする筋疾患診断支援を行った。

D.考察

国内では筋生検検体の約8割の検体を集めて筋病理診断を中心とする筋疾患診断サービスを行った。診断件数においても診断内容においても世界最高水準のものであることが確認された。

この診断サービスに係る費用は研究の一環として研究費で賄われているが、実態は診療支援である。特に「難病の患者に対する医療等に関する法律」が施行され医療費助成の対象となる疾患が増えてその診断基準が整理されていく中で、多くの筋疾患の診断基準において、商業的サービスのない遺伝子診断や筋病理解析が必須条件となっている現実は、事実上、研究者が無償で提供しているサービスが医療制度の根幹を担っていることを明白に示している。加えて、このようなサービス提供は、研究者が夜間や休日などの時間を削って提供しているのが実情であるが、その専門的な知識と技術、労働に対する対価は全く支払われていないのが現実である。このような診断サービスが日本の医療制度を維持するのに必須であることは明白であり、このようないわば「日本の隠れた医療費」に対する早急な財政的対策が求められる。

諸外国との連携については、順調にネットワークを拡大しつつある。特にこれまで

専門家が全くいなかったインドネシアとの接点ができたことは今後の発展に大きく寄与すると期待される。しかし、依然としてアジア域では、筋疾患専門医が存在しない地域があり、今後そのような地域へのアプローチも積極的に行い、筋疾患学分野での先進国である本邦の責務を果たすことが求められる。

E.結論

国内に向けては筋病理診断を中心とする筋疾患診断サービスを提供した。筋病理診断については本邦筋生検総数の約 8 割が国立精神・神経医療研究センターに送られていると推測された。今後は、本サービス維持に必要な費用に対する財政的対策が早急に求められる。国外に向けては、アジア域から医師を受け入れて研修を行うとともに、アウトリーチ活動として現地に赴き、講義･カンファレンス･診療支援などを行い、ネットワーク拡大の基板を形成した。

F.健康危険情報

特になし

G.研究発表

１．論文発表

なし

２．学会発表

なし

H. 知的財産権の出願・登録状況（予定を含む）

１． 特許取得

なし

２． 実用新案登録

なし

３． その他

なし

様式第１９

学 会 等 発 表 実 績

委託業務題目「遺伝性ミオパチーの次世代型統合的診断拠点形成」
機関名　独立行政法人　国立精神・神経医療研究センター

１．学会等における口頭・ポスター発表

発表した成果（発表題目、口頭・ポスター発表の別）	発表者氏名	発表した場所（学会等名）	発表した時期	国内・外の別
Treatment of GNE myopathy（口頭）	Nishino I	バンコク(14th AOMC ANNUAL SCIENTIFIC MEETING 2015)	3.3, 2015	国外
Metabolic Myopathies（口頭）	Nishino I	Egypt(1st Egyptian International Neuromuscular Conference (ENMC))	1.22, 2015	国外
GNE MYOPATHY – WILL IT BE TREATABLE?（口頭）	Nishino I	Soul(Brain Conference 2014 Joint Conference of the KSBNS)	11.6, 2014	国外
Introduction to clinical features of GNE myopathy（口頭）	Nishino I	Berlin, Germany(GNE myopathy Consortium Workshop)	10.12, 2014	国外
Sialyllactose trial on GNE myopathy mouse model（口頭）	Noguchi S	Berlin, Germany(GNE myopathy Consortium Workshop)	10.12, 2014	国外
Therapeutic interventions in GNE-myopathy and possible targets in myofibrillar myopathies（口頭）	Nishino I	Niece,France(13th Interntional Congress on Neuromuscular Diseases)	7.7, 2014	国外
Therapy of DMRV/hIBM (GNE) myopathies（口頭）	Nishino I	Nice,France(13th Interntional Congress on Neuromuscular Diseases)	7.7, 2014	国外
Dominant mutations in ORAI1 cause tubular aggregate myopathy with hypocalcemia via constitutive activation of store-operated Ca2+ channels（口頭）	Endo Y	Berlin, Germany(19th International Congress of the World Muscle Society)	10.8, 2014	国外

発表した成果（発表題目、口頭・ポスター発表の別）	発表者氏名	発表した場所（学会等名）	発表した時期	国内・外の別
An 8-year-old girl with congenital cataracts and motor development delay（口頭）	Wen-Chen Liang	バンコク(14th AOMC ANNUAL SCIENTIFIC MEETING 2015)	3.4.2015	国外
A 35-year-old man with distal muscle weakness, contractures, and persistent hyperCKemia（口頭）	Wenhua Zhu	バンコク(14th AOMC ANNUAL SCIENTIFIC MEETING 2015)	3.4.2015	国外
A case report of TRAPPC11 disease: a wider clinical spectrum with multiple systemic involvement（口頭）	Wen-Chen Liang	上海(The 4th Oriental Congress of Neurology)	3.28.2015	国外
次世代シークエンサーを用いた筋疾患の遺伝子診断システムについて（口頭）	三橋里美	第 3 回骨格筋生物学研究会	3.7.2015	**国内**
Targeted exome sequencing identified a novel genetic disorder in mitochondrial fatty acid β-oxidation.(poster)	Sakai C, Matsushima Y, Sasaki M, Miyamoto Y, Goto Y	Tampere, Finlamd（Euromit 2014）	6.16, 2014	国外
Leigh-like syndrome associated with calcification of the bilateral basal ganglia caused by compound heterozygous mutations in mitochondrial poly(A) polymerase (poster)	Matsushima Y, Hatakeyama H, Takeshita E, Kitamura T, Kobayashi K, Yoshinaga H, Goto Y.	Tampere, Finlamd（Euromit 2014）	6.16, 2014	国外
Mitochondrial Disease.（口頭）	Goto Y	Singapore（Asian & Oceanian Epilepsy Congress 2014.）	8.7, 2014	国外
ECHS1 の変異は呼吸鎖の活性低下を伴う Leigh 脳症を引き起こす.（口頭）	**坂井千香，松島雄一，山口清次，佐々木征行，宮本雄策，後藤雄一**	**福岡（第 14 回日本ミトコンドリア学会年会）**	**12.5，2014**	**国内**

発表した成果（発表題目、口頭・ポスター発表の別）	発表者氏名	発表した場所（学会等名）	発表した時期	国内・外の別
MELAS 脳卒中発作における AQP4 の発現低下. （口頭）	金田大太, 新宅雅幸, 窪田-坂下美恵, 加藤忠史, 後藤雄一	福岡（第 14 回日本ミトコンドリア学会年会）	12.5, 2014	国内
脊髄性筋萎縮症における臨床病型と F 波の多様性（ポスター）	石山昭彦、湯浅正太、本橋裕子、竹下絵里、齋藤貴志、小牧宏文、中川栄二、須貝研司、佐々木征行	第 44 回日本臨床神経生理学会学術大会、博多、福岡	11/19-11/21.2014	国内
Quantitative analysis of surface EMG for pediatric neuromuscular disorders (poster)	Mana Higashihara, Masahiro Sonoo, Akihiko Ishiyama, Yu Nagashima, Haruo Uesugi, Madoka Yoshimura Mori, Miho Murata, Shigeo Murayama, Hirofumi Komaki	Savannah, USA(American association of neuromuscular & electrodiagnostic medicine 61st Annual Meeting)	October 29-November 1, 2014	国外
Selectivity patterns on lower limb skeletal muscle imaging in patients with nemaline myopathy (poster)	Mariko Okubo, Akihiko Ishiyama, Hirofumi Komaki, Eri Takeshita, Takashi Saito, Yoshiaki Saito, Eiji Nakagawa, Kenji. Sugai, Yukiko K. Hayashi, Ichizo Nishino, Masayuki Sasaki	Berlin, Germany(19th international congress of the world muscle society)	October7-October 11, 2014	国外

Association between resting energy expenditure and body weight change in patients with Duchenne muscular dystrophy (poster)	Shinpei Baba a, Satoko Takanoha, Aihiko Ishiyama, Hirofumi Komaki, Eri Takeshita, Hirofumi Imaizumi, Yuji Abe, Mariko Kobayashi, Yusuke Kumazawa, Masayuki Sasaki	Berlin, Germany(19th international congress of the world muscle society)	October7-October 11, 2014	**国外**

２．学会誌・雑誌等における論文掲載

掲載した論文（発表題目）	発表者氏名	発表した場所 （学会誌・雑誌等名）	発表した時期	国内・外の別
Necklace cytoplasmic bodies in hereditary myopathy with early respiratory failure	Uruha A, Hayashi YK, Oya Y, Mori-Yoshimura M, Kanai M, Murata M, Kawamura M, Ogata K, Matsumura T, Suzuki S, Takahashi Y, Kondo T, Kawarabayashi T, Ishii Y, Kokubun N, Yokoi S, Yasuda R, Kira JI, Mitsuhashi S, Noguchi S, Nonaka I, Nishino I	J Neurol Neurosurg Psychiatry	Epub Sep 2014	国外
Ullrich congenital muscular dystrophy: clinicopathological features, natural history and pathomechanism(s)	Yonekawa T, Nishino I	J Neurol Neurosurg Psychiatry	Mar, 2015	国外
Kyphoscoliosis and easy fatigability in a 14-year-old boy	Tanboon J, Hayashi YK, Nishino I	Neuropathology	Feb, 2015	国外
Dominant mutations in ORAI1 cause tubular aggregate myopathy with hypocalcemia via constitutive activation of store-operated Ca2+ channels	Endo Y, Noguchi S, Hara Y, Hayashi YK, Motomura K, Miyatake S, Murakami N, Tanaka S, Yamashita S, Kizu R, Bamba M, Goto YI, Matsumoto N, Nonaka I, Nishino I	Hum Mol Genet	Feb, 2015	国外

DAG1 mutations associated with asymptomatic hyperCKemia and hypoglycosylation of α -dystroglycan	Dong M, Noguchi S, Endo Y, Hayashi YK, Yoshida S, Nonaka I, Nishino I	Neurology	Jan, 2015	国外
Mutation profile of the GNE gene in Japanese patients with distal myopathy with rimmed vacuoles (GNE myopathy)	Cho A, Hayashi YK, Monma K, Oya Y, Noguchi S, Nonaka I, Nishino I	J Neurol Neurosurg Psychiatry	Aug, 2014	国外
Deep sequencing detects very-low-grade somatic mosaicism in the unaffected mother of siblings with nemaline myopathy	Miyatake S, Koshimizu E, Hayashi YK, Miya K, Shiina M, Nakashima M, Tsurusaki Y, Miyake N, Saitsu H, Ogata K, Nishino I, Matsumoto N	Neuromuscul Disord	Jul, 2014	国外

（注１）発表者氏名は、連名による発表の場合には、筆頭者を先頭にして全員を記載すること。
（注２）本様式は excel 形式にて作成し、甲が求める場合は別途電子データを納入すること。

JNNP Online First, published on September 24, 2014 as 10.1136/jnnp-2014-309009

RESEARCH PAPER

Necklace cytoplasmic bodies in hereditary myopathy with early respiratory failure

Akinori Uruha,[1,2,3] Yukiko K Hayashi,[1,2,4] Yasushi Oya,[5] Madoka Mori-Yoshimura,[5] Masahiro Kanai,[5] Miho Murata,[5] Mayumi Kawamura,[6] Katsuhisa Ogata,[7] Tsuyoshi Matsumura,[8] Shigeaki Suzuki,[9] Yukako Takahashi,[10,11] Takayuki Kondo,[11] Takeshi Kawarabayashi,[12] Yuko Ishii,[13] Norito Kokubun,[13] Satoshi Yokoi,[14] Rei Yasuda,[15] Jun-ichi Kira,[16] Satomi Mitsuhashi,[1,2] Satoru Noguchi,[1,2] Ikuya Nonaka,[2,7] Ichizo Nishino[1,2]

• Additional material is published online only. To view please visit the journal online (http://dx.doi.org/10.1136/jnnp-2014-309009).

For numbered affiliations see end of article.

Correspondence to Dr Ichizo Nishino, Department of Neuromuscular Research, National Institute of Neuroscience, NCNP, 4-1-1 Ogawa-Higashi, Kodaira, Tokyo 187-8502, Japan; nishino@ncnp.go.jp

Received 15 July 2014
Revised 2 September 2014
Accepted 7 September 2014

ABSTRACT

Background In hereditary myopathy with early respiratory failure (HMERF), cytoplasmic bodies (CBs) are often localised in subsarcolemmal regions, with necklace-like alignment (necklace CBs), in muscle fbres although their sensitivity and specifcity are unknown.

Objective To elucidate the diagnostic value of the necklace CBs in the pathological diagnosis of HMERF among myofbrillar myopathies (MFMs).

Methods We sequenced the exon 343 of TTN gene (based on ENST00000589042), which encodes the fbronectin-3 (FN3) 119 domain of the A-band and is a mutational hot spot for HMERF, in genomic DNA from 187 patients from 175 unrelated families who were pathologically diagnosed as MFM. We assessed the sensitivity and specifcity of the necklace CBs for HMERF by re-evaluating the muscle pathology of our patients with MFM.

Results TTN mutations were identifed in 17 patients from 14 families, whose phenotypes were consistent with HMERF. Among them, 14 patients had necklace CBs. In contrast, none of other patients with MFM had necklace CBs except for one patient with reducing body myopathy. The sensitivity and specifcity were 82% and 99%, respectively. Positive predictive value was 93% in the MFM cohort.

Conclusions The necklace CB is a useful diagnostic marker for HMERF. When muscle pathology shows necklace CBs, sequencing the FN3 119 domain of A-band in TTN should be considered.

INTRODUCTION

Hereditary myopathy with early respiratory failure (HMERF; OMIM 603689) is an adult-onset progressive myopathy characterised by early presentation of respiratory insufficiency usually during ambulant stage.[1–3] Pathologically, HMERF shares features of myofibrillar myopathy (MFM) besides the key finding of cytoplasmic bodies (CBs).[2 3] Its causative gene TTN, which encodes a gigantic protein, titin,[2 3] is known to be causative also for tibial muscular dystrophy, limb girdle muscular dystrophy type 2J, early-onset myopathy with fatal cardiomyopathy and dilated or hypertrophic cardiomyopathy.[4–10] Interestingly, all patients with HMERF so far identified carry a mutation in exon 343 (based on ENST00000589042) encoding the fibronectin-3 (FN3) 119 domain in the A-band region of titin.[2 3 11–17]

CBs are abnormal protein aggregates visualised usually as red-colored objects on modified Gomori trichrome stain and can be observed in a wide range of myopathic conditions. Nevertheless, they are often conspicuous in MFM and considered as one of the representative pathological findings in MFM.[18] In muscle specimens of HMERF, CBs are often located in the subsarcolemmal region,[12 13 14 19] with a necklace-like alignment, which here we call 'necklace CBs'. However, the utility of necklace CBs in the pathological diagnosis of HMERF is unknown. We therefore tested the sensitivity and specificity of necklace CBs in the diagnosis of HMERF.

METHODS

Patients

National Center of Neurology and Psychiatry (NCNP) functions as a referral centre for muscle pathology and muscle biopsy samples are sent from all over Japan. From 1991 to 2013, 187 patients from unrelated 175 Japanese families have been pathologically diagnosed as MFM at NCNP. In this cohort, mutations were found in known MFM-related genes: DES: 8 families (4.6%), VCP: 8 families (4.6%), FLNC: 6 families (3.4%), DNAJB6: 6 families (3.4%), ZASP: 5 families (2.9%), FHL1: 5 families (2.9%), MYOT: 4 families (2.3%) and BAG3: 1 family (0.6%). No mutation was identified in CRYAB. Clinical information at the time of muscle biopsy was available in all patients.

Genetic analysis

Genomic DNA was isolated from peripheral lymphocytes or frozen muscle as previously described.[20] Exon 343 of TTN was directly sequenced using ABI PRISM 3130 automated sequencer (PE Applied Biosystems). Sequence variants were assessed using publically available databases including 1000 Genomes Project database (http://www.1000genomes.org/), NHLBI Exome Sequencing Project 5400 database (http://evs.gs.washington.edu/EVS/), dbSNP135 (http://www.ncbi.nlm.nih.gov/SNP/) and Human Genetic Variation Browser (http://www.genome.med.kyoto-u.ac.jp/SnpDB/); and

To cite: Uruha A, Hayashi YK, Oya Y, et al. J Neurol Neurosurg Psychiatry Published Online First: [please include Day Month Year] doi:10.1136/jnnp-2014-309009

Table 1 Clinical features of the patients with TTN variants

Patient Number	Age (years)/ sex	Relationship	Mutation (protein level)	Family history (years)	Initial manifestations (years)	Age at gait disturbance/ ambulant	Foot drop (years)	Respiratory disturbance (years)	Artificial ventilation (years)	Cardiac involvement	Dysphagia (years)	Other features
A-1	49/M	Father	p.C31712R		Tripping (46)	46/yes	Yes (NA)	Yes (48)	Yes (49)	RHF	No	No
A-2	26/M	Son			Tripping (20)	22/yes	Yes (22)	Yes*	No	No	No	No
B-1	45/M	Older brother	p.C31712R	Father: Foot drop; sudden death (42) Oldest brother: gait disturbance (32); sudden death (40)	Foot drop (31)	31/yes	Yes (31)	Yes (44)	Yes (45)	No	No	No
B-2	37/M	Younger brother			Foot drop (27)	27/yes	Yes (27)	Yes (34)	Yes (37)	No	No	No
C	34/F		p.C31712R		Fatiguability (26)	29/yes	Yes (31)	Yes (26)	Yes (31)	–	No	Difficulty in opening mouth
D	38/M		p.C31712R		Difficulty in lifting thigh (20)	20/no (32)	Yes (20 s)	Yes (29)	Yes (29)	STC	Yes (28) Artificial nutrition (35)	
E	40/M		p.C31712R	Mother: sudden death (38) Older sister: proximal muscle weakness; respiratory failure (35)	Fatiguability; respiratory failure (31)	31/yes	Yes (NA)	Yes (31)	Yes (37)	RHF, PH	–	
F	52/M		p.C31712R		Foot drop (47)	47/yes	Yes (47)	Yes (50)	Yes (52)	–	Yes (47)	
G-1	58/M	Father	p.C31712R	Grandfather of G-2: died of respiratory failure (45)	Tripping (57)	57/yes	Yes (58)	Yes*	–	–	–	
G-2	29/M	Son			Tripping (20)	20/yes	Yes (20 s)	Yes (29)	Yes (29)	RHF	–	
H	68/F		p.C31712R	Son: distal myopathy; sudden death	Difficulty in standing on right toe (56)	56/yes	No	Yes (68)	Yes (68)	RHF, Af	–	Head drop; forward bent posture
I	43/M		p.C31712R		Fatiguability; weight loss (39)	42/yes	No	Yes (39)	Yes (42)	–	Yes (42)	Myalgia muscle cramp
J	42/F		p.C31712Y		Difficulty lifting thighs (36)	38/Yes	No	Yes*	–	–	–	
K	38/M		p.G31791D		Gait disturbance (28)	28/Yes	Yes (30)	Yes*	Yes (38)	–	Yes (36)	Head drop
L	44/F		p.G31791R		Fatiguability; loss of appetite (40)	41/yes	No	Yes (40)	Yes (44)	STC	–	
M	40/M		p.G31791V	Mother and younger sister: lower leg muscle weakness	Gait disturbance (24)	24/yes	Yes (27)	Yes*	–	2° AVB (type 1)	–	
N	46/M		p.R31783_V31785del		Foot drop; difficulty in opening a bottle (41)	41/yes	Yes (41)	Yes*	–	–	–	Myalgia

*Asymptomatic but found by laboratory tests.
2° AVB (type 1), Mobitz type 1 second degree atrioventricular block; Af, atrial fibrillation; F, female; M, male; NA, not available; PH, pulmonary hypertension; RHF, right-sided heart failure; STC, sinus tachycardia.

softwares to predict functional effects of mutations such as PolyPhen-2 (http://genetics.bwh.harvard.edu/pph2/) and Mutation Taster (http://www.mutationtaster.org/). The description of mutations of TTN conforms to Ensemble sequence ENST00000589042.

In this study a diagnosis of HMERF was made based on the presence of a mutation in exon 343 of TTN, although the possibility that mutations in other parts of the gene cause HMERF cannot be totally excluded.

Re-evaluation of muscle pathology

Muscle pathology was re-evaluated focusing on necklace CBs on modified Gomori trichrome. In the present study, we tentatively defined the presence of necklace CBs as at least two muscle fibres containing CBs exclusively localised in the subsarcolemmal area, covering more than 50% of circumference of each muscle fibre in three non-serial sections (each section was at least 250 µm apart and included at least 300 muscle fibres). CBs were evaluated in all MFM cases, and subsequently the sensitivity and specificity of necklace CBs for the diagnosis of HMERF were calculated. The positive predictive value (PPV) and 95% CIs were calculated with GraphPad Prism V.5.0 (Graph Pad Software, California, USA).

Electron microscopic observation

Biopsied muscle specimens were fixed in 2.5% glutaraldehyde and post-fixed with 2% osmium tetroxide. Semithin sections stained with toluidine blue were examined by light microscopy. Ultrastructural analysis was carried out on longitudinal and transverse ultrathin sections of muscles after staining with uranyl acetate and lead citrate, using Tecnai spirit transmission electron microscope (FEI, Hillsboro, Oregon, USA).

Re-evaluation of clinical data

The clinical information in our cohort together with previous reports[2 3 11–14] showed that respiratory insufficiency before being wheelchair users and selective involvement of semitendinosus muscles on muscle imaging were frequently observed, raising a possibility that these findings might be clues for the diagnosis of HMERF. We therefore reviewed clinical data of our patients with MFM in order to calculate sensitivities, specificities and PPVs of them at the time of muscle biopsy.

Ethics

All of the clinical information and materials used in this study were obtained for diagnostic purpose and permitted for scientific use with written informed consent. All experiments in this study were approved by the Ethical Committee of National Center of Neurology and Psychiatry.

RESULTS

Mutation analysis

Six different heterozygous mutations in exon 343 of TTN were identified in 17 patients from 14 families (table 1). Among them, two mutations, g.284701T>C (c.95134T>C; p.C31712R) and g.284939G>A (c.95372G>A; p.G31791D) were previously reported.[2 3 11 12 14] The former mutation was reported to be the most common in other populations.[11 12] This was also the case in our cohort and the mutation was shared by nine families, while all others were found in single families. The latter mutation was previously reported in a European-American family.[14] Among four novel mutations that we identified, three were missense: g.284702G>A (c.95135G>A; p.C31712Y), g.284938G>C (c.95371G>C; p.G31791R) and g.284939G>T (c.95372G>T; p.G31791V); and one was non-frameshift deletion: g.284913_284921delGAGGGCAGT (c.95346_95354del; p.R31783_V31785del). None of the variants was listed in the

Table 2 Laboratory findings at the time of muscle biopsy

Patient	CK IU/L (normal value)	Respiratory function (%VC, sitting position)	Selective involvement of muscles on imaging test		Muscle pathology		
			Semitendinosus muscle	Anterior compartment of lower legs	CB	Necklaces of CBs	RV
A-1 (49 years)	Normal (value: NA)	Abnormal (value: NA.)	NA	NA	+	+	+
A-2 (26 years)	65 (20–190)	77% (68%, lying)	+	+	+	+	+
B-1 (39 years)	425 (51–197)	84% → 67% (45 years)	+	+	+	+	−
B-2 (32 years)	659 (−200)	82% → 63% (37 years)	+	+	+	+	+
C (31 years)	488 (45–170)	32%	NA (+, 34 years)	NA (+, 34 years)	+	+	−
D (31 years)	375 (51–197)	VC: 0.97 L	+	−*	+	+	−
E (40 years)	234 (62–287)	ABG: $PaCO_2$ 86 mm Hg, PaO_2 56 mm Hg (RA)	+	+	+	+	−
F (50 years)	61 (NA)	41%	+	+	+	−	−
G-1 (58 years)	146 (50–170)	59%	+	+	+	−	−
G-2 (29 years)	142 (50–170)	31%	+	+	+	+	+
H (68 years)	140 (50–170)	ABG: PaCO2 60 mm Hg	+	+	+	+	−
I (43 years)	179 (62–287)	40%	+	+	+	−	−
J (42 years)	364 (45–163)	64%	+	+	+	+	+
K (34 years)	645 (51–197)	67% (55%, lying)	+	+	+	+	+
L (44 years)	139 (43–165)	36%	+	+	+	+	−
M (40 years)	190 (62–287)	61%	−*	+	+	+	+
N (46 years)	799 (62–287)	67%	+	+	+	+	+

In the column of Patient, the same alphabet indicates that they belong to the same family.
*Diffuse muscle involvement.
ABG, arterial blood gas; CB, cytoplasmic body; NA, not available; RV, rimmed vacuole; VC, vital capacity.

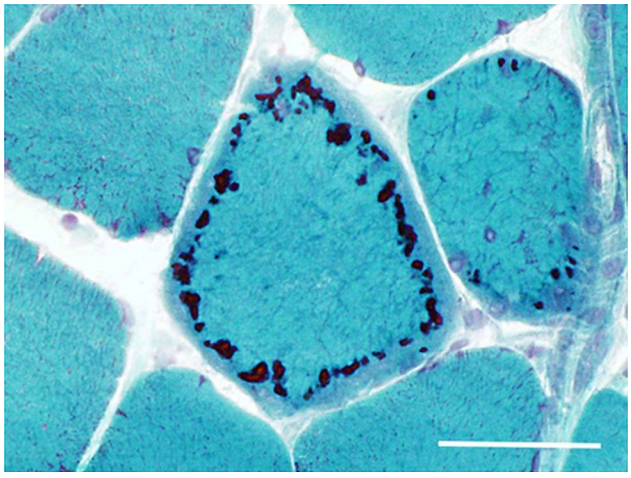

Figure 1 Necklace cytoplasmic bodies. Cytoplasmic bodies are located in line in subsarcolemmal region, often covering the total circumference of a muscle ibre. Modiied Gomori trichrome stain. Bar: 50 µm.

genomic variation databases. The mutated amino acids were highly conserved among species (UCSC Genome Browser). PolyPhen-2 predicted p.C31712Y, p.G31791R and p.G31791V mutations as probably damaging with scores 0.996, 1.000 and 1.000, respectively. Likewise, Mutation Taster predicted the p.C31712Y, p.G31791R, p.G31791V and p.V31782_A31784del mutations to be disease-causing with a probability of 1.000, 1.000, 1.000 and 0.998, respectively. No segregation analysis was possible in any family.

Clinical information of 17 participants with TTN mutations are summarised in tables 1 and 2 and online supplementary table. All patients show clinical signs consistent with HMERF previously reported.[1–3 11–14] The median age of onset was 31 years (range 20–57 years). Four patients developed dysphagia, and one of them required tube feeding.

Table 3 Cross tabulation of necklace cytoplasmic bodies and hereditary myopathy with early respiratory failure

	Patients with myofibrillar myopathies		
Necklace CBs	HMERF	Non-HMERF	Row total
+	14	1	15
% within column	82.4%	0.6%	
% within row	93.3%	6.7%	
–	3	169	172
% within column	17.6%	99.4%	
% within row	1.7%	98.3%	
Column total	17	170	187

CB, cytoplasmic body; HMERF, hereditary myopathy with early respiratory failure.

Sensitivity and speciicity of the necklace of CBs

Among 17 genetically-confirmed patients with HMERF, necklace CBs were found in 14 patients, comprising 0.1–0.8% of the muscle fibres (figure 1). In contrast, none of the 170 patients who had MFM other than HMERF had necklace CBs except for only one patient who had reducing body myopathy, which had been confirmed by the presence of reducing bodies in muscle fibres on menadione-linked α-glycerophosphate dehydrogenase (MAG) stain without substrate and a mutation in the second LIM domain of FHL1 (g.60438G>A; c.377G>A; p.C126Y, based on ENST00000543669; online supplementary figure S1). Based on these results, the sensitivity and specificity of the necklace CBs in HMERF were calculated as 82% (14/ 17, 95% CI 57% to 96%) and 99% (169/170, 95% CI 97% to 100%), respectively (table 3). Since the prevalence of HMERF in the MFM cohort was 9.1% (17/ 187), the PPV was calculated as 93% (95% CI 68% to 100%) based on Bayes' theorem.

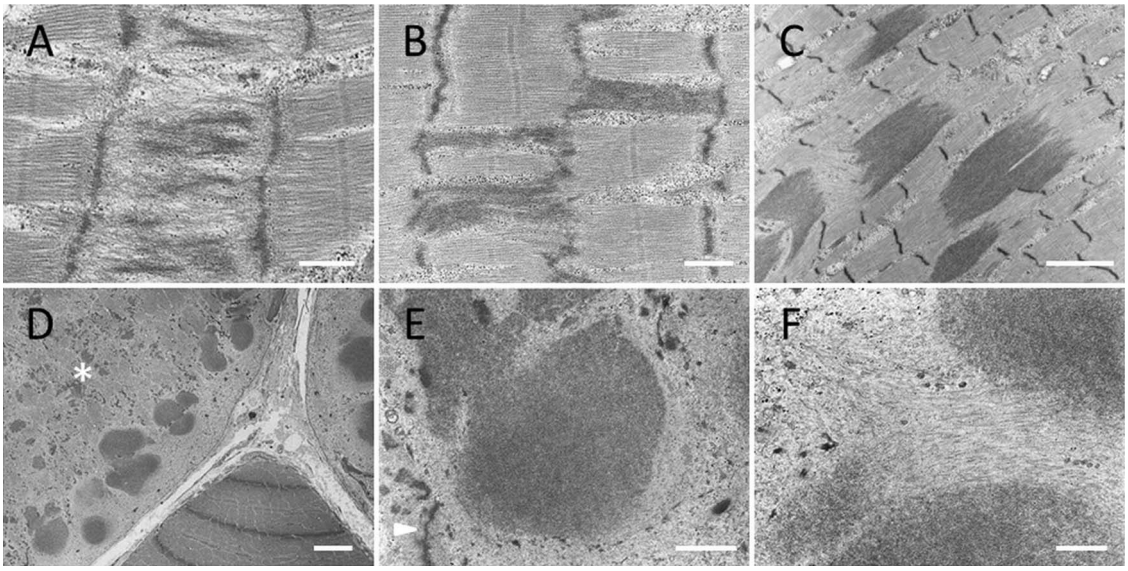

Figure 2 Electron microscope images. (A and B) Sarcomeric disarrangement limited to one sarcomere is observed. (C) Multiple electron-dense inclusions are present in association with Z lines. (D) A ibre containing necklace cytoplasmic bodies (CBs) shows marked myoibrillar disorganisation (asterisk), especially around the CBs. (E) CBs showing a necklace alignment with lower electron density as compared to that of Z line. ⅄: a remnant of Z line. (F) Thin ilamentous structure around the CBs. Lattice-like structure is not seen in the CBs. Bar: 0.5 µm (A, B and F), 1 µm (E), 2 µm (C), and 5 µm (D).

Muscle specimens of the three patients with HMERF had CBs, which are usually located in the subsarcolemmal regions, but did not show the definite necklace-like alignment pattern (online supplementary figure S2). Those three patients shared the same mutation, g.284701T>C (p.C31712R), albeit other nine patients harbouring the same mutation had definite necklace CBs.

Fibres with rimmed vacuoles were occasionally seen, but the sensitivity, specificity and PPV for HMERF were lower than those of the necklace CBs: 47% (8/ 17, 95% CI 23% to 72%), 61% (104/ 170, 95% CI 53% to 69%) and 11% (95% CI 20% to 48%), respectively.

Ultrastructural features

EM samples were available from four patients with HMERF. Sarcomeric disarrangement limited to one sarcomere was observed in all patients (figure 2A, B). In some areas, multiple electron-dense inclusions associated with Z line were surrounded by disorganised myofibrils (figure 2C). Fibres with necklace CBs were included only in one sample. These fibres showed marked myofibrillar disorganisation (figure 2D, asterisk), especially in the vicinity of the CBs (figure 2D, E). The CBs had a lower electron density as compared with that of the Z line and contained dense and mildly filamentous components, without lattice-like structure (figure 2E, F). Small number of CBs were partly surrounded by thin filaments (figure 2F).

Sensitivity and speciicity of respiratory dysfunction and muscle imaging data

Using the data at the time of muscle biopsy about the respiratory function of 102 participants in the MFM cohort, the sensitivity, specificity and PPV of the respiratory insufficiency before being wheelchair users (below 80% of vital capacity or over 45 mm Hg of $PaCO_2$) were calculated as 88% (14/16, 95% CI 62% to 99%), 94% (81/86, 95% CI 87% to 98%) and 74% (95% CI 49% to 91%), respectively (table 2 and 4). In five non-HMERF participants presenting respiratory insufficiency during the ambulant stage, one had a mutation in VCP, but no causative genes were identified in four participants as far as we have screened.

As for the muscle imaging at the time of muscle biopsy, the sensitivity of selective muscle involvement of semitendinosus muscles as shown in figure 3 was 93% (14/ 15; table 4). The specificity could not be calculated due to the limited number of images available in non-HMERF participants.

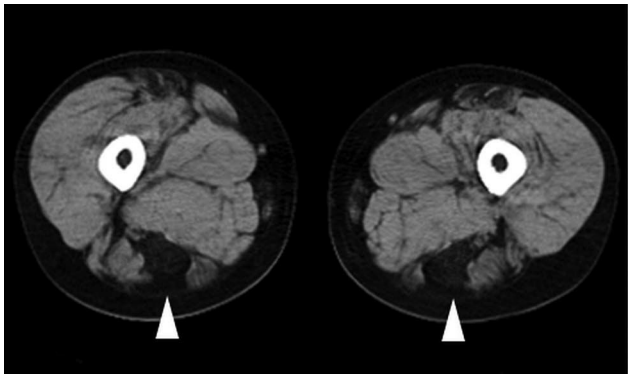

Figure 3 Muscle image. Representative image showing preferential involvement of semitendinosus muscles. CT images of skeletal muscles in proximal legs of the patient K. ⚠: semitendinosus muscles.

DISCUSSION

We have demonstrated that necklace CBs had high specificity for a diagnosis of HMERF (99%), with sensitivity 82% and PPV 93% in our MFM cohort. In this study, all 15 patients with necklace CBs had HMERF except for only one who had reducing body myopathy due to a mutation in FHL1, without mutation in exon 343 of TTN. Although we judged this case as having necklace CBs retrospectively, CBs in this case are smaller in size and scattered in the subsarcolemmal region in muscle fibres, giving an appearance different from typical necklace CBs in HMERF (online supplementary figure S1), suggesting that the specificity of necklace CBs could be substantially 100%. In addition, muscle pathology of this patient showed typical reducing bodies in scattered fibres on MAG stain without substrate, and thus differential diagnosis between reducing body myopathy and HMERF was not a problem in practise.

Interestingly, even in three patients with HMERF without typical necklace CBs, CBs are aligned in the subsarcolemmal regions in muscle fibres, albeit they do not encompass more than half of the myofibre circumference (online supplementary figure S2), suggesting that this unique subsarcolemmal alignment pattern is likely to be related to the dysfunction of titin due to exon 343 mutations although the detailed mechanism is still unknown.

On electron microscopy (EM), CBs in the patients differ slightly from typical CBs seen in other various diseases. While typical CBs consists of a core with electron density similar to Z line,[21] the CBs in HMERF show lower density. Furthermore, thin filaments, which compose a halo of typical CBs, are rarely seen around the CBs. Interestingly, the sarcomeric disarrangement appears to progress in order of figure 2A, C, suggesting a possibility that this sarcomeric disarrangement may ultimately produce the CBs.

Several groups reported that CBs in HMREF are reactive to antibodies to myofibrillar proteins including myotilin, αB-crystallin, actin (phalloidin), filamin C, dystrophin, and γ-sarcoglycan, but not for titin on immunohistochemical analysis.[11 12 14 19] Although similar findings were obtained in our observation (data not shown), the pathophysiological significance of CBs in HMERF has still not been elucidated.

We found four novel variants in exon 343 of TTN including three heterozygous missense mutations [g.284702G>A (p.C31712Y), g.284938G>C (p.G31791R) and g.284939G>T (p.G31791V)], and a heterozygous deletion variant [g.284913_284921del (p.R31783_V31785del)]. These variants were not described in any of the publically available databases. Mutated amino acids are highly conserved among species. Also

Table 4 Sensitivity, specificity, and positive predictive value of laboratory findings for HMERF

	Respiratory disturbance in the ambulant stage	Selective affected semitendinosus muscles on muscle imaging	Necklace CBs on muscle pathology
Sensitivity	88% (14/16)	93% (14/15)	82% (14/17)
Specificity	94% (81/86)	NA	99% (169/170)
PPV	74%	NA	93%

At the time of muscle biopsy.
Respiratory disturbance: <80% of %VC or >45 mm Hg of $PaCO_2$. PPVs were calculated by the HMERF prevalence of 9.1% in the MFM cohort.
CB, cytoplasmic body; HMERF, hereditary myopathy with early respiratory failure; MFM, myofibrillar myopathy; NA, not available, PPV, positive predictive value; VC, vital capacity.

Table 5 Mutations in the FN3 119 domain of A-band in TTN in HMERF

DNA change	Amino acid change	Origin	Family	Reference
g.284693C>G	p.P31709R (p.P30068R)	French		3
g.284701T>C	p.C31712R (p.C30071R)	Swedish, British, Finnish, Italian, Spanish, Argentinian (European ancestry), East Indian, Japanese	A, B, C, D, E, F, G, H, I	2, 3, 11, 12, 14
g.284702G>A	p.C31712Y (p.C30071Y)	Japanese	J	*
g.284752T>C	p.W31729R (p.W30088R)	British		12
g.284754G>C	p.W31729C (p.W30088C)	German		12
g.284753G>T	p.W31729L (p.W30088L)	Japanese		13
g.284762C>T	p.P31732L (p.P30091 L)	Italian, French, British, Portuguese, Swedish		11, 12, 15, 16, 17
g.284913_284921del	p.R31783_V31785del (p.R30142_V30144del)	Japanese	N	*
g.284925C>G	p.N31786K (p.N30145 K)	British		11
g.284939G>A	p.G31791D (p.G30150D)	American (European ancestry), Japanese	K	14
g.284938G>C	p.G31791R (p.G30150R)	Japanese	L	*
g.284939G>T	p.G31791V (p.G30150V)	Japanese	M	*

*Possible novel mutation. Titin reference: ENST00000589042 and ENST00000591111, a former transcript, inside the brackets.
HMERF, hereditary myopathy with early respiratory failure.

the variants were predicted to be pathogenic by the plural prediction software programs. Furthermore, in single-base substitutions, other types of substitutions of the same amino acids (p. C31712R and p.G31791D) have already been reported in other families with HMERF (table 5).[2 3 11 12 14] Thus, although segregation analysis was not possible, the variants are highly likely to be pathogenic.

Previous reports suggested that HMERF might not be extremely rare in Caucasian populations.[11 12] In UK, in patients with HMERF with p.C31712R (p.C30071R, based on ENST00000591111), mutation in exon 343 of TTN was identified in 5.5% of the MFM cohort.[11] Patients have also been identified in Asian populations including Japanese and Indian, suggesting that patients with HMERF are likely to be distributed worldwide.[13 14 22] Here, we confirmed the presence of patients with HMERF in Japan. Furthermore, among all the 175 MFM families in our Japanese cohort, 14 families (8%) had HMERF with mutations in the exon 343 of TTN, which renders TTN the most frequent causative gene for MFM in our cohort although there still remains a possibility that there may be an undisclosed major causative gene as causative mutations have not been identified in more than 60% of the MFM families.

Clinical features of participants with HMERF described in this study coincide with those in previous reports for most parts: affected individuals usually present with predominant distal leg muscle weakness followed by chronic respiratory failure.[1–3 11–14] Interestingly, dysphagia was seen in 4 of the 17, which was rarely described in the literature.[13] Dysphagia seems to be mostly mild, but was severe in one patient, who required tube feeding.

Skeletal muscle imaging has been reported to show preferential involvement of semitendinosus, obturator, sartorius, gracilis, iliopsoas muscles and anterior compartment of lower legs, suggesting such imaging findings are useful for the diagnosis of HMERF.[3 11 12 19] Particularly, selective involvement of semitendinosus muscles is commonly observed. Our study showed a sensitivity of 93%, which is compatible with 95–100% reported by previous studies.[3 12] Unfortunately, skeletal muscle imaging was not available in many of our patients with MFM other than HMERF, and thus it was impossible to calculate the specificity and PPV of the selective involvement of semitendinosus muscles. However, it may not be so specific since such finding was observed also in other MFMs caused by mutations in DES, CRYAB and MYOT.[23 24]

In conclusion, the necklace CB is a useful pathological marker in the diagnosis of HMERF. When muscle pathology shows necklace CBs, sequencing the FN3 119 domain of the A-band in TTN should be considered.

Author afiliations
[1]Department of Clinical Development, Translational Medical Center, National Center of Neurology and Psychiatry (NCNP), Tokyo, Japan
[2]Department of Neuromuscular Research, National Institute of Neuroscience, NCNP, Tokyo, Japan
[3]Department of Education, Interdisciplinary Graduate School of Medicine and Engineering, University of Yamanashi, Yamanashi, Japan
[4]Department of Neurophysiology, Tokyo Medical University, Tokyo, Japan
[5]Department of Neurology, National Center Hospital, NCNP, Tokyo, Japan
[6]Department of Neurology, Japanese Red Cross Society, Wakayama Medical Center, Wakayama, Japan
[7]Institute of Clinical Research/Department of Neurology, National Hospital Organization Higashisaitama Hospital, Saitama, Japan
[8]Department of Neurology, National Hospital Organization Toneyama National Hospital, Osaka, Japan
[9]Department of Neurology, Keio University School of Medicine, Tokyo, Japan
[10]Department of Neurology, Osaka Red Cross Hospital, Osaka, Japan
[11]Department of Neurology, Graduate School of Medicine, Kyoto University, Kyoto, Japan
[12]Department of Neurology, Institute of Brain Science, Hirosaki University Graduate School of Medicine, Aomori, Japan
[13]Department of Neurology, Dokkyo Medical University, Tochigi, Japan
[14]Department of Neurology, Nagoya University Graduate School of Medicine, Nagoya, Japan
[15]Department of Neurology, National Hospital Organization Maizuru Medical Center, Kyoto, Japan
[16]Department of Neurology, Neurological Institute, Graduate School of Medical Sciences, Kyushu University, Fukuoka, Japan

Acknowledgements The authors thank Ms Kaoru Tatezawa, Ms Yoriko Kojima, Ms Kazu Iwasawa, Mr Takao Uchikai, and Ms Kanako Goto in NCNP for their technical assistance.

Contributors AU was involved in the conceptualisation and design of the study, data analysis and interpretation, literature review and drafting the manuscript. YKH was involved in the conceptualisation and design of the study, data analysis and interpretation, and manuscript revision for intellectual content. YO, MM-Y, MK, MM, MK, KO, TM, SS, YT, TK, TK, YI, NK, SY, RY, and JK were involved in the collection of clinical data. SM and SN were involved in the data interpretation (molecular data) and manuscript revision for intellectual content. IkN was involved in the supervision of pathological analysis and interpretation and manuscript revision for intellectual content. IcN was involved in the supervision of all aspects, including study design, data analysis and interpretation, and manuscript preparation.

Funding This study was supported partly by JSPS KAKENHI Grant Number of 24659437; partly by Research on Rare and Intractable Diseases, Comprehensive Research on Disability Health and Welfare and Applying Health Technology from the Ministry of Health, Labour and Welfare of Japan; and partly by Intramural Research Grant 23-5 and 26-8 for Neurological and Psychiatric Disorders of NCNP.

Competing interests None.

Ethics approval Ethical Committee of National Center of Neurology and Psychiatry.

Provenance and peer review Not commissioned; externally peer reviewed.

REFERENCES

1 Edström L, Thornell LE, Albo J, et al. Myopathy with respiratory failure and typical myofbrillar lesions. J Neurol Sci 1990;96:211–28.
2 Ohlsson M, Hedberg C, Brådvik B, et al. Hereditary myopathy with early respiratory failure associated with a mutation in A-band titin. Brain 2012;135:1682–94.
3 Pfeffer G, Elliott HR, Griffn H, et al. Titin mutation segregates with hereditary myopathy with early respiratory failure. Brain 2012;135:1695–713.
4 Haravuori H, Mäkelä-Bengs P, Udd B, et al. Assignment of the tibial muscular dystrophy locus to chromosome 2q31. Am J Hum Genet 1998;62:620–6.
5 Hackman P, Vihola A, Haravuori H, et al. Tibial muscular dystrophy is a titinopathy caused by mutations in TTN, the gene encoding the giant skeletal-muscle protein titin. Am J Hum Genet 2002;71:492–500.
6 Carmignac V, Salih MA, Quijano-Roy S, et al. C-terminal titin deletions cause a novel early-onset myopathy with fatal cardiomyopathy. Ann Neurol 2007;61:340–51.
7 Gerull B, Gramlich M, Atherton J, et al. Mutations of TTN, encoding the giant muscle flament titin, cause familial dilated cardiomyopathy. Nat Genet 2002;30:201–4.
8 Itoh-Satoh M, Hayashi T, Nishi H, et al. Titin mutations as the molecular basis for dilated cardiomyopathy. Biochem Biophys Res Commun 2002;291:385–93.
9 Herman DS, Lam L, Taylor MRG, et al. Truncations of titin causing dilated cardiomyopathy. New Eng J Med 2012;366:619–28.
10 Satoh M, Takahashi M, Sakamoto T, et al. Structural analysis of the titin gene in hypertrophic cardiomyopathy: identifcation of a novel disease gene. Biochem Biophys Res Commun 1999;262:411–17.
11 Pfeffer G, Barresi R, Wilson IJ, et al. Titin founder mutation is a common cause of myofbrillar myopathy with early respiratory failure. J Neurol Neurosurg Psychiatry 2014;85:331–8.
12 Palmio J, Evilä A, Chapon F, et al. Hereditary myopathy with early respiratory failure: occurrence in various populations. J Neurol Neurosurg Psychiatry 2014;85:345–53.
13 Izumi R, Niihori T, Aoki Y, et al. Exome sequencing identifes a novel TTN mutation in a family with hereditary myopathy with early respiratory failure. J Hum Genet 2013;58:259–66.
14 Toro C, Olivé M, Dalakas MC, et al. Exome sequencing identifes titin mutations causing hereditary myopathy with early respiratory failure (HMERF) in families of diverse ethnic origins. BMC Neurol 2013;13:29.
15 Vasli N, Böhm J, Le Gras S, et al. Next generation sequencing for molecular diagnosis of neuromuscular diseases. Acta Neuropathol 2012;124:273–83.
16 Hedberg C, Melberg A, Dahlbom K, et al. Hereditary myopathy with early respiratory failure is caused by mutations in the titin FN3 119 domain. Brain 2014;137(Pt 4):e270.
17 Lange S, Edström L, Udd B, et al. Reply: Hereditary myopathy with early respiratory failure is caused by mutations in the titin FN3 119 domain. Brain 2014;137(Pt 6): e279.
18 Schröder R, Schoser B. Myofbrillar Myopathies: A clinical and myopathological Guide. Brain Pathol 2009;19:483–92.
19 Tasca G, Mirabella M, Broccolini A, et al. An Italian case of hereditary myopathy with early respiratory failure (HMERF) not associated with the titin kinase domain R279W mutation. Neuromuscul Disord 2010;20:730–4.
20 Cho A, Hayashi YK, Momma K, et al. Mutation Profle of the GNE gene in Japanese patients with distal myopathy with rimmed vacuoles (GNE myopathy). J Neurol Neurosurg Psychiatry. 2014;85:914–17.
21 Macdonald RD, Engel AG. The cytoplasmic body: another structural anomaly of the Z disk. Acta Neuropathol 1969;14:99–107.
22 Uruha A, Nishino I. Think worldwide: hereditary myopathy with early respiratory failure (HMERF) may not be rare. J Neurol Neurosurg Psychiatry 2014;85:248.
23 Fisher D, Kley RA, Stratch K, et al. Distinct muscle imaging patterns in myofbrillar myopathies. Neurology 2008;71:758–65.
24 Wattjes MP, Kley RA, Fischer D. Neuromuscular imaging in inherited muscle diseases. Eur Radiol 2010;20:2447–60.

Necklace cytoplasmic bodies in hereditary myopathy with early respiratory failure

Akinori Uruha, Yukiko K Hayashi, Yasushi Oya, et al.

J Neurol Neurosurg Psychiatry published online September 24, 2014
doi: 10.1136/jnnp-2014-309009

Notes

REVIEW

Ullrich congenital muscular dystrophy: clinicopathological features, natural history and pathomechanism(s)

Takahiro Yonekawa,[1,2] Ichizo Nishino[1,3]

[1]Department of Neuromuscular Research, National Institute of Neuroscience, National Center of Neurology and Psychiatry (NCNP), Kodaira, Tokyo, Japan
[2]Department of Child Neurology, National Center Hospital, NCNP, Kodaira, Tokyo, Japan
[3]Department of Clinical Development, Translational Medical Center, NCNP

Correspondence to
Dr Ichizo Nishino, Department of Neuromuscular Research, National Institute of Neuroscience, NCNP, 4-1-1, Ogawa-Higashicho, Kodaira, Tokyo 187 8502, Japan; nishino@ncnp.go.jp

Received 15 April 2014
Revised 12 May 2014
Accepted 25 May 2014
Published Online First 17 June 2014

ABSTRACT

Collagen VI is widely distributed throughout extracellular matrices (ECMs) in various tissues. In skeletal muscle, collagen VI is particularly concentrated in and adjacent to basement membranes of myofibers. Ullrich congenital muscular dystrophy (UCMD) is caused by mutations in either COL6A1, COL6A2 or COL6A3 gene, thereby leading to collagen VI deficiency in the ECM. It is known to occur through either recessive or dominant genetic mechanism, the latter most typically by de novo mutations. UCMD is well defined by the clinicopathological hallmarks including distal hyperlaxity, proximal joint contractures, protruding calcanei, scoliosis and respiratory insufficiency. Recent reports have depicted the robust natural history of UCMD; that is, loss of ambulation by early teenage years, rapid decline in respiratory function by 10 years of age and early-onset, rapidly progressive scoliosis. Muscle pathology is characterised by prominent interstitial fibrosis disproportionate to the relative paucity of necrotic and regenerating fibres. To date, treatment for patients is supportive for symptoms such as joint contractures, respiratory failure and scoliosis. There have been clinical trials based on the theory of mitochondrion-mediated myofiber apoptosis or impaired autophagy. Furthermore, the fact that collagen VI producing cells in skeletal muscle are interstitial mesenchymal cells can support proof of concept for stem cell-based therapy.

INTRODUCTION

Collagen VI is an important component of the ECM of skeletal muscle and is involved in maintaining tissue integrity by providing a structural link between different ECM molecules and in promoting adhesion,[1 2] proliferation,[3] migration[4] and survival[5] of various cell types. Collagen VI-related myopathies are the hereditary myopathies caused by mutations in either COL6A1, COL6A2 or COL6A3 gene, each encoding a subunit of collagen VI. Patients have the clinicopathological features of a muscle disorder as well as of a connective tissue disorder, although the link between this defect of ECM and phenotype remains to be fully elucidated.

Recent advance in molecular biology has evolved the aetiological definition of collagen VI-related myopathies; these myopathies are known to encompass a clinical continuum with Ullrich congenital muscular dystrophy (UCMD) and Bethlem myopathy (BM) at each end of the spectrum, originally described separately.[6–8] Intermediate phenotypes, named as mild UCMD or severe BM, have been known but less well defined as there is currently no clear-cut boundary between two major phenotypes. In addition, it should be noted that genotype–phenotype correlation is very difficult to establish; for example, both extremes of the clinical spectrum are seen in patients with p.Gly284Arg mutation in the COL6A1 gene, the most commonly observed mutation, while half had an intermediate phenotype.[9] In this context, several researchers have proposed the clinical stratification of patients with collagen VI-related myopathies (figure 1A).[10–12]

The hallmarks of UCMD include marked distal joint hyperlaxity associated with proximal joint contractures, a rigid spine and normal intelligence. Furthermore, children presenting UCMD phenotype have been referred to as having 'early severe' or 'moderately progressive' course of early-onset collagen VI-related myopathies according to maximal motor ability and disease progression.[10–12] Thus, UCMD is relatively well defined as compared with BM or intermediate phenotypes.

CLINICAL PICTURE

In 1930, Otto Ullrich described two boys with an unusual congenital myopathy characterised by muscle weakness and wasting, marked distal joint looseness and contracture of the proximal joints since birth or early infancy and termed this new condition "Kongenitale, atonisch-skelerotische Muskeldystrophie, ein weiterer Typus der heredodegenerativen Erkrankungen des neuromuskulären Systems".[6 7] Subsequent publications confirmed a likely autosomal-recessive inheritance and a recognisable pattern of disease.[13] The diagnostic clinical and molecular criteria for UCMD have been proposed by the European Neuromuscular Centre.[14]

Epidemiology

UCMD is the second most common congenital muscular dystrophy (CMD) after CMD with laminin α2 deficiency (also known merosin-deficient CMD; or MDC1A) in Europe,[15] after Fukuyama CMD in Japan[16] and after α-dystroglycanopathies in Australia.[17] The prevalence of UCMD is reported to be 1.3 per million in Northern England.[18]

Perinatal features and development

Prenatal movements might be reduced in fetuses with UCMD.[19] Some patients have congenital hip dislocation, torticollis and transient kyphotic deformity.[19 20] Multiple joint contractures may be evident at birth, affecting the elbows, knees, spine

To cite: Yonekawa T, Nishino I. J Neurol Neurosurg Psychiatry 2015;86:280–287.

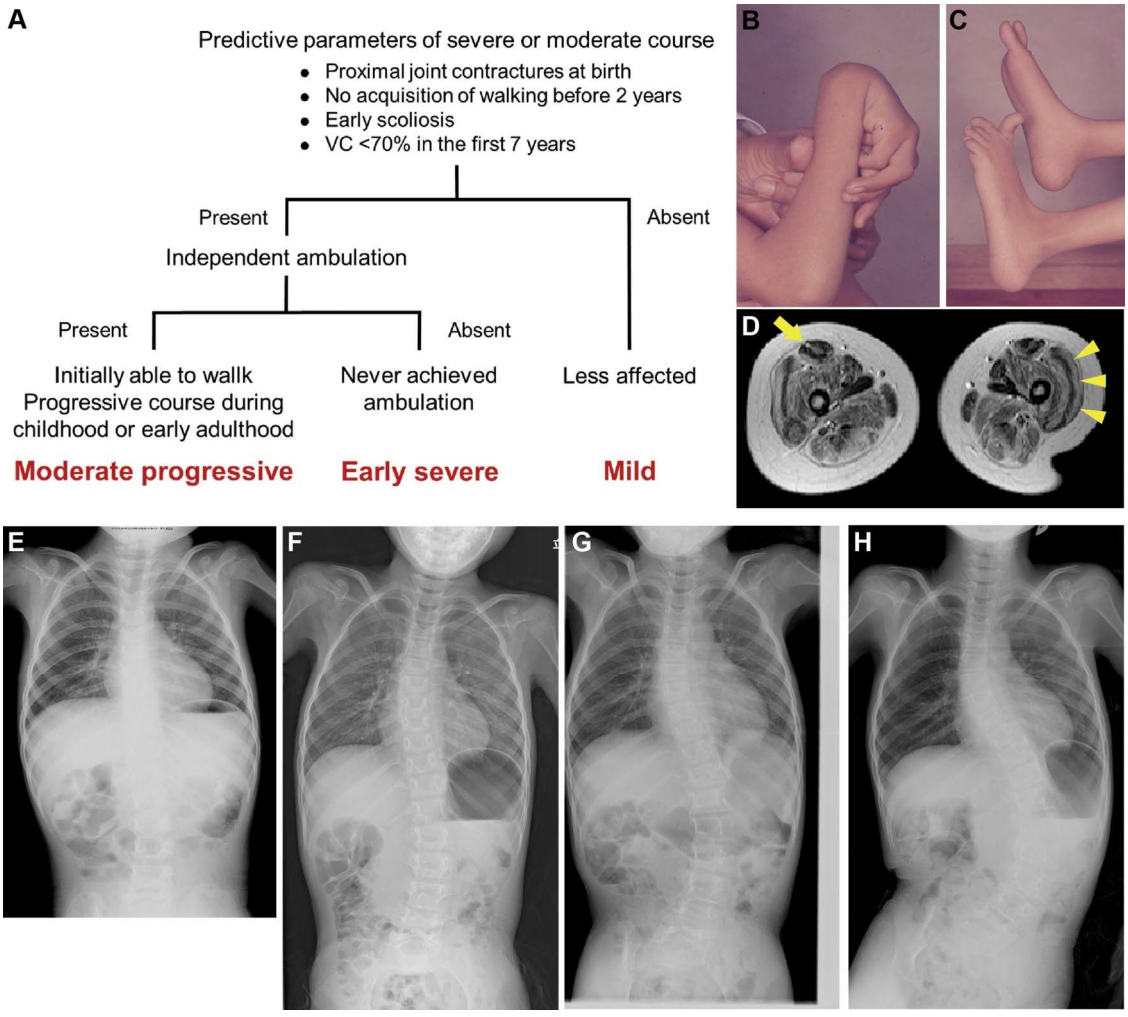

Figure 1 Phenotypic stratification of early-onset collagen VI-related myopathies; modification from Quijano-Roy et al[10] and Briñas et al[11] (A). Typical distal hyperlaxity and protruding calcanei in a patient with Ullrich congenital muscular dystrophy (UCMD) (B,C). Diagnostic muscle MRI findings of the thigh (D): fatty regeneration along the fascia in the centre of the rectus femoris (arrow) and in the periphery of the vastus lateralis with relative sparing of its central part (arrowheads). Early-onset and rapidly progressive scoliosis in UCMD (E–H). E, 3.7; F, 6.1; G, 6.9; H, 7.9 years of age at assessment. (Images courtesy of Drs Ikuya Nonaka and Akihiko Ishiyama).

(kyphoscoliosis) and ankles. Arthrogryposis multiplex are seen in 20.0% of patients.[19] Some transient feeding difficulties or poor sucking might occur in the neonatal period.[19 20]

The most common presentations are delayed motor milestone and proximal muscle weakness. Patients with UCMD usually become able to sit independently with or without delay.[19] The majority of patients with typical UCMD achieve the ability to walk by 2 years of age. The age at independent ambulation is reported to be 1.7±0.8 and 1.7±0.5 years in English and Japanese natural history studies, respectively.[19 20] This group is referred to as having 'moderate progressive' disease in the phenotypic stratification of early-onset collagen VI-related myopathy (figure 1A).[10 11] In the remaining patients, ambulation is never achieved. Those with the most severe presentation, accounting for 19.4–25.7% of UCMD patients,[11 19] are referred to as having 'early-severe' disease (figure 1A). However, even these severely affected children can usually learn to roll, crawl and maintain a sitting position. Patients who never walk due to severe contractures that prevent an upright posture may walk on their knees for a certain period of time. Achievement of speaking phrases is not delayed, ranging from 12 to 25 months of age.[19]

Clinical manifestations

Patients show generalised muscle weakness predominantly in trunk and proximal limbs. Neck flexors are weak. Facial weakness is reported respectively in 24.1% and 30.8% of patients in two different studies.[19 20] The most striking feature is hyperlaxity of the distal joints (figure 1B), although it can be absent in severely affected individuals. Spinal rigidity, scoliosis and various proximal joint contractures develop with progression of the disease. Typically, initially flexible distal joints, such as fingers, wrists and ankles, eventually become contractured with time. Interestingly, calcanei are often protruded posteriorly (figure 1C). Distal joint hyperlaxity, proximal joint contractures, scoliosis and protruding calcaneous are observed in >50% patients in a Japanese cohort.[19] Many patients have a characteristic facial appearance with round-shaped face with slight drooping of the lower lid and prominent ears.[15] Intelligence is normal. Other features include follicular hyperkeratosis over the extensor surfaces of upper and lower limbs, a softer consistency of the skin in the palms and soles and the tendency to keloid formation.[15] Respiratory insufficiency is not common at birth, although it becomes a critical complication of the disease as the condition progresses. Cardiac involvement is not documented to date.[21 22]

Serum creatine kinase (CK) activity in patients with UCMD is usually within normal range or only mildly elevated,[19–21] which is unusual in other (congenital) muscular dystrophies. Electromyography shows action potentials of low amplitude and short duration.[13] Muscle MRI shows a characteristic pattern on transverse T1-weighted images—diffuse involvement of the thigh muscles with relative sparing of the medial muscles (sartorius, gracilis and adductor longus).[23] Rectus femoris is variably involved with a typical central area of high signal, called 'central shadow'.[23] In vastus lateralis, the peripheral part is mainly involved and signal intensity is markedly increased while the central part is relatively spared (figure 1D).[23]

Muscle pathology and collagen VI immunohistochemistry

Variable degrees of histological changes can be observed in muscle biopsies from patients with UCMD. The spectrum includes fibre size variation affecting both fast and slow fibres, type 1 fibre predominance, increased endomysial connective tissue or adipose tissue, increased number of internal nuclei and mild necrotic and regenerating process along with indirect evidence of regenerating fibres such as the presence of fibres containing fetal myosin.[21 24] One report described that, early in the disease, UCMD presents as a non-dystrophic myopathy with predominant fibre atrophy, showing a bimodal size distribution of type 1 fibres or a diagnostic pattern of congenital fibre-type disproportion.[25] Unlike other muscular dystrophies, interstitial fibrosis seems disproportionately prominent considering the relative paucity of necrotic and regenerating fibres in UCMD.

Collagen VI is widely distributed throughout ECMs in various tissues. In skeletal muscle, collagen VI is found in the epimysial, perimysial and endomysial interstitium, but it is concentrated in particular in and adjacent to basement membranes of myofibers, blood vessels and intramuscular nerves. Muscle biopsies from UCMD patients can show anything from mild reduction of endomysial or basal lamina collagen VI staining to complete deficiency (CD) of collagen VI in the ECM. We previously showed that, in the majority of patients with UCMD, collagen VI is present in the interstitium but is absent from the sarcolemma by using double immunostaining for collagen IV and VI (figure 2), and named it 'sarcolemma specific collagen VI deficiency (SSCD)'.[26] Electron microscopic findings support a lack of connection between collagen VI microfibrils in the interstitium and the basal lamina, leading to SSCD.[26] Space is observed between muscle fibres and connective tissue that are normally closely attached. Basal lamina appear intact even in degenerating muscle fibres with disorganised myofibrils. These findings suggest a loose connection between the basal lamina and other ECM collagens in UCMD.[27] Collagen VI is deficient also in capillaries in muscle.[13] The absence or alteration of collagen VI can be demonstrated by immunocytochemistry of cultured skin fibroblasts, although this analysis is available only in limited laboratories. In skin, collagen VI expression is decreased in the papillary dermis and skin hair follicles, but not in vessels, peripheral nerves, smooth muscle and sweat glands.[13] One report described that collagen VI levels were greatly decreased in peripheral blood macrophages from three patients with UCMD.[28]

Natural history of disease

Muscle weakness is slowly progressive. Most affected children become able to walk independently but eventually lose ambulation often by early teenage years. Loss of ambulation is reported to occur at 10.7±4.8, 10.1±4.4 and 8.8±2.9 years of age in English, French and Japanese group of patients with UCMD, respectively.[11 19 20] However, this can be widely variable: some patients never walk while others can still walk even beyond late teens. After loss of ambulation, progression of muscle weakness becomes less prominent. In contrast, the contractures can still be progressive, particularly in the ankles, knees, hips and elbows, aggravating physical disability. These clinical features may well be in line with strikingly progressive interstitial fibrosis on muscle pathology.

Respiratory insufficiency usually occurs after the loss of ambulation. It is noteworthy, however, some patients have impending respiratory dysfunction while they are still ambulant. Progressive decline in the predicted forced vital capacity (FVC) or vital capacity (VC) is observed from the preschool age to the early teens.[19 20] Of note, restrictive respiratory dysfunction develops rapidly in the first decade of life; indeed, %predicted FVC declines by 6.6±1.9%/year from 6 to 10 years of age compared to by 0.4±3.0%/year from 11 to 15 years of age.[20] Similarly, VC declines exponentially with a sharp decrease by 10 years of age.[19] This may well be associated with proximal joint and vertebral contractures together with weakness of the diaphragm. The introduction of non-invasive ventilation (NIV) is usually sufficient to treat this situation effectively for many years. The percentage of patients with NIV increases with age; half require NIV by age 11–12 years.[12 19] Natural history study from UK reported that age at initiation of NIV was 14.3 ±4.7 years, with a mean FVC of 20%.[20] The other two studies have recently reported similar findings: an estimated predicted VC of 36% at the time of initiation of NIV at 11.2±3.6 years in a Japanese cohort[19] and an average FVC of 34% just before NIV initiation at 11.3±4.0 years in a large international cohort,[12] demonstrating a remarkable consistency of the pulmonary function declining in patients with UCMD among different cohorts, regardless of different approaches to data acquisition.

Scoliosis, which may require surgical correction, is a common complication.[15 20] Substantial scoliosis appears as early as preschool years and its onset precedes loss of ambulation.[19 20] Development of scoliosis in Duchenne muscular dystrophy (DMD) is strongly related to the loss of walking ability—scoliosis is not typically evident in ambulatory patients and develops after they become wheelchair dependent. In contrast, in UCMD, scoliosis develops even when patients are still ambulant and is progressive from early stage. In our cohort, a maximum progression rate of Cobb angle was 16.2±10.0°/year.[19] Importantly, scoliosis progresses rapidly within years, once it starts (figure 1E–H). The early-onset and rapidly progressive scoliosis in UCMD may well accelerate physical disability, such as difficulty sitting, standing and walking, and cause pain. More importantly, scoliosis can aggravate respiratory function by reducing the rib cage compliance in combination with other proximal joint contractures.

Differential diagnosis

Differential diagnosis includes wide range of neuromuscular disorders in infants and children, such as other forms of muscular dystrophy, congenital myopathies, spinal muscular atrophy (SMA), especially type 2 and 3, and other diseases of connective tissue such as Ehlers–Danlos syndrome (EDS). However, combination of normal or minimally elevated CK levels, lack of cardiac manifestation and specific pattern of thigh muscle involvement is often suggestive of UCMD. Brain MRI is usually normal unlike other CMD forms such as MDC1A, Walker–Warburg syndrome, muscle-eye-brain disease and Fukuyama CMD, which may show structural abnormalities or white matter

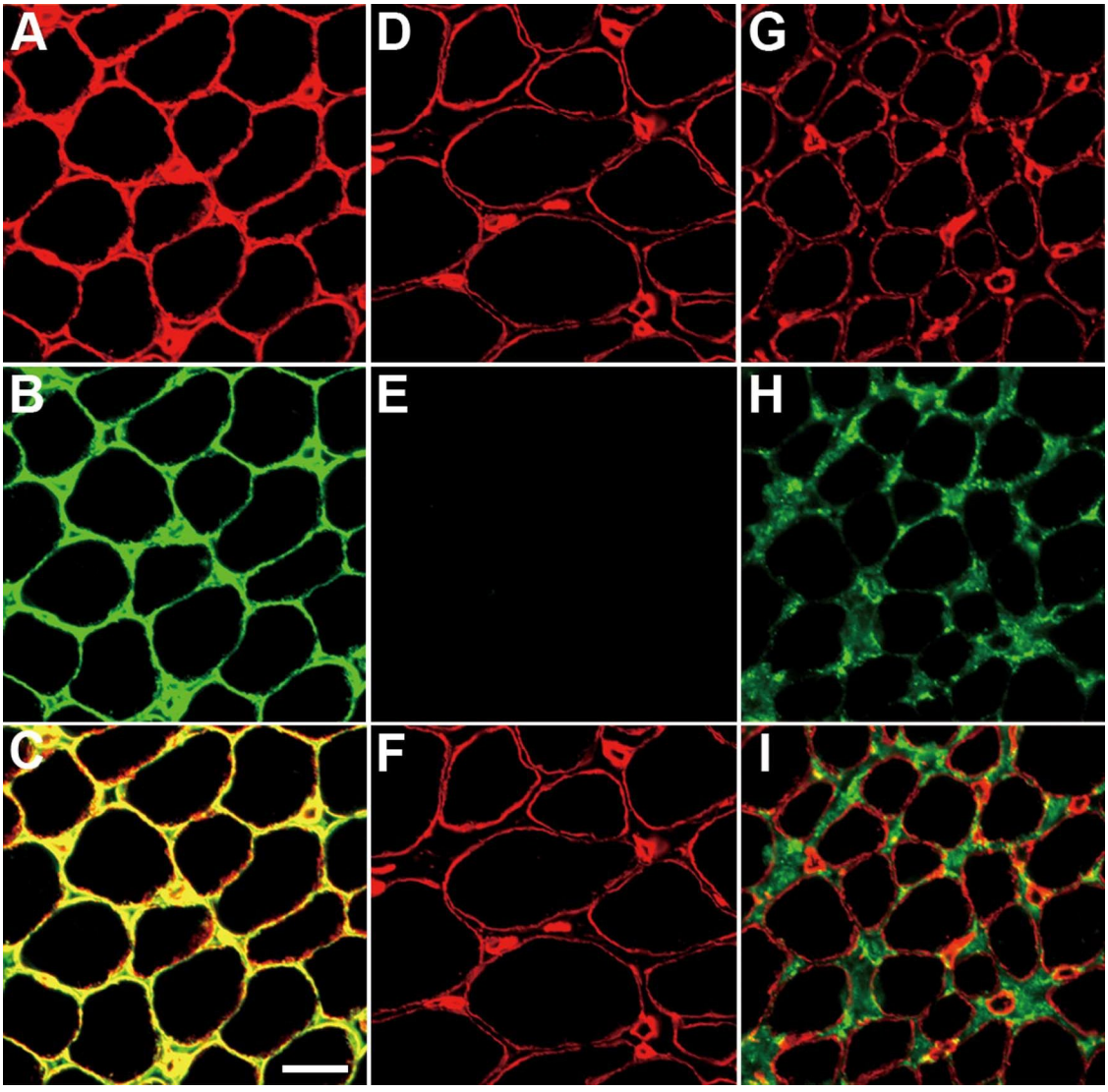

Figure 2 Double immunostaining for collagen IV and VI. (A–C) Patient with non-diagnostic muscle pathology; (D–F) UCMD patient with CD; (G–I) UCMD patient with SSCD. (A,D,G) Immunostaining for collagen IV. Collagen IV is present in the sarcolemma. (B,E,H) Immunostaining for collagen VI. Collagen VI is absent in a patient with CD, while it is present in the interstitium but markedly reduced in a patient with SSCD. (C,F,I) Merged images. Both collagen IV and VI are present in the sarcolemma in a patient with non-diagnostic pathology, as indicated by yellow; in contrast, collagen VI is absent in the sarcolemma in a patient with SSCD, as indicated by only red. UCMD, Ullrich congenital muscular dystrophy; CD, complete collagen VI deficiency; SSCD, sarcolemma-specific collagen VI deficiency, bar 20 µm.

changes. RYR1-related core myopathy, including central core disease (CCD) and multiminicore disease, may also show similar clinical features as they can multiple joint contractures and spinal deformity. Progressive respiratory muscle involvement, often disproportionate to the skeletal muscle weakness, is also seen in multiminicore disease. However, significant respiratory insufficiency is unusual in CCD. Interestingly, a recent report demonstrated that muscle pathology in a patient with a heterozygous COL6A3 gene mutation included cores, rods and lobulated fibres.[29] SMA is characterised by fasciculation and diagnosed by identifying mutations in the SMN gene. EDS may mimic UCMD in terms of joint laxity. Furthermore, various types of EDS are commonly associated with mild to moderate muscle weakness. Muscle pathology can demonstrate mild myopathic features but necrotic fibres and fibrosis are absent and collagen VI staining is normal.[30]

Of particular importance is rigid spine with muscular dystrophy type 1 (RSMD1) in forms of CMD, which results from mutations in the SEPN1 gene, because it can show a significant clinical overlap in the late stage of the disease. RSMD1 patients typically show combination of mild or moderate proximal muscle weakness, Achilles tendon tightness, spinal rigidity and scoliosis, and require ventilator assistance in the first decade of life,[15] similarly to UCMD.

Management

Treatment for patients with UCMD is supportive for symptoms such as respiratory insufficiency and scoliosis, and is dependent on age of the individual and severity of symptoms. Respiratory failure is a common complication of UCMD and careful follow-up with regular assessments of respiratory function, including spirometry and nocturnal oximetry studies, is important to detect asymptomatic decline in patients. In a recent review based on expert consensus on the standard care for CMD, cough assistance using mechanical insufflation-exsufflation is generally accepted as the method to improve cough efficiency.[22] Other methods such as

breath stacking with Ambu bag maintain thoracic compliance and reduce the risk of chronic atelectasis.[22] Respiratory support with nocturnal NIV usually becomes necessary in the first or second decade of life for patients[12 19] and might be effective in reducing symptoms and promoting quality of life. There are times when chronic ventilation can require an invasive application via tracheostomy.

For scoliosis, conservative management including standing frame, positioning and bracing is widely used, although controversial whether those approaches are preventive.[22] However, scoliosis may require active management including spinal surgery to prevent progression, although there have been no formal studies on the efficacy of scoliosis surgery. The choice of the instrumentation such as growing rods depends on the age of the individual, his/her ability to grow and the severity of scoliosis.[22] Suggested contraindications to spinal surgery includes family decision, very poor or deteriorating cardiac status and/or respiratory status, very young age, potential loss of function after spinal fixation and severe scoliosis.[22] Severe respiratory insufficiency may not be a contraindication in certain high specialised centres. In fact, one study on surgical correction of spinal deformity from Japan reported that scoliosis surgery was successfully performed in three patients with UCMD at 11, 13 and 17 years of age, respectively[31]; spinal surgery, however, did not prevent deterioration of respiratory function in these patients, suggesting that at such older ages pulmonary and chest wall compliance might be too severely compromised for patients to benefit from scoliosis surgery, and earlier surgical intervention may be more beneficial. Indeed, a single case report described that slower decline of predicted VC in a patient after scoliosis surgery performed at 5 years of age compared with another patient who had undergone surgical correction of scoliosis at 9 years of age.[19] Further studies are necessary to conclude the efficacy of early scoliosis surgery.

Equipment recommended for assistance in standing, ambulation and/or other forms includes walking frames, standing frames, swivel walker, knee-ankle-foot orthoses, ankle-foot orthoses, scooters and wheelchairs.[22] The joint contractures of patients with UCMD in particular seem to be progressive and regular stretching is recommended to maintain a certain level of mobility of the joints. In addition, feeding and swallowing difficulties can be encountered in UCMD.[20] Issues of feeding and nutrition are multifactorial and closely related to other areas of care; for example, nocturnal hypoventilation can affect appetite and growth and respiratory insufficiency can result in easy fatigue and difficulty in swallowing.[22] Consultation with a nutrition specialist is often helpful to boost energy intake. Some children may need a temporary or permanent gastric feeding tube support to maintain an adequate nutritional and fluid intake.[20 21] Survival has not been fully documented under the current standards of medical care, but failure to introduce adequate respiratory support might lead to the death of teenagers with UCMD.[11 21] With the availability of effective respiratory interventions, patients commonly survive into adulthood to date, and other potential aspects of the disease could surface.

MOLECULAR DIAGNOSIS, PATHOGENESIS AND THERAPEUTIC AVENUES

Collagen VI is a ubiquitously expressed ECM protein composed of three α-chains, α1, α2 and α3. The three chains are encoded by the genes COL6A1 and COL6A2 on chromosome 21q22.3 and COL6A3 on chromosome 2q37.[13] The basic monomer, made up of two globular domains connected by a triple helical structure, is composed of one of each of the these α-chain subunits (1:1:1 ratio). Prior to secretion into the extracellular space, the two basic monomers assemble into dimers (two antiparallel, overlapping monomers) and such dimers associate in a staggered parallel orientation to form tetramers (four monomers) in the cytoplasm.[13 32] Outside the cell, these tetramers, the secreted form of collagen VI, associate in an end-to-end fashion to form collagen VI microfibrillar structures, which interacts with collagen IV and other ECM components including proteoglycans decorin and biglycan, collagen I, hyaluronan, heparin and integrin.[13 33]

Collagen VI gene mutations in UCMD

UCMD used to be regarded as an autosomal-recessive disorder. However, soon after the initial discovery of recessive mutations in the COL6A2 gene,[34 35] a total of four patients with sporadic UCMD were found to carry de novo autosomal-dominant mutations in either COL6A1, COL6A2 or COL6A3.[36 37] UCMD is now known to be caused by either recessive or dominant genetic mechanism, the latter most typically occur as de novo mutations.[32] This is most likely because these dominant mutations are associated with too severe phenotype to allow patients to produce their offspring. In contrast, in BM, the phenotype is typically mild enough for patients to produce children, resulting in autosomal-dominant inheritance condition.[8 13]

The most common types of mutations are point mutations, exon skipping and mutations leading to premature termination codons (PTCs).[32] Among point mutations, missense changes affecting glycine residues in the Gly-Xaa-Yaa motifs of the N-terminal triple helical domains are the most common and are often dominant de novo.[32 33] Splice mutations resulting in in-frame exon skipping are generally dominant de novo mutations.[32 33] These dominant mutations can result in secretion of some mutant-containing tetramers into the extracellular space; in the multistep collagen VI intracellular assembly process, only 1/16 of the tetramers produced by patients with dominant mutations could be composed entirely of normal α-chains, thus exerting a dominant negative effect.[37] This leads to loss of normal localisation of collagen VI in the basement membrane and eventually results in a severe phenotype. Nonsense mutations and small deletions or insertions inducing PTCs with consequent nonsense-mediated mRNA decay (NMD), an mRNA quality control mechanism that degrades aberrant mRNAs containing PTCs, and loss of the mutated chain are mostly inherited as recessive mutations.[32 33] Patients with these mutations are unable to assemble or secrete functional collagen VI protein, as all three α-chains are required to form a collagen VI monomer. Thus, such functional null alleles, which underlie typical UCMD, mostly lead to CD mode of collagen VI in skeletal muscles.[16 26 33 34] On the other hand, complete deletions of one copy of these genes also act in a recessive fashion. In support of this notion, carriers of the deletion are in fact clinically asymptomatic, indicating that complete haploinsufficiency of any of the three collagen VI genes does not cause the disease. Interestingly, two reports demonstrated that autosomal-recessive inheritance can also underlie BM, in which patients carried a truncating or null COL6A2 mutation associated with missense changes in the partnering allele lying within the C2 domain of the α2 chain.[38 39] Furthermore, myosclerosis syndrome was reported to be responsible for a homozygous nonsense COL6A2 mutation.[40] Unlike nonsense mutations associated with UCMD, the mutated mRNA escaped NMD and was translated into a truncated α2 chain, but secreted collagen VI was reduced and structurally abnormal and thus did not correctly localise in the basement membrane of myofibers. These facts suggest that the

severity of collagen VI gene mutations and the resulting functional abnormality of collagen VI in the ECM dictate a phenotypic spectrum of collagen VI-related myopathies, meaning that a fundamentally different genetic and biochemical mechanism among these myopathies can no longer be assumed.

We previously showed that there are two modes of collagen VI deficiency, CD and SSCD,[26] which respectively result from recessive and de novo dominant mutations in the collagen VI genes.[16] There is no straightforward correlation between protein levels and phenotypes; CD, however, is most likely to be associated with the more severe phenotype than SSCD.[11 19] Unlike patients with CD, a great heterogeneity in the maximal motor capacity was observed in patients with SSCD, ranging from no acquisition of walking ability to retaining ambulation throughout childhood.

Properties of collagen VI and its pathological roles

Collagen VI is widely distributed throughout ECMs in various tissues, including muscle, skin, tendon, cartilage, intervertebral discs, lung, blood vessels and adipose tissue.[4] Given the clinical features seen in patients with collagen VI-related myopathies, the tissues in which collagen VI has the most important roles include muscle and tendon. In muscle, the cell source producing collagen VI is the interstitial mesenchymal cell.[41 42] In tendons, abundant collagen VI is present in immediate pericellular ECM of the resident tendon fibroblasts.[43]

Collagen VI contributes to the properties of the local ECM microenvironment by forming a discrete network of beaded microfilaments, which interact with a large number of matrix molecules and cell surface receptors. One possible molecule mediating its interaction would be collagen type IV, the most important collagenous component of basement membranes.[13] On the other hand, collagen VI might be indirectly linked to muscle cell surface receptors via biglycan and the dystrophin-associated protein complex, as collagen VI binds to biglycan,[13] which interacts with the sarcoglycan and dystroglycan complex.[33] The functions of collagen VI pertaining to various cell types also include the promotion of adhesion,[1 2] proliferation,[3] migration[4] and survival.[5 44 45] Attachment of cells to the ECM is important for preventing apoptosis,[46] which could be particularly relevant for muscle disorders that directly involve interactions between matrix and muscle, as is the case for high early implanted cell death, partially due to 'anoikis', in cell transplantation treatment of DMD.[47] Studies with cultured fibroblasts from patients with UCMD have shown that mutant cells or mutated collagen VI exhibit decreased adherence to their surroundings, emphasising that loss of cell ECM interactions is the key mechanism of collagen VI-related myopathies.[2 48] Collagen VI also has crucial roles in the regulation and differentiation of adipocytes.[49]

Studies on muscle fibres from Col6a1$^{-/-}$ mice, engineered by genetic ablation of the Col6a1 gene,[50] and human myoblast cultures has suggested that collagen VI may be involved in preventing myofiber apoptosis, which seems to be mediated by regulating the mitochondrion-mediated cell death cascade[5 51]; a key event appears to be inappropriate opening of the mitochondrial permeability transition pore. These findings therefore link a defect of the ECM to mitochondrial dysfunction followed by apoptosis that is preventable by inactivation of cyclophilin D by using cyclosporine A, its derivative Debio025 or genetic inactivation of cyclophilin D.[51–53] However, there are contradictory reports in which researchers did not find evidence of myofiber apoptosis in biopsied muscles from UCMD patients or Col6a3 mutant mice muscles,[54 55] suggesting that muscle cell death by apoptosis is not a universal phenomenon in all patients and collagen VI-deficient mice.

In addition, a study of the autophagic process in muscles of Col6a1$^{-/-}$ mice revealed that autophagy was not induced efficiently, which determines the presence of dysfunctional organelles in muscle fibres.[56] A similar alteration of autophagy was also detected in muscle biopsies derived from nine patients with UCMD or BM.[56] This defective autophagy provides the link between the previously described mitochondrial dysfunction and myofiber degeneration. These data thus provide a basis for novel therapeutic targets to reactivate of the autophagic flux by either nutritional approaches[57] or by pharmacological and genetic tools in collagen VI deficient skeletal muscle.

Therapeutic advances

The events responsible for myofiber atrophy and loss might be different in UCMD than in other forms of muscular dystrophy with prominent membrane fragility such as DMD. To date, no single hypothesis can fully explain variation in fibre size, ongoing interstitial fibrogenesis and adipogenesis even in mild necrotic and regenerating process in UCMD or provide all targets for therapies, although important clues have been discovered.

Pathological hypotheses leading to myofiber degeneration in collagen VI-deficient skeletal muscle have been proposed and therapeutic targets have been suggested. There have been pilot studies on patients with UCMD based upon the theory of mitochondrial dysfunction or impaired autophagy.[51–53 57] A recent report has shown that collagen VI is a key component of satellite cell niche and lack of collagen VI causes impaired muscle regeneration and reduced satellite cell self-renewal capability after injury in Col6a1$^{-/-}$ mice.[58] Additionally, when normal collagen VI is supplied in vivo by grafting wild-type interstitial mesenchymal cells, the biochemical properties of collagen VI-deficient muscles are ameliorated and satellite cell defects also rescued.[58] These results can open new venues for a better understanding of the pathomechanism underlying collagen VI-related myopathies. Furthermore, multipotent mesenchymal stem cell (MSC) is the most common type of adult stem cells and is isolated from several sources such as bone marrow and adipose tissue. Another report has recently shown that transplanted human adipose-derived stem cells, with phenotypic and functional features of mesenchymal progenitors, secrete collagen VI protein in Col6a1$^{-/-}$ mice.[59] Thus, MSC-based therapy can be an attractive option as transplanted cells are able to self-renew and to differentiate into collagen VI-producing cells in skeletal muscle.[41 42]

Advances in molecular genetics provide gene-based therapies; that is, antisense oligonucleotide or small interfering RNA (siRNA) inhibition of mutant transcripts exerting dominant negative effects[60–62] and upregulation of mutant transcripts by specific inhibition of NMD.[63] As 60–80% of UCMD cases are attributed to dominant negative mutations,[11 16] the allele-specific antisense approach can be applied to the majority of patients. Recent reports have shown that siRNA-mediated knockdown of SMG-1 and Upf1, essential components for NMD, or SMG-8, a subunit of SMG-1 kinase, gives rise to the upregulation of mutant triple-helical collagen VI, thus ameliorating mutant phenotypes from UCMD fibroblasts with a homozygous frameshift mutation causing a PTC in the COL6A2 gene.[64 65]

CONCLUSION

UCMD is caused by mutations in either COL6A1, COL6A2 or COL6A3 gene, thereby leading to collagen VI deficiency in the ECM. We here presented the clinicopathological features, robust

natural history and the current supportive care for symptoms. Of special interest is progressive interstitial fibrosis even in very mild necrotic and regenerating process in muscle. Patients with UCMD have unique manifestations attributable to both muscle and connective tissue disorders. Collagen VI contributes to the properties of the local ECM microenvironment by forming a discrete network of beaded microfilaments, which interact with a large number of matrix molecules and cell surface receptors. Advanced researches have provide important clues to explain how collagen VI deficiency in the ECM can cause the development of muscle weakness in Col6a1$^{-/-}$ mice or patients with UCMD, although the link between the ECM defect and phenotype remains to be fully elucidated. Further studies are necessary to elucidate exactly how collagen VI deficiency in the ECM makes muscle cells vulnerable to apoptosis or interstitial fibrogenesis and adipogenesis strikingly progressive.

Acknowledgements The authors thank Drs Ikuya Nonaka, Hirofumi Komaki and Akihiko Ishiyama for their valuable assistance. This study was supported by Intramural Research Grant (23-5) for Neurological and Psychiatric Disorders of NCNP, Research on Rare and Intractable Diseases and Research on Applying Health Technology from the Ministry of Health, Labour and Welfare of Japan.

Contributors TY performed literature search and wrote the manuscript; IN was involved in literature search and preparation of the manuscript.

Competing interests None.

Provenance and peer review Commissioned; externally peer reviewed.

REFERENCES

1 Aumailley M, Specks U, Timpl R. Cell adhesion to type VI collagen. Biochem Soc Trans 1991;19:843–7.
2 Kawahara G, Okada M, Morone N, et al. Reduced cell anchorage may cause sarcolemma-specific collagen VI deficiency in Ullrich disease. Neurology 2007;69:1043–9.
3 Atkinson JC, Rühl M, Becker J, et al. Collagen VI regulates normal and transformed mesenchymal cell proliferation in vitro. Exp Cell Res 1996;228:283–91.
4 Iyengar P, Espina V, Williams TW, et al. Adipocyte-derived collagen VI affects early mammary tumor progression in vivo, demonstrating a critical interaction in the tumor/stroma maicroenvironment. J Clin Invest 2005;115:1163–76.
5 Irwin WA, Bergamin N, Sabatelli P, et al. Mitochondrial dysfunction and apoptosis in myopathic mice with collagen VI deficiency. Nat Genet 2003;35:367–71.
6 Ullrich O. Kongenitale, atonisch-skelerotische Muskeldystrophie, ein weiterer Typus der heredodegenerativen Erkrankungen des neuromuskulären Systems. Z Ges Neurol Psychiat 1930;126:171–201.
7 Ullrich O. Kongenitale, atonisch-skelerotische Muskeldystrophie. Monatsschr Kinderheilkd 1930;47:502–10.
8 Bethlem J, van Wijngaarden GK. Benign myopathy, with autosomal dominant inheritance. A report on three pedigrees. Brain 1976;99:91–100.
9 Butterfield RJ, Foley AR, Dastgir J, et al. Position of glycine substitutions in the triple helix of COL6A1, COL6A2, and COL6A3 is correlated with severity and mode of inheritance in collagen VI myopathy. Hum Mutat 2013;34:1558–67.
10 Quijano-Roy S, Allamand V, Riahi N, et al. Predictive factors of severity and management of respiratory and orthopaedic complications in 16 Ullrich CMD patients [abstract]. Neuromuscul Disord 2007;17:844.
11 Briñas L, Richard P, Quijano-Roy S, et al. Early onset collagen VI myopathies: Genetic and clinical correlations. Ann Neurol 2010;68:511–20.
12 Foley AR, Quijano-Roy S, Collins J, et al. Natural history of pulmonary function in collagen VI-related myopathies. Brain 2013;136:3625–33.
13 Lampe AK, Bushby KM. Collagen VI related muscle disorders. J Med Genet 2005;42:673–85.
14 Pepe G, Bertini E, Bonaldo P, et al. Bethlem myopathy (BETHLEM) and Ullrich scleroatonic muscular dystrophy: 100th ENMC International Workshop, 23–24 November 2001, Naarden, the Netherlands. Neuromuscul Disord 2002;12:984–93.
15 Muntoni F, Voit T. The congenital muscular dystrophies in 2004: a century of exciting progress. Neuromuscul Disord 2004;14:635–49.
16 Okada M, Kawahara G, Noguchi S, et al. Primary collagen VI deficiency is the second most common congenital muscular dystrophy in Japan. Neurology 2007;69:1035–42.
17 Peat RA, Smith JM, Compson AG, et al. Diagnosis and etiology of congenital muscular dystrophy. Neurology 2008;71:312–21.
18 Norwood FL, Harling C, Chinnery PF, et al. Prevalence of genetic muscle disease in Northern England: in depth analysis of a muscle clinic population. Brain 2009;132:3175–86.
19 Yonekawa T, Komaki H, Okada M, et al. Rapidly progressive scoliosis and respiratory deterioration in Ullrich congenital muscular dystrophy. J Neurol Neurosurg Psychiatry 2013;84:982–9.
20 Nadeau A, Kinali M, Main M, et al. Natural history of Ullrich congenital muscular dystrophy. Neurology 2009;73:25–31.
21 Mercuri E, Yuva Y, Brown SC, et al. Collagen VI involvement in Ullrich syndrome: a clinical, genetic, and immunohistochemical study. Neurology 2002;58:1354–9.
22 Wang CH, Bönnemann CG, Rutkowski A, et al. Consensus statement on standard of care for congenital muscular dystrophies. J Child Neurol 2010;25:1559–81.
23 Mercuri E, Lampe A, Allsop J, et al. Muscle MRI in Ullrich congenital muscular dystrophy and Bethlem myopathy. Neuromuscular Disord 2005;15:303–10.
24 Nonaka I, Une Y, Ishihara T, et al. A clinical and histological study of Ullrich's disease (congenital atonic-sclerotic muscular dystrophy). Neuropediatrics 1981;12:197–208.
25 Schessl J, Goemans NM, Magold AI, et al. Predominant fiber atrophy and fiber type disproportion in early Ullrich disease. Muscle Nerve 2008;38:1184–91.
26 Ishikawa H, Sugie K, Murayama K, et al. Ullrich disease due to deficiency of collagen VI in the sarcolemma. Neurology 2004;62:620–3.
27 Ishikawa H, Sugie K, Murayama K, et al. Ullrich disease: collagen VI deficiency: EM suggests a new basis for muscular weakness. Neurology 2002;59:920–3.
28 Gualandi F, Curci R, Sabatelli P, et al. Macrophages: a minimally invasive tool for monitoring collagen VI myopathies. Muscle Nerve 2011;44:80–4.
29 Claeys KG, Schrading S, Bozkurt A, et al. Myopathy with lobulated fibers, cores, and rods caused by a mutation in collagen VI. Neurology 2012;79:2288–90.
30 Voermans NC, van Alfen N, Pillen S, et al. Neuromuscular involvement in various types of Ehlers-Danlos syndrome. Ann Neurol 2009;65:687–97.
31 Takaso M, Nakazawa T, Imura T, et al. Surgical correction of spinal deformity in patients with congenital muscular dystrophy. J Orthop Sci 2010;15:493–501.
32 Allamand V, Briñas L, Richard P, et al. ColVI myopathies: where do we stand, where do we go? Skelet Muscle 2011;1:30–42.
33 Bönnemann CG. The collagen VI-related myopathies: muscle meets its matrix. Nat Rev Neurol 2011;7:379–90.
34 Camacho VO, Bertini E, Zhang RZ, et al. Ullrich congenital muscular dystrophy is caused by recessive mutations in collagen type VI. Proc Natl Acad Sci USA 2001;98:7516–21.
35 Higuchi I, Shiraishi T, Hashiguchi T, et al. Frameshift mutation in the collagen VI gene causes Ullrich's disease. Ann Neurol 2001;50:261–5.
36 Pan TC, Zhang RZ, Sudano DG, et al. New molecular mechanism for Ullrich congenital muscular dystrophy: a heterozygous in-frame deletion in the COL6A1 gene causes a severe phenotype. Am J Hum Genet 2003;73:355–69.
37 Baker NL, Morgelin M, Peat R, et al. Dominant collagen VI mutations are a common cause of Ullrich congenital muscular dystrophy. Hum Mol Genet 2005;14:279–93.
38 Gualandi F, Urciuolo A, Martoni E, et al. Autosomal recessive Bethlem myopathy. Neurology 2009;73:1883–91.
39 Foley AR, Hu Y, Zou Y, et al. Autosomal recessive inheritance of classic Bethlem myopathy. Neuromuscul Disord 2009;19:813–17.
40 Merlini L, Martoni E, Grumati P, et al. Autosomal recessive myosclerosis myopathy is a collagen VI disorder. Neurology 2008;71:1245–53.
41 Zou Y, Zhang RZ, Sabatelli P, et al. Muscle interstitial fibroblasts are the main source of collagen VI synthesis in skeletal muscle: implications for congenital muscular dystrophy dystrophy types Ullrich and Bethlem. J Neuropathol Exp Neurol 2008;67:144–54.
42 Braghetta P, Ferrari A, Fabbro C, et al. An enhancer required for transcription of the Col6a1 gene in muscle connective tissue is induced by signals released from muscle cells. Exp Cell Res 2008;314:3508–18.
43 Ritty TM, Roth R, Heuser JE. Tendon cell array isolation reveals a previously unknown fibrillin-2-containing macromolecular assembly. Structure 2003;11:1179–88.
44 Rühl M, Sahin E, Johannsen M, et al. Soluble collagen VI drives serum-starvated fibroblast through S phase and prevents apoptosis via down-regulation of Bax. J Biol Chem 1999;274:34361–8.
45 Howell SJ, Doane KJ. Type VI collagen increases cell survival and prevents anti-β1 integrin-mediated apoptosis. Exp Cell Res 1998;241:230–41.
46 Chiarugi P, Giannoni E. Anoikis: a necessary death program for anchorage-dependent cells. Biochem Pharmacol 2008;76:1352–64.
47 Gerard C, Forest MA, Beauregard G, et al. Fibrin gel improves the survival of transplanted myoblasts. Cell transplant 2012;21:127–37.
48 Kawahara G, Ogawa M, Okada M, et al. Diminished binding of mutated collagen VI to the extracellular matrix surrounding myocytes. Muscle Nerve 2008;38:1192–5.
49 Nakajima I, Muroya S, Tanabe R, et al. Extracellular matrix development during differentiation into adipocyte with a unique increase in type V and VI collagen. Biol Cell 2002;94:197–203.
50 Bonaldo P, Braghtta P, Zanetti M, et al. Collagen VI deficiency induces early onset myopathy in the mouse: an animal model for Bethlem myopathy. Hum Mol Genet 1998;7:2135–40.
51 Bernardi P, Bonaldo P. Dysfunction of mitochondria and sarcoplasmic reticulum in the pathogenesis of collagen VI muscular dystrophies. Ann NY Acad Sci 2008;1147:303–11.

52 Tiepolo T, Angelin A, Palma E, et al. The cyclophilin inhibitor Debio025 normalizes mitochondrial function, muscle apoptosis and ultrastructural defects in Col6a−/− myopathic mice. Br J Pharmacol 2009;157:1045–52.
53 Palma E, Tiepolo T, Angelin A, et al. Genetic ablation of cyclophilin D rescues mitochondrial defects and prevents muscle apoptosis in collagen VI myopathic mice. Hum Mol Genet 2009;18:2024–31.
54 Paco S, Ferrer I, Jou C, et al. Muscle fiber atrophy and regeneration coexist in collagen VI-deficient human muscle: role of calpain-3 and nuclear factor-κB signaling. J Neuropathol Exp Neurol 2012;71:894–906.
55 Pan TC, Zhang RZ, Markova D, et al. COL6A3 protein deficiency in mice leads to muscle and tendon defects similar to human collagen VI congenital muscular dystrophy. J Biol Chem 2013;288:14320–31.
56 Grumati P, Coletto L, Sabatelli P, et al. Autophagy is defective in collagen VI muscular dystrophies, and its reactivation rescues myofiber degeneration. Nat Med 2010;16:1313–20.
57 Low protein diet in patients with collagen VI related myopathies (LPD). http://clinicaltrials.gov/ct2/show/NCT01438788 (accessed 3 Feb 2014).
58 Urciuolo A, Quarta M, Morbidoni V, et al. Collagen VI regulates satellite cell self-renewal and muscle regeneration. Nat commun 2013;4:1964.
59 Alexeev V, Arita M, Donahue A, et al. Human adipose-derived stem cell transplantation as a potential therapy for collagen VI-related congenital muscular dystrophy. Stem Cell Res Ther 2014;5:21. http://stemcellres.com/content/5/1/21
60 Gualandi F, Manzati E, Sabatelli P, et al. Antisense-induced messenger depletion corrects a COL6A2 dominant mutation in Ullrich myopathy. Hum Gene Ther 2012;23:1313–8.
61 Bolduc V, Zou Y, Ko D, et al. siRNA-mediated allele-specific silencing of a COL6A3 mutation in a cellular model of dominant Ullrich muscular dustrophy. Mol Ther Nucleic Acids 2014;3:e147
62 Noguchi S, Ogawa M, Kawahara G, et al. Allele-specific gene silencing of mutant mRNA restores cellular function in Ullrich congenital muscular dystrophy fibroblasts. Mor Ther Nucleic Acids (In press).
63 Usuki F, Yamashita A, Higuchi I, et al. Inhibition of nonsense-mediated mRNA decay rescues the phenotype in Ullrich's disease. Ann Neurol 2004;55:740–4.
64 Usuki F, Yamashita A, Kashima I, et al. Specific inhibition of nonsense-mediated mRNA decay components, SMG-1 or Upf1, rescues the phenotype of Ullrich disease fibroblasts. Mol Ther 2006;14:351–60.
65 Usuki F, Yamashita A, Shiraishi T, et al. Inhibition of SMG-8, a subunit of SMG-1 kinase, ameliorates nonsense-mediated mRNA decay-exacerbated mutant phenotypes without cytotoxicity. Proc Natl Acad Sci USA 2013;110:15037–42.

JNNP

Ullrich congenital muscular dystrophy: clinicopathological features, natural history and pathomechanism(s)

Takahiro Yonekawa and Ichizo Nishino

J Neurol Neurosurg Psychiatry 2015 86: 280-287 originally published online June 17, 2014
doi: 10.1136/jnnp-2013-307052

NEUROPATHOLOGY

Neuropathology 2015; **35**, 91–93 doi:10.1111/neup.12147

Neuropathology Education

Kyphoscoliosis and easy fatigability in a 14-year-old boy

Jantima Tanboon,[1] Yukiko K. Hayashi,[2,3,4] Ichizo Nishino[3,4] and Tumtip Sangruchi[1]

[1]Department of Pathology, Faculty of Medicine, Siriraj Hospital, Mahidol University, Bangkok, Thailand, [2]Department of Neurophysiology, Tokyo Medical University, [3]Department of Neuromuscular Research, National Institute of Neuroscience, and [4]Department of Clinical Development, Translational Medical Center, National Center of Neurology and Psychiatry, Tokyo, Japan

CLINICAL COURSE

The patient was a 14-year-old Thai boy who presented at an orthopedic clinic with kyphoscoliosis first detected 1 year prior to medical attention. He was the first child of non-consanguineous parents; the pregnancy and delivery were uneventful. He had normal developmental milestones. The patient noticed easy fatigability after exercise which worsened during the past year. His younger brother was 10 years old and healthy. There was no history of neuromuscular disease in his family. His father passed away due to an unrelated incident. General examination revealed a body weight of 30 kg and a height of 149 cm, bilateral ptosis, high-arched palate, kyphoscoliosis, and asymmetrical chest wall. Proximal muscle weakness of grade 4 by Medical Research Council Scale in all extremities and areflexia were noted. The muscle tone was normal. Serum CK was 49 IU/L. Echocardiogram showed mild pulmonary and tricuspid regurgitation. Pulmonary function tests showed restrictive lung disease; the forced vital capacity was 1.56 L (51% of predicted). Sleep study revealed apnea-hypopnea index 13.6 per hour associated with severe oxygen desaturation (minimum SpO_2 39.0%).

PATHOLOGICAL FINDINGS

Muscle biopsy from the right quadriceps showed varying fiber sizes with type 1 hypotrophy and type 2 hypertrophy. The type 1 fibers were predominant (91%). Cap structures were seen in 32% of all fibers (Fig. 1). Ultrastructurally, the cap structures were composed of disorganized thin myofibrils and thickened Z-lines (Fig. 2). Nemaline rods were not present. Genetic analysis using genomic DNA identified a heterozygous c.415_417delGAG (p.Glu139del) in exon 4 of *TPM2*. The genetic tests were not performed in other family members.

DIAGNOSIS

TPM2-related cap myopathy.

DISCUSSION

Cap myopathy is a rare congenital myopathy characterized by presence of muscle fibers with cap structures on muscle biopsy and prominent respiratory muscle involvement. It is associated with dominant mutations in *TPM2*, *TPM3* and *ACTA1* genes, in descending order.[1,2]

Histologically, in cases with genetic results, cap structures range from 4% to 100% in muscle fibers.[1] Fidzianska reported two neonatal-onset cases with childhood death containing caps in 70–75% of fibers and two other childhood-onset cases with slowly progressive course containing caps in 20–30% of fibers, suggesting association of disease severity and the frequency of cap structure.[3] The number of caps seems to increase as the patients have aged.[4,5]

Onset of cap myopathy ranges from the neonatal period to childhood. Respiratory insufficiency is usually the major problem in patient management. The other common clinical manifestations include neonatal hypotonia, high-arched palate, myopathic facies and scoliosis. Muscle weakness is predominant in proximal muscles, which is non-specific. Serum CK is usually normal or slightly elevated. A case with distinctive abnormal cardiac function[6] and several cases with mild non-specific cardiac abnormalities have been reported.[1] Interestingly, one of the reported cases shows continuous gradual clinical improvement.[5]

Since all three causative genes in cap myopathy are also associated with nemaline myopathy (NM), it is not surprising to have concurrent caps and rods in the same patients[2,7]

Correspondence: Jantima Tanboon, MD, Department of Pathology, Faculty of Medicine, Siriraj Hospital, Mahidol University, Bangkok Noi, Bangkok 10700, Thailand. Email: jtanboon@gmail.com

Received 14 July 2014 and accepted 20 July 2014; published online 28 August 2014.

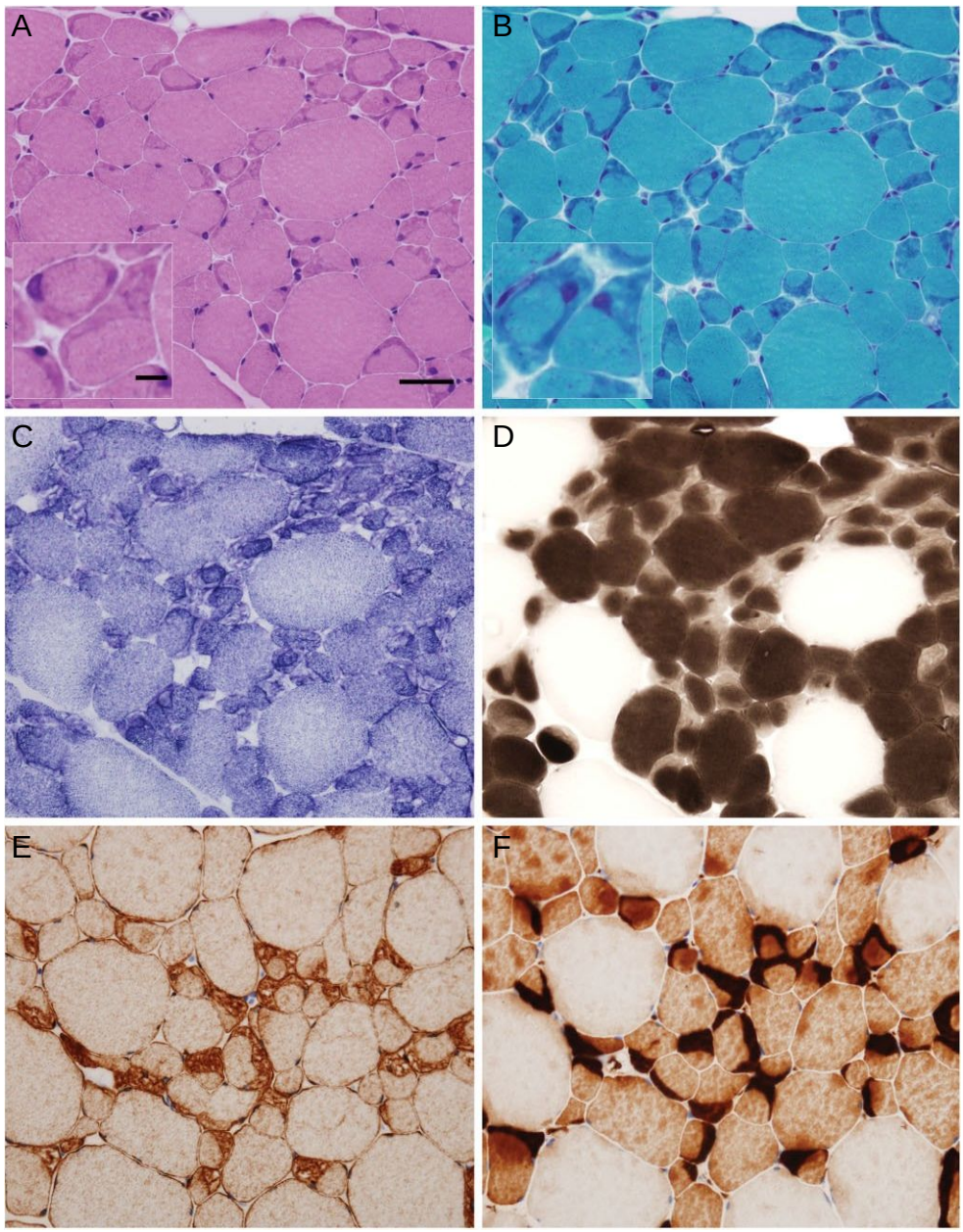

Fig. 1 Cap structures at the periphery of the small fibers in HE stain (A). Caps are highlighted by modified Gomori trichrome stain (B) and nicotinamide adenine dehydrogenase tetrazolium reductase stain (C). The small fibers are type 1 demonstrated by ATPase stain (pH 4.4) and the cap areas are negatively stained (D). The caps are positive for desmin (E) and alpha-actinin (F). Bar = 50 μm, inset bar = 10 μm.

or have a family member with NM[4,8] although cap myopathy is much less common. Muscle biopsy findings of some cap myopathy patients were consistent with congenital fiber type disproportion (CFTD) at a younger age.[5,8] This may represent either a disease spectrum or insufficient tissue sampling since CFTD is also associated with *TPM2* and *TPM3* mutations.[2] Most cap myopathy patients are sporadic yet a few probable autosomal dominant familial cap myopathy cases have been reported.[1,7] It is likely that most cases are affected by *de novo* dominant mutations causing too severe phenotypes to have offspring. Overlapping phenotypes between cap and nemaline myopathies include facial muscle weakness, high-arched palate and respiratory complications. The severity of both myopathies can range from mild to fatal.

The most common recurrent mutation in cap myopathy is p.Glu139del in exon 4 of *TPM2* gene and this mutation seems to be mostly related to cap myopathy, although six patients with different phenotypes have been reported.[2,6,7,9] Most patients with p.Glu139del, including our case, devel-

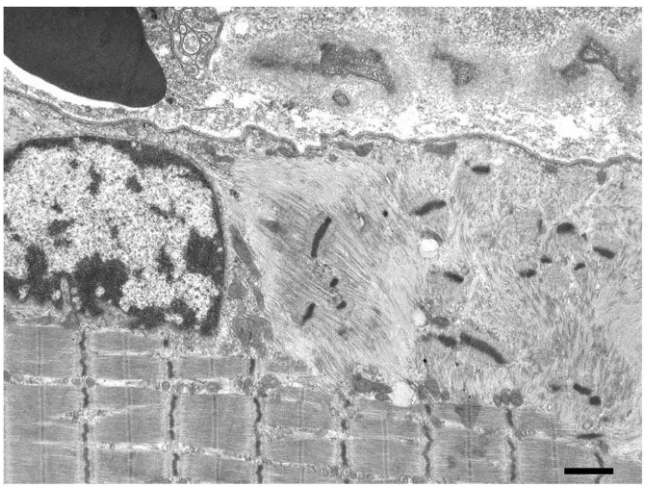

Fig. 2 Electron microscopy study of the cap structures shows disorganized thin myofibrils and thickened Z-lines. Bar = 1 μm.

oped symptoms during childhood, except for one case that presented in the neonatal period.[9] Our patient and two of the reported cases noticed developed scoliosis in a short period of time.[6,7] This feature has not been documented in cap myopathy patients with other mutations. It is possible yet inconclusive that p.Glu139del might affect axial muscles in later stage but progress at a faster rate compared to the other mutations.

In conclusion, we report a case of cap myopathy in a 14-year-old Thai boy. It is the first case reported from Asia and shares a common mutation, p.Glu139del, which was previously identified in patients with European ancestry.[2,6,7,9]

ACKNOWLEDGMENTS

The authors thank Ms. Rangsima Nguenvattana for her secretarial work on the preparation of this manuscript. This work was supported partly by Research on Intractable Diseases, Comprehensive Research on Disability Health and Welfare, and Applying Health Technology from the Ministry of Health Labour and Welfare; partly by Intramural Research Grant 23-5 for Neurological and Psychiatric Disorders of National Center of Neurology and Psychiatry.

DISCLOSURES

All authors report no disclosures.

REFERENCES

1. Schreckenbach T, Schroder JM, Voit T *et al*. Novel TPM3 mutation in a family with cap myopathy and review of the literature. *Neuromuscul Disord* 2014; **24**: 117–124.
2. Marttila M, Lehtokari VL, Marston S *et al*. Mutation update and genotype-phenotype correlations of novel and previously described mutations in TPM2 and TPM3 causing congenital myopathies. *Hum Mutat* 2014; **35**: 779–790.
3. Fidzianska A. "Cap disease" – a failure in the correct muscle fibre formation. *J Neurol Sci* 2002; **201**: 27–31.
4. Cuisset JM, Maurage CA, Pellissier JF *et al*. "Cap myopathy": case report of a family. *Neuromuscul Disord* 2006; **16**: 277–281.
5. Ohlsson M, Quijano-Roy S, Darin N *et al*. New morphologic and genetic findings in cap disease associated with beta-tropomyosin (TPM2) mutations. *Neurology* 2008; **71**: 1896–1901.
6. Clarke NF, Domazetovska A, Waddell L, Kornberg A, McLean C, North KN. Cap disease due to mutation of the beta-tropomyosin gene (TPM2). *Neuromuscul Disord* 2009; **19**: 348–351.
7. Tasca G, Fattori F, Ricci E *et al*. Somatic mosaicism in TPM2-related myopathy with nemaline rods and cap structures. *Acta Neuropathol* 2013; **125**: 169–171.
8. Tajsharghi H, Ohlsson M, Lindberg C, Oldfors A. Congenital myopathy with nemaline rods and cap structures caused by a mutation in the beta-tropomyosin gene (TPM2). *Arch Neurol* 2007; **64**: 1334–1338.
9. Lehtokari VL, Ceuterick-de Groote C, de Jonghe P *et al*. Cap disease caused by heterozygous deletion of the beta-tropomyosin gene TPM2. *Neuromuscul Disord* 2007; **17**: 433–442.

Human Molecular Genetics, 2015, Vol. 24, No. 3 637–648
doi:10.1093/hmg/ddu477
Advance Access published on September 16, 2014

Dominant mutations in ORAI1 cause tubular aggregate myopathy with hypocalcemia via constitutive activation of store-operated Ca^{21} channels

Yukari Endo[1,2,4], Satoru Noguchi[1,2,*], Yuji Hara[5,6], Yukiko K. Hayashi[1,2,7], Kazushi Motomura[1], Satoko Miyatake[8], Nobuyuki Murakami[9], Satsuki Tanaka[10], Sumimasa Yamashita[11], Rika Kizu[12], Masahiro Bamba[13], Yu-ichi Goto[1,3], Naomichi Matsumoto[8], Ikuya Nonaka[2] and Ichizo Nishino[1,2]

[1]Department of Clinical Development, Translational Medical Center, National Center of Neurology and Psychiatry, Kodaira, Tokyo 187-8556, Japan, [2]Department of Neuromuscular Research and [3]Department of Mental Retardation and Birth Defect Research, National Institute of Neuroscience, National Center of Neurology and Psychiatry, Kodaira, Tokyo 187-8502, Japan, [4]Department of Pediatrics, Kyoto University Graduate School of Medicine, Kyoto 606-8507, Japan, [5]Department of Synthetic Chemistry and Biological Chemistry, Graduate School of Engineering, Kyoto University, Kyoto 615-8510, Japan, [6]Tokyo Women's Medical University Institute for Integrated Medical Sciences (TIIMS), Shinjuku, Tokyo 162-8666, Japan, [7]Department of Neurophysiology, Tokyo Medical University, Tokyo 160-8402, Japan, [8]Department of Human Genetics, Graduate School of Medicine, Yokohama City University, Yokohama 236-0004, Japan, [9]Department of Pediatrics, Dokkyo Medical University, Koshigaya Hospital, Koshigaya, Saitama 343-8555, Japan, [10]Department of Diabetes and Endocrinology, Osaka Saiseikai Nakatsu Hospital, Osaka 530-0012, Japan, [11]Division of Pediatric Neurology, Kanagawa Children's Medical Center (KCMC), Yokohama 232-8555, Japan, [12]Division of Pediatrics, Yokosuka Kyosai Hospital, Yokosuka, Kanagawa 238-8558, Japan and [13]Division of Pediatrics, Kawasaki Municipal Hospital, Kawasaki, Kanagawa 210-0013, Japan

Received June 28, 2014; Revised August 26, 2014; Accepted September 10, 2014

The store-operated Ca^{21} release-activated Ca^{21} (CRAC) channel is activated by diminished luminal Ca^{21} levels in the endoplasmic reticulum and sarcoplasmic reticulum (SR), and constitutes one of the major Ca^{21} entry pathways in various tissues. Tubular aggregates (TAs) are abnormal structures in the skeletal muscle, and although their mechanism of formation has not been clarified, altered Ca^{21} homeostasis related to a disordered SR is suggested to be one of the main contributing factors. TA myopathy is a hereditary muscle disorder that is pathologically characterized by the presence of TAs. Recently, dominant mutations in the STIM1 gene, encoding a Ca^{21} sensor that controls CRAC channels, have been identified to cause tubular aggregate myopathy (TAM). Here, we identified heterozygous missense mutations in the ORAI1 gene, encoding the CRAC channel itself, in three families affected by dominantly inherited TAM with hypocalcemia. Skeletal myotubes from an affected individual and HEK293 cells expressing mutated ORAI1 proteins displayed spontaneous extracellular Ca^{21} entry into cells without diminishment of luminal Ca^{21} or the association with STIM1. Our results indicate that STIM1-independent activation of CRAC channels induced by dominant mutations in ORAI1 cause altered Ca^{21} homeostasis, resulting in TAM with hypocalcemia.

*To whom correspondence should be addressed at: Department of Neuromuscular Research, National Institute of Neuroscience, National Center of Neurology and Psychiatry, 4-1-1, Ogawahigashi-cho, Kodaira, Tokyo 187-8502, Japan. Tel: +81 423461712; Fax: +81 423461742. Email: noguchi@ncnp.go.jp

INTRODUCTION

Calcium (Ca^{2+}) signals are crucial for controlling a broad range of cellular functions, including secretion, excitation, contraction, motility, metabolism, transcription, growth, cell division and apoptosis (1). In the striated muscle, the sarcoplasmic reticulum (SR) is a primary Ca^{2+}-storage organelle, and Ca^{2+} released from the SR directly activates the contraction of myofibrils via excitation – contraction coupling regulation (2). Depletion of Ca^{2+} in the SR activates a store-operated Ca^{2+} entry (SOCE) pathway that is used to replenish intracellular calcium stores (3,4). In non-excitable cells and the skeletal muscle, SOCE is coordinated by stromal-interacting molecule 1 (STIM1), an endoplasmic reticulum (ER)/SR Ca^{2+} sensor, and ORAI1, a plasma membranous calcium release-activated Ca^{2+} (CRAC) channel, following Ca^{2+} ion release from intracellular stores (5 – 8). Specifically, when the ER/SR Ca^{2+} store is depleted, oligomerization and translocation of STIM1 to adjacent ER/SR-plasma membrane junctions are induced (9). Within these junctions, oligomeric STIM1 interacts with and activates ORAI1 (10–12).

Recessive mutations in ORAI1 are known to cause severe combined immunodeficiency (SCID, MIM 612782), which is characterized by a severe defect in T-cell activation accompanied by muscle hypotonia (13,14). In this disease, mutated ORAI1 leads to its deficiency in the plasma membrane resulting in loss of function of SOCE. Homozygous nonsense mutations in STIM1 also cause primary immunodeficiency (15) (MIM612783). Recently, dominant missense mutations in STIM1 were revealed to cause tubular aggregate myopathy (TAM) (16). TAM is a rare form of myopathy that can show either autosomal-dominant or -recessive inheritance (17), and is pathologically characterized by the presence of tubular aggregates (TAs). A gain of function of mutated STIM1 due to disruption of its Ca^{2+}-sensing domain was suggested as the main pathomechanism underlying STIM1-related TAM. More recently, Stormorken syndrome, which is characterized by thrombocytopenia, muscle fatigue, asplenia and congenital miosis, was also reported to be caused by a gain-of-function STIM1 mutation (18,19). Stormorken syndrome displays histological evidence of myopathy with TAs (18). However, the mechanism underlying muscle weakness and TA formation from abnormal Ca^{2+} influx has not been well established.

TAs are abnormal structures in muscle fibers that are morphologically characterized based on light and electron microscopic observations (20,21). TAs appear as accumulations of densely packed tubules, which are suggested to arise from the SR as they contain numerous SR proteins (21,22). Conceivably, the formation of TAs is triggered by some functional consequences due to disruptions in the SR-T-tubule junction, such as altered Ca^{2+} homeostasis (20). Alternatively, TAs are thought to be derived from reshaping of the SR caused by aggregation of misfolded membranous proteins (23). TAs are also observed in certain types of muscle diseases, including periodic paralysis, congenital myasthenic syndromes, alcohol- and drug-induced myopathy and TAM (21,22). However, the precise mechanism of TA formation remains to be clarified.

In this study, we performed whole exome sequencing in three families suffering from genetically undiagnosed TAM and found pathogenic mutations in the ORAI1. In addition, we demonstrated STIM1-independent activation of CRAC channels in myotubes derived from an affected individual, suggesting that this abnormal activation is the basic mechanism of this disease.

RESULTS

Clinical characterization of individuals with TAM

The clinical features of the included families are listed in Table 1 and Supplementary Material, Table S1. The common characteristic symptoms among the families were diffuse muscle weakness, marked and bilateral ankle joint contractures, rigid spine and hypocalcemia. Disease onset ranged from childhood to adolescence. Muscle weakness progressed slowly, and although all of the affected individuals were ambulant, half of them required the use of high-heeled shoes to walk correctly. All affected members in Family A and Family B showed mildly decreased serum Ca^{2+} levels and relatively low intact parathyroid hormone (PTH) levels, which were still within the normal range. In computed tomography imaging of II-3a, III-2a and II-3b, paraspinal, gastrocnemius and soleus muscles were markedly replaced by fat, which might explain ankle joint contractures and rigid spine. Trapezius, latissimus dorsi, gluteus medius, hamstrings and adductor muscles in the thigh showed severe atrophy and fat infiltration (Fig. 1). Affected members in Family A also showed central nervous system involvement as follows: individual II-3a showed calcification in the cerebellum, basal ganglia and cerebral corticomedullary junction; individual III-2a showed mild intellectual disability (IQ: 63, based on the Weschler Intelligence Scale for Children III). None of the included individuals showed characteristic signs of Stormorken syndrome, such as congenital miosis, bleeding diathesis and thrombocytopenia (Supplementary Material, Table S1).

Pathological findings

TAs were found in muscle fibers of four affected individuals (II-3a in Fig. 2; I-2b and II-1c in Supplementary Material, Fig. S1; II-1b, pictures not shown). The TAs appeared as bright red inclusions in muscle fibers following modified Gomori trichrome (mGt) staining (Fig. 2A) and showed high enzymatic activity following NADH-tetrazolium reductase (NADH-TR) staining (Fig. 2B), but were negative for succinate dehydrogenase (SDH) expression (Fig. 2C), reflecting characteristics of the SR but not the mitochondria. Under electron microscopy, the TAs appeared as aggregates composed of numerous straight tubules aligned in parallel in a longitudinal dimension and were arranged in a honeycomb-like structure in the transverse dimension (Fig. 2D). At higher magnification, each tubule showed double-walled membranes (Fig. 2E and F). All these findings were compatible with previously reported features of TAs (20). In addition to TAs, all biopsy samples demonstrated chronic dystrophic changes based on the presence of regenerating fibers, increased internal nuclei, fiber size variation in both type 1 and type 2 fibers and endomysial fibrosis. Type 1 fiber predominance was also observed (Table 2).

The ORAI1 gene is mutated in TAM-affected individuals

In order to identify the genetic cause of dominantly inherited TAM, we performed whole exome sequencing on two affected

Table 1. Clinical characterization of TAM families

	Family A		Family B			Family C
	II-3	III-2	I-2	II-1	II-3	II-1
Sex	Female	Male	Female	Female	Male	Male
Mutation	c.292G.A	c.292G.A	c.292G.A	c.292G.A	c.292G.A	c.412C.T
Predicted protein impact	p.Gly98Ser	p.Gly98Ser	p.Gly98Ser	p.Gly98Ser	p.Gly98Ser	p.Leu138Phe
Muscle disorders						
Onset	Childhood	Childhood	NI	Childhood	Childhood	Adolescence
Patterns of weakness	Lower limbs proximal; upper limbs proximal	Diffuse	Diffuse	Diffuse	Diffuse	Diffuse
Disease course	Slowly progressive	Slowly progressive	Slowly progressive	Slowly progressive	Slowly progressive	Slowly progressive
Serum CK (IU/L) (normal range)	65 (45–170)	1300 (61–255)	300 (–200)	960 (–200)	684 (–200)	213 (37–142)
Joint contractures						
Onset	Childhood	Childhood	NI	Childhood	Childhood	Adolescence
Ankle	Bilateral, severe	Bilateral, severe	Bilateral, severe	Bilateral, severe	Bilateral, severe	NI
Surgical treatment	NP	NP	13 years old	10 years old	11 years old	NP
Rigid spine	+	+	+	+	+	+
Hypocalcemia						
Onset	Childhood	Childhood	NI	Childhood	Neonatal	NI
Serum calcium (mg/dl) (normal range)	7.7 (8.8–10.2)	8.5 (8.8–10.2)	8.1 (9.0–10.2)	7.7 (9.0–10.2)	7.8 (9.0–10.2)	NI
Serum intact PTH (pg/ml) (normal range)	9 (10–65)	NI (NI)	26 (10–65)	22 (10–65)	19 (10–65)	NI
Treatment	+	+	NI	NI	+	
Other symptoms	Diabetes, calcification in the brain	Intellectual disability	–	–	–	–

NI, no information; NP, not performed; CK, creatinine kinase.

(II-3a and III-2a) and two non-affected members (I-2a and III-2a) of Family A and in all five members of Family B (I-1b, I-2b, II-1b, II-2b and II-3b) (Fig. 3A and Supplementary Material, Table S2). In total, 41 variants from Family A and 34 variants from Family B were extracted based on the assumption of autosomal-dominant inheritance and with reference to the dbSNP135, the 1000 Genomes Project database, the National Heart, Lung, and Blood Institute (NHLBI) Exome Variant Server and Human Genetic Variation Database (HGVD) for Japanese genetic variants (Supplementary Material, Table S3). Among all extracted variants, we identified only one common variant, a heterozygous c.292G.A mutation in ORAI1 (RefSeq accession number NM_032790.3) in both families (Table 1 and Fig. 3A and Supplementary Material, Tables S4 and S5). This mutation was confirmed by Sanger sequencing in all affected members and was absent in the unaffected members (Supplementary Material, Fig. S2). We also found an additional heterozygous missense mutation, c.412C.T in ORAI1, in the third TAM family by Sanger sequencing (Fig. 3A and Supplementary Material, Fig. S2). The mutation was not listed in dbSNP137, 1000 Genomes or HGVD. Both mutations were predicted to result in amino acid changes in the ORAI1 protein: p.Gly98Ser in the transmembrane (TM) 1 domain and p.Leu138Phe in the TM2 domain (Fig. 3B). The amino acid residues Gly at 98 and Leu at 138 show high evolutionary conservation (Fig. 3C). The impact of these variations was also predicted to be damaging based on in silico analysis with SIFT and PolyPhen-2 (data not shown). The crystal structure of Drosophila Orai1 determined by Hou et al. (24) and reported in the Molecular Modeling Database (MMDB ID: 105660) (Fig. 3D) shows that Gly98 is localized to face to the pore of the CRAC channel (white) and Leu138 is in the interface between TM1 and 2 (yellow).

Localization and expression of ORAI1 in the skeletal muscles from TAM

To analyze the localization of ORAI1 in the skeletal muscles of TAM, we investigated skeletal muscle cryosections from an individual with TAM (II-3a, II-1c) using immunohistochemistry (Fig. 4). SERCA1, an SR protein, was strongly labeled in the aggregates, as previously reported (20,21). ORAI1 and STIM1 co-localized with SERCA1 in the aggregates. Moreover, dihydropyridine receptor (DHPR), which is present in T-tubules, was also involved in the aggregates and co-localized with ORAI1, as expected (21) (Fig. 4).

On western blotting, the expression levels of ORAI1, STIM1, SERCA1 and SERCA2 in the skeletal muscles from an affected individual (II-1c) were similar to that of the skeletal muscles from unaffected individuals (Supplementary Material, Fig. S3).

TAM cells showed constitutive extracellular Ca^{21} influx via the CRAC channel without depletion of SR Ca^{21} stores

To explore whether the identified mutations are pathogenic, we monitored Ca^{2+} entry into myotubes prepared from muscle cells of an affected individual with the c.292G.A (p.Gly98Ser) mutation. Intracellular Ca^{2+} concentration ($[Ca^{2+}]_i$) was monitored using Fura-2 as a Ca^{2+} indicator and was recorded by using fluorescence ratiometry with excitation at 340 and 380 nm. The experiments revealed a significantly higher $[Ca^{2+}]_i$ level in TAM myotubes than in control cells [normal human skeletal

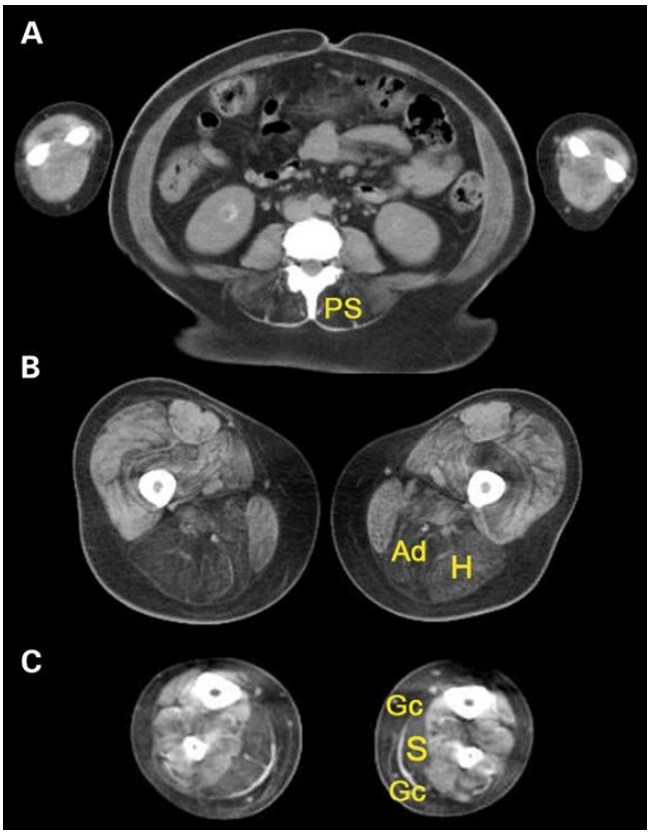

Figure 1. Computed tomographic imaging of TAM. Paraspinal (PS), hamstrings (H), adductor muscles in the thigh (Ad), soleus (S) and gastrocnemius (Gc) muscles of affected individual II-3a were markedly replaced by fat.

muscle cells (SKMCs)] when the extracellular Ca^{2+} concentration was 2 mM, which was assumed to match that of the in vivo environment, and 20 mM (Fig. 5A and B). Upon application of a CRAC channel inhibitor, 50 mM 2-aminoethoxydiphenyl borate [2-APB (25)] or 10 mM 3,5-bistrifluoromethyl pyrazole derivative (BTP2) (26), the $[Ca^{2+}]_i$ levels in TAM myotubes were not elevated (Fig. 5A). Another inhibitor, 1-[2-(4-methoxyphenyl)-2-[3-(4-methoxyphenyl) ethyl-1H-imidazole hydrochloride (SKF-96365), was also effective although the response was slower. These results indicated that the higher Ca^{2+} influx in TAM myotubes occurred via CRAC channels. In addition, an Mn^{2+} quenching assay of intracellular Fura-2 fluorescence was performed (Fig. 5C). Mn^{2+} is known to enter cells via CRAC channels and shows very high affinity to Fura-2. The extracellular Mn^{2+} influx causes quenching of intracellular Fura-2 fluorescence. TAM myotubes showed an Mn^{2+} quenching that was distinct from that of normal myotubes, implicating the activation of CRAC channels. We also examined thapsigargin (TG) treatment to TAM myotubes to induce Ca^{2+} depletion in the SR. TG induced extracellular Ca^{2+} influx in normal myotubes in a dose-dependent manner in extracellular 2 mM Ca^{2+} medium. On the other hand, similar extracellular Ca^{2+} influx levels were observed in TAM myotubes with and without TG treatment (Fig. 5D). Thus, TAM cells showed constitutive Ca^{2+} influx to the cytosol via the CRAC channel without depletion of the SR Ca^{2+} store. It should be noted that slightly higher $[Ca^{2+}]_i$ elevation was observed with higher concentrations of TG treatment (Fig. 5D), indicating that the store-operated Ca^{2+} influx-inducing system may still function in TAM myotubes.

Gly98Ser and Leu138Phe mutations in ORAI1 caused spontaneous activation of the CRAC channel

We also tested the impact of the c.292G.A (Gly98Ser) and c.412C.T (Leu138Phe) mutations in ORAI1 on induction of spontaneous Ca^{2+} influx. $[Ca^{2+}]_i$ was measured at 24–36 h after transfection to HEK293 cells of mutated and wild-type ORAI1 cDNAs. The transfected green fluorescent protein (GFP)-tagged ORAI1 and Myc-tagged ORAI1 localized on the plasma membranes, and the mutated ORAI1 also localized to the cell surface membrane (Fig. 6A). Western blotting of expressed ORAI1 protein showed multiple bands at 25–50 kDa, indicating the presence of different glycosylated forms, similar to previous reports (27,28) (Fig. 6B). Although glycosylated forms of Gly98Ser-mutated ORAI1 were slightly decreased, there were no differences in band patterns observed among Gly98Ser-mutated, Leu138Phe-mutated and wild-type (WT) ORAI1 after PNGase F treatment.

The Gly98Ser and Leu138Phe ORAI1 mutants caused a dramatic elevation of $[Ca^{2+}]_i$ following application of 2 mM Ca^{2+} in the medium when compared with the WT protein (2 mM Ca^{2+} in Fig. 6C). Cells transfected with the Gly98Ser or Leu138Phe mutants exhibited high levels of $[Ca^{2+}]_i$ even under conditions of extracellular Ca^{2+} depletion (0 mM Ca^{2+} region in Fig. 6C). In addition, the Mn^{2+} quenching assay revealed that the cells transfected with Gly98Ser or Leu138 Phe mutants showed distinct Mn^{2+} quenching rates from those transfected with the WT protein (Fig. 6D). It should be noted that the spontaneous Ca^{2+} and Mn^{2+} influx observed in the mutated ORAI1-expressing cells did not require co-expression of STIM1 or TG-induced Ca^{2+} store depletion in the ER. Moreover, the elevated resting $[Ca^{2+}]_i$ induced by both ORAI1 mutants was reduced by application of 2-APB (Supplementary Material, Fig. S4), which indicated the specific activation of CRAC channels. These results clearly demonstrate that both the c.292G.A (Gly98Ser) and c.412C.T (Leu138Phe) mutations in ORAI1 cause constitutive CRAC channel activation in a STIM1-independent manner.

DISCUSSION

Based on the inheritance mode in the affected families and the functional analyses of mutated ORAI1 proteins, we concluded that the constitutive activation of CRAC channels by dominant mutations in ORAI1 caused TAM in the three families. In support of this notion, dominant mutations in STIM1 have been reported to cause TAM by constitutive activation of SOCE (16). In that report, the mutated STIM1 spontaneously clustered and translocated to the plasma membrane independently of Ca^{2+} stores in the SR, and consequently led to activation of the CRAC channel, resulting in higher cytosolic Ca^{2+} levels. More recently, Nesin et al. (18) reported that activating mutations in STIM1 and ORAI1 caused overlapping syndromes of TAM and congenital miosis. Interestingly, the authors suggested that a dominant mutation in ORAI1 caused prolonged activation

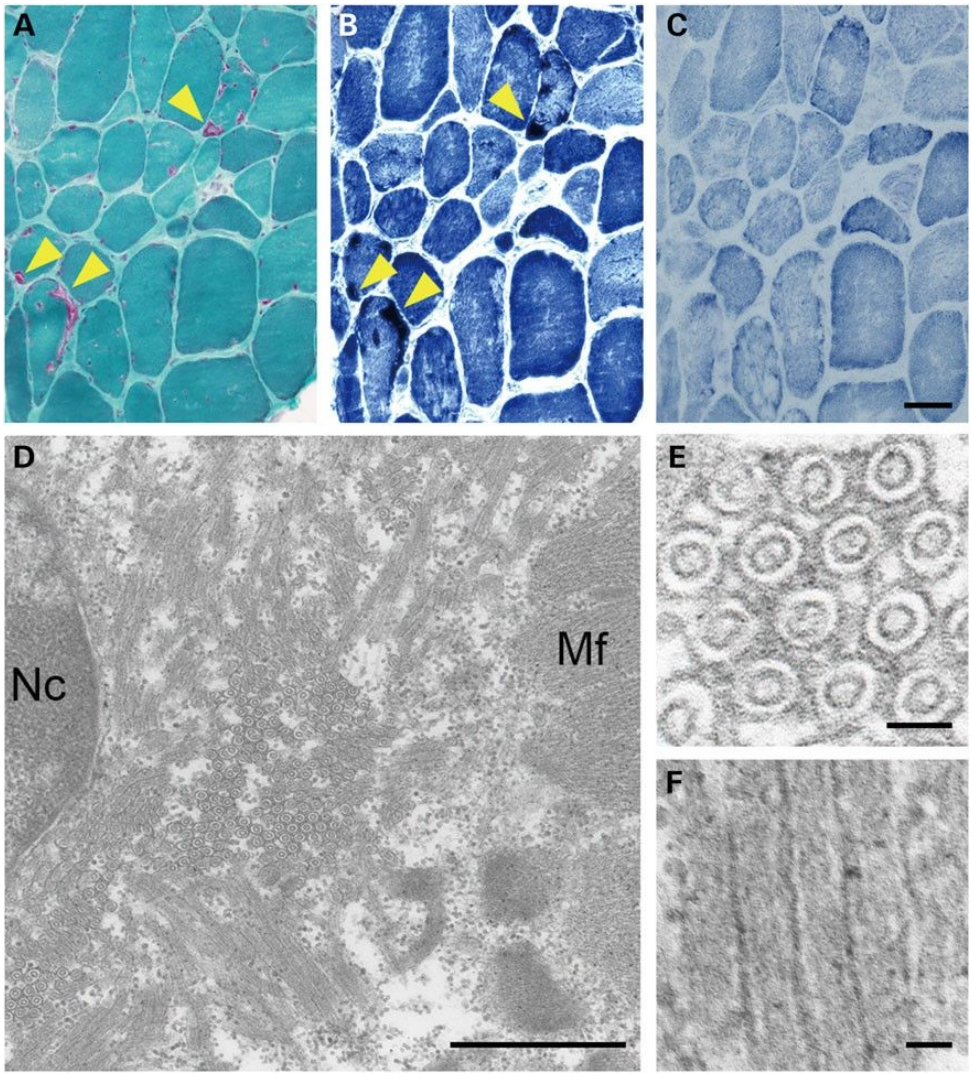

Figure 2. Histology and electron microscopy of a muscle biopsy sample from affected individual II-3a. Histological analysis of transverse sections revealed aggregations with mGt (A) and NADH-TR (B) but not SDH (C) staining. Ultrastructural analysis demonstrated prominent tubular aggregation with double-walled membranes in transversal (D and E) and longitudinal (F) sections. Nc, nucleus; Mf, myofibrils. Arrows, tubular aggregates (TAs). Scale bars, 50 mm (C); 1 mm (D); 100 nm (E); 50 nm (F).

of CRAC channels that required association with STIM1. On the other hand, in the present study, we showed that the two mutations in ORAI1 directly caused constitutive opening of the channel, resulting in higher cytosolic Ca^{2+} influx independent of either Ca^{2+} stores in the SR or STIM1 activation.

ORAI1 is a tetra-spanning TM protein in the plasma membrane (Fig. 3C) (8), and acts as a pore subunit of the CRAC channel (29). The CRAC channel consists of a hexamer of ORAI1 proteins, and the TM helices (TM1 – 4) of each monomer are arranged in three concentric rings. Six TM1 helices make up an inner ring of helices and line the ion pore, while the TM2 and TM3 helices constitute a middle ring that surrounds the TM1 helices (24) (Fig. 3D). The mutation c.292G.A (Gly98Ser) was identified in the TM1 domain directly beside the pore (white residues in Fig. 3D). The other mutation, p.412C.T (Leu138Phe), was identified in the TM2 domain directly facing TM1 (yellow residues in Fig. 3D).

Many studies have elucidated the roles of amino acid residues in TM1 in channel activity as well as in the ion selectivity of SOCE channels (8,29 – 33). In particular, Arg91 is mutated in SCID (13) and is thought to act as both a barrier as well as a provider of electrostatic stabilization to the elongated pore that is controlled via interaction with STIM1, and Glu106 determines ion selectivity (8) (Fig. 3C). Similarly, the importance of Gly98 for channel activity has also been suggested based on in vitro experiments (31). Interestingly, Gly98 has been predicted to be located exactly two a-helical turns from both the Arg91 and Glu106 sites (Fig. 3C). Ala replacement at Gly98 results in failure of channel activity, whereas Asp or Pro replacement at this position results in a negative charge or hydrophilic properties, which in turn cause constitutive channel opening as well as reduced ion selectivity in a STIM1-independent manner (31,33). Our experiments revealed that a Ser replacement of Gly at position 98 may also confer the protein with a hydrophilic

Table 2. Histological characterization of TAM families

	Family A	Family B			Family C
	II-3	I-2	II-1	II-3	II-1
Age at muscle biopsy	42 years	NI	10 years	5 years	42 years
Tubular aggregates	Type I and II fibers	+	Type I and II fibers	2	Type I and II fibers
Fiber size variation	+	NI	+	+	+
Regenerating fibers	+	NI	+	2	+
Increased internal nuclei (% of fibers)	Single 14%	NI	Single 15%	Single 5%	Single, multiple 20%
Type I fiber predominance (% of fibers)	70%	NI	71%	93%	73%

NI, no information.

property that is sufficient to cause constitutive channel activation, similar to the effect of Pro replacement.

In contrast to TM1, the roles of specific amino acid residues in TM2 have not been well investigated. In our experiment, the mutation c.412C.T (p.Leu138Phe) in TM2 also caused constitutive SOCE channel activation. Interestingly, basal $[Ca^{2+}]_i$ levels in Leu138Phe-expressing HEK293 cells were lower than those were in Gly98Ser-expressing cells. Further studies are necessary to fully understand the impact of these mutations on CRAC channels.

Of particular note, the mechanism underlying the muscle weakness caused by a constitutively activated CRAC channel might be associated with altered Ca^{2+} homeostasis in a manner different from that derived from its loss of function. Individuals affected with SCID owing to recessive loss-of-function mutations in ORAI1 or STIM1 were reported to show muscle hypotonia (13 – 15) and decreased Ca^{2+} influx. Transgenic mice with muscle-specific expression of dominant-negative Orai1 have also been reported and exhibited reduced body weight, muscle mass and fiber cross-sectional area, and increased susceptibility to fatigue, which might have been due to SR Ca^{2+} depletion (34). On the other hand, ORAI1-related TAM is caused by elevation of $[Ca^{2+}]_i$ levels in the skeletal muscle cells, similar to STIM1-related TAM. Therefore, preventing excessive extracellular Ca^{2+} influx is a potential therapeutic strategy for TAM.

The mechanism of TA formation in the skeletal muscle has remained elusive thus far. However, our results support the hypothesis that TA formation is related to disordered Ca^{2+} homeostasis. Recent efforts on the identification of causative genes in TA-presenting muscle diseases also provide a clue into this mechanism. Recessive mutations in GFPT1 and DPAGT1, which are both involved in protein N-glycosylation, have been shown to be causative factors of myasthenic syndrome with TAs (35,36). Furthermore, the functional importance of N-glycosyl modification of STIM1 was recently reported (27). A mutation at the N-glycosylation site in STIM1 results in a strong gain of function by increasing the number of active Orai1 channels, indicating the significance of N-glycosylation for the function of STIM. Thus, activation of CRAC channels may result in the formation of TAs in skeletal muscles, although further analyses of CRAC channel activation in skeletal muscles of GFPT1- and DPAGT1-mutated individuals are required to confirm this hypothesis.

The finding of c.292G.A (p.Gly98Ser) ORAI1 mutation in two unrelated families would not be due to a founder effect. This mutation in Family A probably occurred de novo in II-3a because individual I-1a did not show any symptoms of myopathy in his lifetime and individual I-2a does not have the mutation. Regarding to the mutation in Family B, we could not judge whether it is de novo or not, because of limited information.

The clinical and histological features of ORAI1-mutated TAM are similar to those of TAM caused by STIM1 mutations, regarding onset of the disease, progression of weakness, involvement of contractures, presence of TAs in both type I and type II fibers, fiber size variation and type I fiber predominance. However, the patterns of affected muscles are slightly different: individuals with ORAI1-mutated TAM exhibit diffuse weakness in all limbs, and the characteristic patterns in the selectivity of atrophy, whereas those with STIM1-mutated TAM show proximal muscle weakness only in the lower limbs (16). Severe ankle contractures and a rigid spine were common characteristics observed in the families included in the present study, although STIM1-mutated TAM was not likely. Furthermore, eye-movement defects, which were reported in STIM1-mutated TAM individuals studied by Böhm et al. (16), congenital miosis, bleeding diathesis and thrombocytopenia are not detected in individuals with ORAI1-mutated TAM. This discrepancy could be explained by differences in the expression patterns of STIM1, ORAI1 and their homologues (ORAI2, ORAI3 and STIM2).

Although ORAI1 transcripts are expressed in multiple tissues, including the skeletal muscle, in humans and mice (28,37), it is not clear why other organs were saved. Orai1 expression is low in the brain (28); therefore, the intellectual disability observed in individual III-2a in the present study might be unrelated to the ORAI1 mutation. The calcification in the brain of individual II-3a could be attributed to long-term hypocalcemia.

Another characteristic clinical feature of ORAI1-mutated TAM is hypocalcemia. Serum Ca^{2+} levels are controlled mainly through the action of PTH and 1,25(OH)2D3 (38). These hormones increase the serum Ca^{2+} level through their actions on the bone, kidney and intestine; impaired activity of either hormone leads to hypocalcemia. In this study, the five individuals analyzed showed mildly decreased serum Ca^{2+} levels and rather low PTH levels, which were nonetheless within the normal range. PTH is secreted by parathyroid cells and the secretion volume is controlled by the extracellular Ca^{2+} intensity. In ORAI1-mutated TAM individuals, PTH levels are improperly low in spite of the presence of hypocalcemia. This condition is classified as PTH-insufficient hypoparathyroidism on the basis of the criteria for the differential diagnosis of hypocalcemia

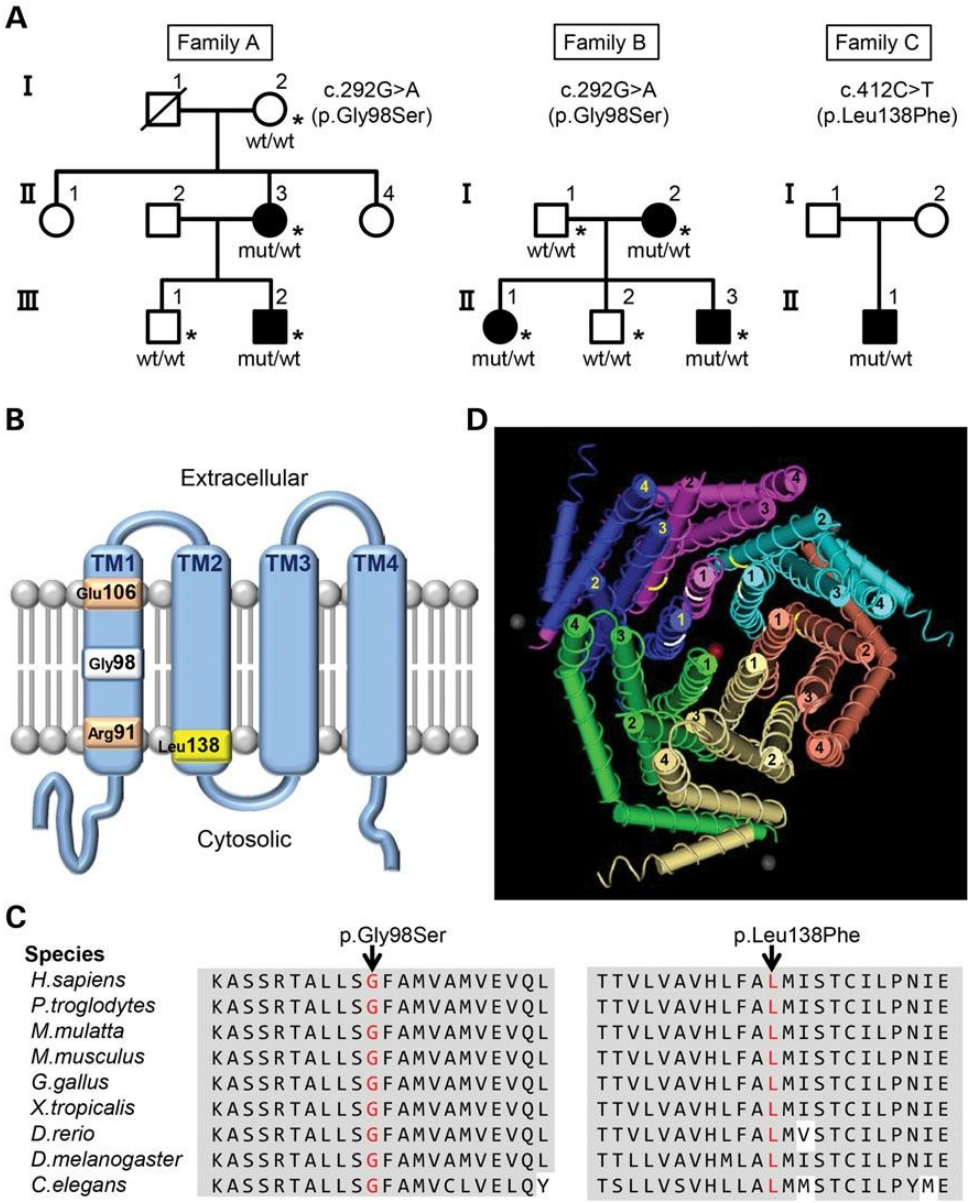

Figure 3. Genetic analysis of autosomal-dominant TAM and modeling the effects of mutations in ORAI1. (A) Pedigrees indicated dominant inheritance of TAM, and sequence analysis confirmed the segregation of the heterozygous mutations with the disease. * Individuals who were analyzed by exome sequencing. ORAI1 genotypes are shown below the individuals in the pedigrees. (B) Schematic depiction of a single ORAI1 subunit. Upper side, extracellular; lower side, cytosolic. Gly98Ser and Leu138Phe are highlighted in white and yellow, respectively. Arg91 and Glu106, critical amino acids for channel function, are shown in orange. (C) Amino acid sequence conservation of ORAI1. The affected amino acids (red) have been highly conserved during evolution. (D) Crystal structure of the Drosophila melanogaster SOCE channel. The crystal structure was obtained from the Molecular Modeling Database (MMDB ID: 105660). This structure shows that the channel is formed from a hexamer of ORAI subunits. Each subunit is represented in a different color. The ion pore is located at the center of the channel (red circle), and the transmembrane helices are arranged in three concentric rings. Six TM1 helices (1) make up an inner ring of helices and line the ion pore. The TM2 (2) and TM3 (3) helices constitute a middle ring that surrounds the transmembrane portion of the TM1 helices and separates them from TM4 helices (4), which are arranged in an outer ring. The position of Gly98 in TM1 is highlighted in white, and that of Leu138 in TM2 is highlighted in yellow.

(39). Although the precise pathomechanisms are not known, ORAI1-mutated TAM might cause decreased PTH secretion.

In summary, we identified heterozygous missense mutations in ORAI1 that cause TAM with hypocalcemia via constitutive activation of CRAC channels. Our results, together with those of previous reports (16,19), will contribute to establishing a new disease entity whose pathomechanism is associated with intracellular Ca^{2+} elevation to induce muscle weakness and TA formation in the skeletal muscles. The detailed pathomechanism linking intracellular Ca^{2+} elevation to muscle weakness and TA formation in the skeletal muscles should be clarified.

MATERIALS AND METHODS

Materials

Three unrelated Japanese families affected by TAM were selected based on pathological examinations. All clinical

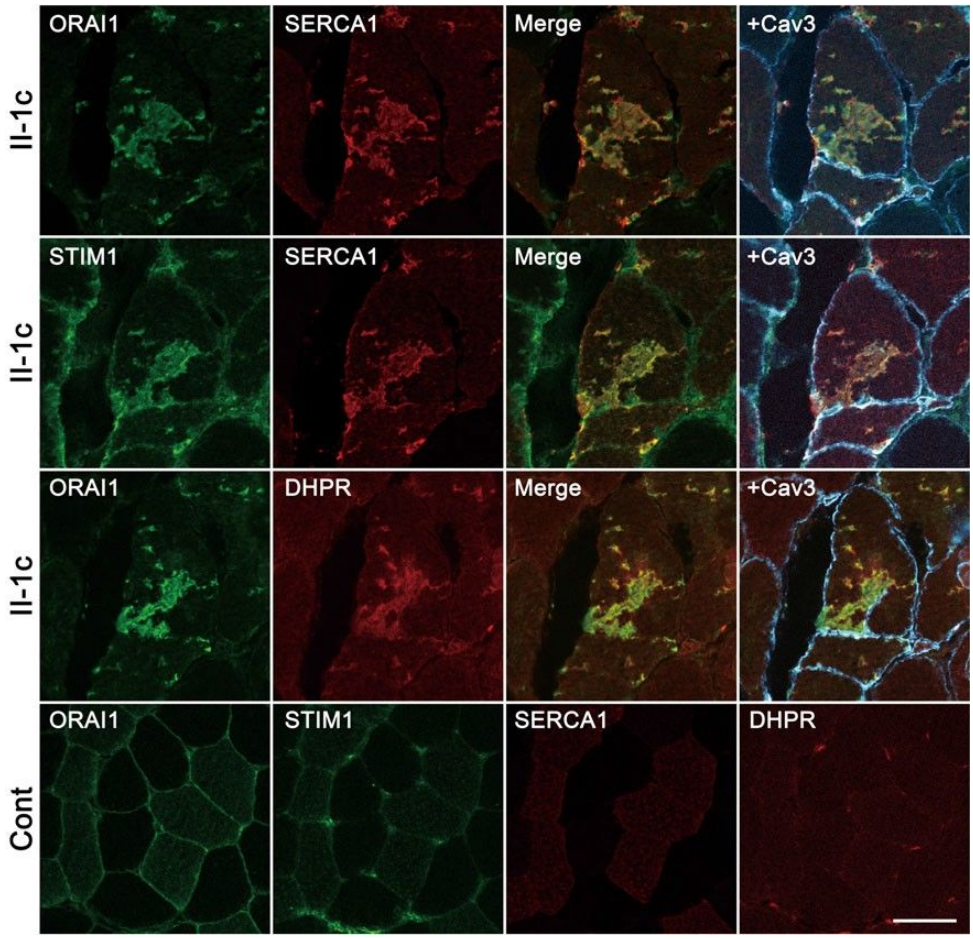

Figure 4. Immunohistochemical analysis of the skeletal muscle from an individual affected with TAM (II-1c). Immunofluorescence showed that SERCA1, ORAI1, STIM1 and DHPR localized in TAs. Scale bar, 50 mm. Cont, skeletal muscle from an unaffected person.

materials used in this study were obtained with written informed consent for research use. All experiments performed in this study were approved by the Ethical Committee of the National Center of Neurology and Psychiatry (NCNP).

Histological analyses

Muscle samples were taken from the biceps brachii. Muscles were frozen in liquid nitrogen-cooled isopentane and stored at 2808C. Serial frozen sections (10 mm thick) were histochemically stained with mGt, NADH-TR or SDH. Immunohistochemistry was performed using 8 mm thick serial frozen sections according to the standard protocols (40). The primary antibodies used were as follows: anti-Orai1 (O8264, 1:200 dilution; Sigma-Aldrich), anti-STIM1 (H-180, 1:50; Santa Cruz Biotechnology), anti-SERCA1 (VE121G9, 1:200; Abcam), anti-RYR1 (XA7B6, 1:200; Developmental Studies Hybridoma Bank) and anti-DHPR (IIID5E1, 1:100; Developmental Studies Hybridoma Bank). Anti-caveolin antibody (N-18, 1:100; Santa Cruz Biotechnology) was also used for labeling the sarcolemma (plasma membrane of the muscle fiber). After incubation with primary antibodies, the sections were incubated with appropriate Alexa Fluor 488-, 568- and 647-conjugated secondary antibodies (1:600; Invitrogen). The sections were observed under an LSM710 confocal laser microscope (Carl Zeiss).

Electron microscopy

Muscle specimens were fixed in 2.5% glutaraldehyde and post-fixed with 2% osmium tetroxide. Ultrathin sections of muscles stained with uranyl acetate and lead citrate were observed under a transmission electron microscope (FEI; Hillsboro, OR, USA).

Exome sequencing

Genomic DNA was isolated from muscle specimens or peripheral blood lymphocytes using standard techniques. Exome sequencing was carried out in subjects I-2a, II-3a, III-1a and III-2a from Family A, and in subjects I-1b, I-2b, II-1b, II-2b and II-3b from Family B. Exons of genomic DNA samples were captured and sequenced using Agilent in-solution enrichment methodology and the Illumina HiSeq1000 sequencer. Briefly, 3 mg of each genomic DNA sample was fragmented to 150 – 200 bp by sonication. Paired-end fragment libraries were prepared by using a kit from Agilent Technologies. Purified libraries (750 ng) were hybridized to the SureSelect oligonucleotide probe capture library for 24 h (Sure Select Human All Exon kit V4, 50 Mb; Agilent). The captured DNA sample was then sequenced on an Illumina HiSeq1000 as paired-end 100-base reads. Image analysis and base calling were performed using

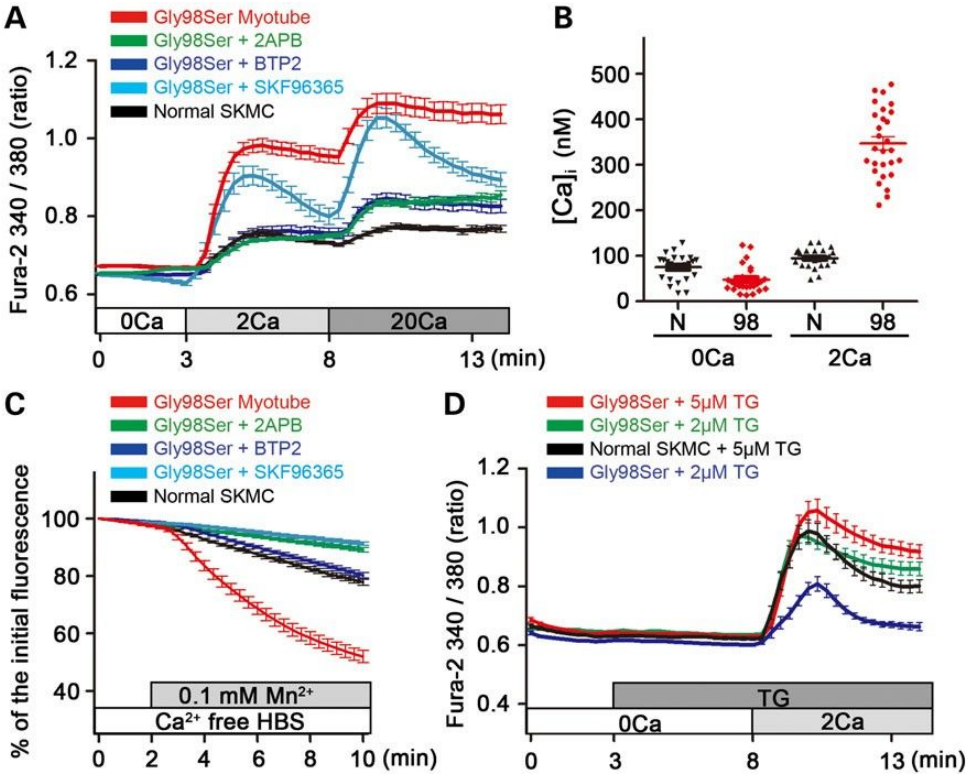

Figure 5. Cytosolic Ca^{2+} measurement and Mn^{2+} quenching assay of myotubes from an individual affected with TAM. (A) Cytosolic Ca^{2+} was measured with Fura-2 in myotubes from affected individual II-3b (red: Gly98Ser myotube, n ¼ 29 cells) and normal human skeletal muscle (black: normal SKMC, n ¼ 26 cells), using single-cell Ca^{2+} imaging. First, cells were placed in an extracellular solution containing 0 mM Ca^{2+} (0Ca). After 3 min, the extracellular solution was changed to 2 mM Ca^{2+} (2Ca), and then to 20 mM Ca^{2+} (20Ca) at 8 min. Myotubes from affected individual were experimentally treated with 50 mM 2-APB (green: Gly98Ser +2APB, n ¼ 17 cells), with 10 mM BTP-2 (blue: Gly98Ser +BTP2, n ¼ 17 cells) or with 20 mM SKF96365 (cyan: Gly98Ser +SKF96365, n ¼ 15). (B) Resting $[Ca^{2+}]_i$ in myotubes from TAM. 0Ca, N: normal SKMC98, n ¼ 26; 0Ca, 98: Gly98Ser myotube, n ¼ 25; 2Ca, N: normal SKMC98, n ¼ 27; 2Ca, 98: Gly98Ser myotube, n ¼ 28. (C) Fluorescence quenching due to the Mn^{2+} influx was observed in Fura-2-loaded Gly98Ser myotubes (red, n ¼ 32 cells) and normal SKMC myotubes (black, n ¼ 21 cells), using single-cell Ca^{2+} imaging. Mn^{2+} (0.1 mM) was added to nominally Ca^{2+}-free HBS. Gly98Ser myotubes were treated with 50 mM 2-APB (green: Gly98Ser + 2APB, n ¼ 17 cells), with 10 mM BTP-2 (blue: Gly98Ser + BTP2, n ¼ 17 cells) or with 20 mM SKF96365 (cyan: Gly98Ser +SKF96365, n ¼ 39 cells). (D) Store-operated Ca^{2+} entry in myotubes. Ca^{2+} stores in the SR were depleted by treatment with 2 mM TG or 5 mM TG. Red, Gly98Ser myotubes with 5 mM TG, n ¼ 20 cells; green, Gly98Ser myotubes with 2 mM TG, n ¼ 25 cells; black, normal SKMC myotubes with 5 mM TG, n ¼ 27 cells; blue, normal SKMC myotubes with 2 mM TG, n ¼ 25 cells.

the Illumina Real-Time Analysis Pipeline version 1.13, with default parameters.

Bioinformatics analysis

Reads were aligned to hg19 with Burrows-Wheeler Aligner (41). Duplicate reads were removed using Picard for downstream analysis. Local realignments around indels and regions for low base quality scores were performed with the Genome Analysis Toolkit (42) (GATK) for recalibration. Single-nucleotide variants and small indels were identified using GATK UnifiedGenotyper (version 1.6) and filtered according to the Broad Institute's best-practice guidelines. Genetic variation was annotated with the NCNP in-house pipeline (amelief), consisting of gene annotation [using ANNOVAR (43)] and detection of known polymorphisms using dbSNP135, the 1000 Genomes, NHLBI Exome Variant Server (ESP5400) and HGVD for Japanese genetic variants. Candidates of mutations identified in exome sequencing were validated by Sanger sequencing on an ABI Prism 3130 DNA Analyzer (Applied Biosystems). Segregation analysis of within-family variants was carried out using the primer sets designed to amplify exons corresponding to the sequence under accession NM_032790. PCR conditions and primer sequences for ORAI1 mutation analysis are available upon request.

Western blotting of the skeletal muscles

Frozen skeletal muscles were sliced and suspended in the buffer containing 10 mM Tris – HCl, 0.6 mM KCl and 1 mM EDTA. After a centrifugation at 1200g for 10 min, the supernant was centrifuged at 20 000g for 90 min. The resulting pellet was solubilized in laemmli's sample buffer. An equal amount of proteins (10 mg) were electrophoresed on 4 – 20% polyacrylamide gradient gel (Bio-Rad). The primary antibodies used were as follows: anti-Orai1 (O8264, 1:1000 dilution; Sigma-Aldrich), anti-STIM1 (H-180, 1:500; Santa Cruz Biotechnology), anti-SERCA1 (VE121G9, 1:1000; Abcam) and anti-caveolin-3 antibody (Clone 26, 1:1000; BD Transduction Laboratories). The blots were coupled with the peroxidase-conjugated secondary antibodies, and developed using the ECL detection kit (Millipore Corporation).

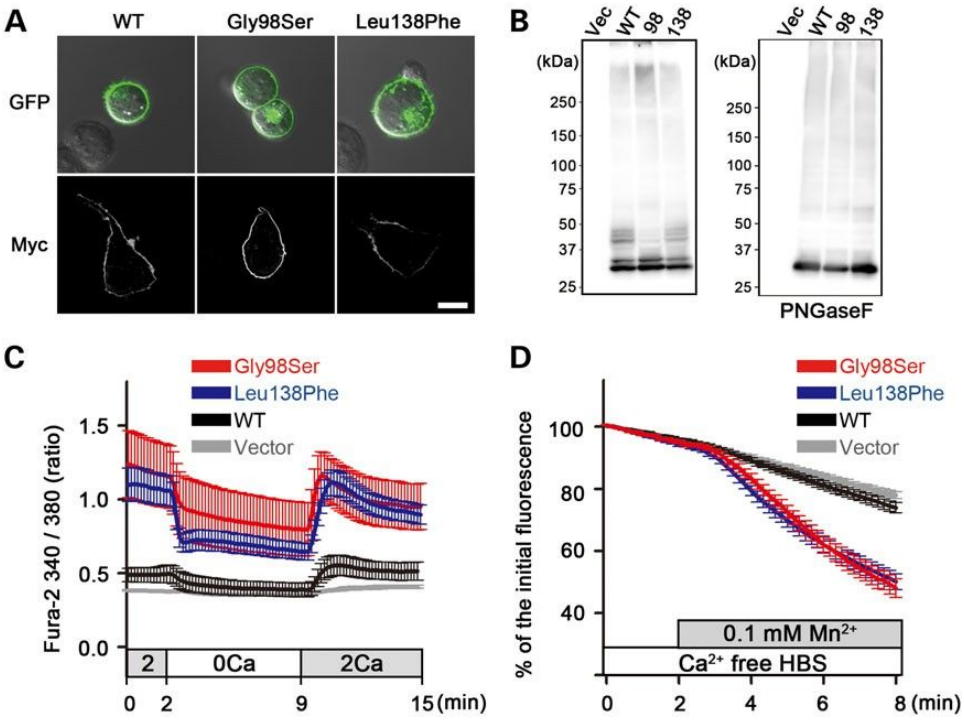

Figure 6. Characterization of ORAI1 mutants. (A) Localization of transfected ORAI1 constructs. HEK 293 cells were transfected with EGFP-tagged ORAI1 (WT, Gly98Ser, Leu138Phe) or Myc-tagged ORAI1 (WT, Gly98Ser, Leu138Phe). Upper panels, phase contrast (white and black) and GFP fluorescence (green). Lower panels, fluorescent micrographs for Myc-ORAI1. (B) Western blot of Myc-tagged ORAI1 proteins expressed in HEK cells (left panel). PGNaseF treatment (right panel). Vec, vector; 98, ORAI1 with Gly98Ser; 138, ORAI1 with Leu138Phe. (C) Cytosolic Ca^{2+} was measured in HEK293 cells expressing WT ORAI1 (black, n ¼ 35 cells) and ORAI1 mutants, Gly98Ser (red, n ¼ 28 cells) or Leu138Phe (blue, n ¼ 37 cells) and vector (gray, n ¼ 32 cells). Extracellular solution was first changed to 0 mM Ca^{2+} (0Ca) then to 2 mM Ca^{2+} (2Ca). (D) Mn^{2+} quenching assay. After application of 0.1 mM Mn^{2+} solution, fluorescence quenching of Fura-2 was observed in HEK293 cells expressing WT ORAI1 (black, n ¼ 34 cells) and ORAI1 mutants, G98S (red, n ¼ 42 cells) or L138F (blue, n ¼ 43 cells), and vector (gray, n ¼ 46 cells).

Construction of ORAI1 mutants

The construction of WT and mutant human ORAI1 cDNA in the expression vectors pCMV-Myc and pEGFP-N1 (Clontech) was described previously (44). A Myc tag was fused to the N-terminus of ORAI1, and a EGFP tag was fused to the C-terminus of ORAI1 without its termination codon. All ORAI1 mutants were generated with the Quick Change Site-Directed Mutagenesis Kit (Stratagene). Information on primer sequences and conditions for cloning and PCR is available upon request.

Transfection of ORAI1 constructs to HEK293 cells

HEK293 cells obtained from the RIKEN Bioresource Center were maintained in Dulbecco's modified Eagle medium (D-MEM; Wako) supplemented with 10% fetal bovine serum (FBS; Life Technologies), 2 mM glutamine, 30 units/ml penicillin and 30 mg/ml streptomycin. ORAI1 constructs were transfected using X-tremeGENE9 (Roche Applied Science). For observation of ORAI1 mutants in cells, EGFP-tagged ORAI1 constructs were also introduces. For western blots, Myc-tagged ORAI1 constructs were introduced. For $[Ca^{2+}]_i$ measurement, Myc-tagged ORAI1 constructs were co-transfected with the pDsRed-Monomer-C1 vector (Clontech).

Localization of ORAI1 protein in HEK293 cells

Confocal and phase contrast images were taken at 2 days post-transfection on an LSM-710 microscope (Carl Zeiss).

Expression of ORAI1 protein in HEK293 cells

HEK293 cells were harvested at 2 days post-transfection. The cells were lysed with Tris-buffered saline containing 1% Triton X-100 and protease inhibitors (cOmplete EDTA-free; Roche). The extracts were boiled in the presence of sodium dodecyl sulfate sample buffer and subjected to western blot analysis. An equal amount of the supernatant fractions (75 mg proteins) was subjected to SDS–PAGE (SuperSep Ace, 5–20% gradient gel, Wako). The protein-transferred membrane was incubated with anti-Myc antibody (9E10, 1:2000; Wako). After incubating with anti-mouse IgG (H+L) secondary antibody conjugated with horseradish peroxidase (GE Healthcare), the expression of ORAI1-Myc was detected using Immunostar Zeta (Wako). To confirm glycosylated patterns of ORAI1, lysate samples (75 mg each) were incubated with PNGase F (Roche; 3 U/sample), for 6 h at 378C and subjected to SDS–PAGE.

Cell culture for $[Ca^{21}]_i$ measurement and Mn^{21} quenching assay

Skeletal muscle cells of a TAM-affected individual (II-3b) and normal human SKMCs (Clonetics) were seeded onto collagen-coated glass cover slips and cultured in D-MEM/Ham's F-12 medium (1:1) supplemented with 20% FBS (Invitrogen), 100 units/ml penicillin and 100 mg/ml streptomycin. After the cells reached confluence, the culture media were switched to differentiation media [D-MEM/Ham's F-12 Medium (1:1)

supplemented with 5% horse serum (Invitrogen), 100 units/ml penicillin and 100 mg/ml streptomycin]. Six days following induction of differentiation, myotubes were used for $[Ca^{2+}]_i$ imaging or a Mn^{2+} quenching assay.

Transfected HEK293 cells were lifted using trypsin and seeded onto poly-L-lysine-coated glass cover slips at 8 h post-transfection. Note that trypsinized cells were cultured in low-Ca^{2+} D-MEM (Life Technologies), which was supplemented with 10% FBS, 2 mM glutamine, 30 units/ml penicillin, 30 mg/ml streptomycin, 0.2 mM $CaCl_2$ and 10 mM La^{3+}, to prevent Ca^{2+} overload-induced cell death (31). $[Ca^{2+}]_i$ imaging was performed at 24–36 h after transfection.

Measurement of changes in $[Ca^{21}]_i$

HEK293 cells on cover slips were loaded with Fura-2 by incubation in low-Ca^{2+} D-MEM containing 5 mM Fura-2/AM (Dojindo Laboratories) at 378C for 40 min, and washed with imaging solution (2Ca). The cover slips were then placed in a perfusion chamber mounted on the stage of a microscope (Axio-observer Z1; Carl Zeiss). Transfected cells were identified by detection of fluorescence from pDsRed-Monomer. Fura-2 fluorescence images of the cells were recorded and analyzed with Physiology software (Carl Zeiss). The 340/380 nm ratios of images were recorded at 10 s intervals. The compositions of $[Ca^{2+}]_i$ imaging solutions are listed in Supplementary Material, Table S6. Fura-2/AM was loaded into skeletal myotubes on cover slips in the same manner used for HEK293 cells but in nominally Ca^{2+}-free HEPES-buffered saline (HBS) (Supplementary Material, Table S6). The cover slips were then placed in a perfusion chamber mounted on the stage of the microscope (IX70; Olympus). Fura-2 fluorescence images of the myotubes were recorded and analyzed with MetaMorph Imaging Software (Molecular Devices). The images were recorded at 20 s intervals. Compositions of $[Ca^{2+}]_i$ imaging solutions are listed in Supplementary Material, Table S6. For measurement of the resting $[Ca^{2+}]_i$, Fura-2/AM was loaded to myotubes at 0Ca and 2Ca, respectively, and $[Ca^{2+}]_i$ imaging was performed. The resting $[Ca^{2+}]_i$ was calculated as previously reported (45).

Mn^{21} quenching assay

Extracellular Mn^{2+} entry was measured through monitoring the decline in the fluorescence intensity of Fura-2 at an isosbestic excitation wavelength of 360 nm and recording the emitted fluorescence at 510 nm (46) by using the same system as used for the $[Ca^{2+}]_i$ measurement. The compositions of nominally Ca^{2+}-free HBS and 0.1 mM $MnCl_2$ solutions are listed in Supplementary Material, Table S6.

Statistical analysis

Graphics were prepared and statistical analyses were performed with GraphPad Prism (GraphPad Software). Data are presented as mean + SEM. All data were analyzed using unpaired t-tests in comparisons between two samples and ANOVA in comparisons among three samples.

WEB RESOURCES

Online Mendelian Inheritance in Man (OMIM), http://www.omim.org/.
dbSNP, http://www.ncbi.nlm.nih.gov/projects/SNP/.
1000 Genomes Project, http://www.1000genomes.org/.
NHLBI Exome Sequencing Project (ESP) Exome Variant Server, http://eversusgs.washington.edu/EVS/.
HGVD, http://www.genome.med.kyoto-u.ac.jp/SnpDB/.
MutationTaster, http://www.mutationtaster.org/.
SIFT, http://sift.jcvi.org.
PolyPhen-2, http://genetics.bwh.harvard.edu/pph2/.
MMDB, http://www.ncbi.nlm.nih.gov/Structure/MMDB/mmdb.shtml.
BWA, http://bio-bwa.sourceforge.net/.
Picard, http://picard.sourceforge.net/.
GATK, http://www.broadinstitute.org/gatk/.
ANNOVAR, http://www.openbioinformatics.org/annovar/.

SUPPLEMENTARY MATERIAL

Supplementary Material is available at HMG online.

ACKNOWLEDGEMENTS

We thank T. Uchiumi, K. Goto, A. Kaminaga, K. Tatezawa and M. Ogawa for technical assistance. The antibodies XA7B6 for anti-RYR1 and IIID5E1 for anti-DHPR developed by K.P. Campbell were obtained from the Developmental Studies Hybridoma Bank developed under auspices of the NICHD and maintained by the University of Iowa, Department of Biology, Iowa City, IA52242.

Conflict of Interest statement. None declared.

FUNDING

This work was supported by an Intramural Research Grant (26-8, 25-5, 23-4) for Neurological and Psychiatric Disorders of the NCNP (to S.N., Y.H., I.N.) and by a Research on Applying Health Technology grant (H23-JITSUYOUKA(NANBYOU)-IPPAN-008, H26-ITAKU(NAN)-IPPAN-081) from the Ministry of Health, Labour and Welfare (to I.N.).

REFERENCES

1. Shoback, D. (2008) Clinical practice. Hypoparathyroidism. New Eng. J. Med., 359, 391–403.
2. Rossi, A.E. and Dirksen, R.T. (2006) Sarcoplasmic reticulum: the dynamic calcium governor of muscle. Muscle Nerve, 33, 715–731.
3. Vig, M., Peinelt, C., Beck, A., Koomoa, D.L., Rabah, D., Koblan-Huberson, M., Kraft, S., Turner, H., Fleig, A., Penner, R. and Kinet, J.P. (2006) CRACM1 is a plasma membrane protein essential for store-operated Ca^{2+} entry. Science, 312, 1220–1223.
4. Yeromin, A.V., Zhang, S.L., Jiang, W., Yu, Y., Safrina, O. and Cahalan, M.D. (2006) Molecular identification of the CRAC channel by altered ion selectivity in a mutant of Orai. Nature, 443, 226–229.
5. Liou, J., Kim, M.L., Heo, W.D., Jones, J.T., Myers, J.W., Ferrell, J.E. and Meyer, T. (2005) STIM is a Ca^{2+} sensor essential for Ca^{2+}-store-depletion-triggered Ca^{2+} influx. Curr. Biol., 15, 1235–1241.
6. Roos, J., DiGregorio, P.J., Yeromin, A.V., Ohlsen, K., Lioudyno, M., Zhang, S., Safrina, O., Kozak, J.A., Wagner, S.L., Cahalan, M.D. et al. (2005) STIM1, an essential and conserved component of store-operated Ca^{2+} channel function. J. Cell Biol., 169, 435–445.
7. Zhang, S.L., Yu, Y., Roos, J., Kozak, J.A., Deerinck, T.J., Ellisman, M.H., Stauderman, K.A. and Cahalan, M.D. (2005) STIM1 is a Ca^{2+} sensor that

activates CRAC channels and migrates from the Ca^{2+} store to the plasma membrane. Nature, 437, 902–905.
8. Prakriya, M., Feske, S., Gwack, Y., Srikanth, S., Rao, A. and Hogan, P.G. (2006) Orai1 is an essential pore subunit of the CRAC channel. Nature, 443, 230–233.
9. Stathopulos, P.B., Li, G.-Y., Plevin, M.J., Ames, J.B. and Ikura, M. (2006) Stored Ca^{2+} depletion-induced oligomerization of stromal interaction molecule 1 (STIM1) via the EF-SAM region: an initiation mechanism for capacitive Ca^{2+} entry. J. Biol. Chem., 281, 35855–35862.
10. Luik, R.M., Wu, M.M., Buchanan, J. and Lewis, R.S. (2006) The elementary unit of store-operated Ca^{2+} entry: local activation of CRAC channels by STIM1 at ER-plasma membrane junctions. J. Cell Biol., 174, 815–825.
11. Park, C.Y., Hoover, P.J., Mullins, F.M., Bachhawat, P., Covington, E.D., Raunser, S., Walz, T., Garcia, K.C., Dolmetsch, R.E. and Lewis, R.S. (2009) STIM1 clusters and activates CRAC channels via direct binding of a cytosolic domain to Orai1. Cell, 13, 876–890.
12. Wu, M.M., Buchanan, J., Luik, R.M. and Lewis, R.S. (2006) Ca^{2+} store depletion causes STIM1 to accumulate in ER regions closely associated with the plasma membrane. J. Cell Biol., 174, 803–813.
13. Feske, S., Gwack, Y., Prakriya, M., Srikanth, S., Puppel, S.-H., Tanasa, B., Hogan, P.G., Lewis, R.S., Daly, M. and Rao, A. (2006) A mutation in Orai1 causes immune deficiency by abrogating CRAC channel function. Nature, 441, 179–185.
14. McCarl, C.A., Picard, C., Khalil, S., Kawasaki, T., Röther, J., Papolos, A., Kutok, J., Hivroz, C., Ledeist, F., Plogmann, K., Ehl, S. et al. (2009) ORAI1 deficiency and lack of store-operated Ca^{2+} entry cause immunodeficiency, myopathy, and ectodermal dysplasia. J. Allergy Clin. Immunol., 124, 1311–1318.
15. Picard, C., McCarl, C.-A., Papolos, A., Khalil, S., Lüthy, K., Hivroz, C., LeDeist, F., Rieux-Laucat, F., Rechavi, G., Rao, A. et al. (2009) STIM1 mutation associated with a syndrome of immunodeficiency and autoimmunity. New Eng. J. Med., 360, 1971–1980.
16. Böhm, J., Chevessier, F., Maues De Paula, A., Koch, C., Attarian, S., Feger, C., Hantaï, D., Laforêt, P., Ghorab, K., Vallat, J.M. et al. (2013) Constitutive activation of the calcium sensor STIM1 causes tubular-aggregate myopathy. Am. J. Hum. Genet., 92, 271–278.
17. Jain, D., Sharma, M.C., Sarkar, C., Suri, V., Sharma, S.K., Singh, S. and Das, T.K. (2008) Tubular aggregate myopathy: a rare form of myopathy. J. Clin. Neurosci., 15, 1222–1226.
18. Nesin, V., Wiley, G., Kousi, M., Ong, E.C., Lehmann, T., Nicholl, D.J., Suri, M., Shahrizaila, N., Katsanis, N., Gaffney, P.M., Wierenga, K.J. and Tsiokas, L. (2014) Activating mutations in STIM1 and ORAI1 cause overlapping syndromes of tubular myopathy and congenital miosis. Proc. Natl Acad. Sci. USA, 11, 4197–4202.
19. Misceo, D., Holmgren, A., Louch, W.E., Holme, P.A., Mizobuchi, M., Morales, R.J., De Paula, A.M., Stray-Pedersen, A., Lyle, R., Dalhus, B. et al. (2014) A dominant STIM1 mutation causes Stormorken syndrome. Hum. Mutat., 35, 556–564.
20. Chevessier, F., Marty, I., Paturneau-Jouas, M., Hantaï, D. and Verdière-Sahuqué, M. (2004) Tubular aggregates are from whole sarcoplasmic reticulum origin: alterations in calcium binding protein expression in mouse skeletal muscle during aging. Neuromus. Disord., 14, 208–216.
21. Chevessier, F., Bauché-Godard, S., Leroy, J.-P., Koenig, J., Paturneau-Jouas, M., Eymard, B., Hantaï, D. and Verdière-Sahuqué, M. (2005) The origin of tubular aggregates in human myopathies. J. Pathol., 207, 313–323.
22. Salviati, G., Pierobon-Bormioli, S., Betto, R., Damiani, E., Angelini, C., Ringel, S.P., Salvatori, S. and Margreth, A. (1985) Tubular aggregates: sarcoplasmic reticulum origin, calcium storage ability, and functional implications. Muscle Nerve, 8, 299–306.
23. Schiaffino, S. (2012) Tubular aggregates in skeletal muscle: just a special type of protein aggregates? Neuromuscul. Disord., 22, 199–207.
24. Hou, X., Pedi, L., Diver, M.M. and Long, S.B. (2012) Crystal structure of the calcium release-activated calcium channel Orai. Science, 338, 1308–1313.
25. Prakriya, M. and Lewis, R.S. (2001) Potentiation and inhibition of Ca^{2+} release-activated Ca^{2+} channels by 2-aminoethyldiphenyl borate (2-APB) occurs independently of IP(3) receptors. J. Physiol., 536, 3–19.
26. Ishikawa, J., Ohga, K., Yoshino, T., Takezawa, R., Ichikawa, A., Kubota, H. and Yamada, T. (2003) A pyrazole derivative, YM-58483, potently inhibits store-operated sustained Ca^{2+} influx and IL-2 production in T lymphocytes. J. Immunol., 170, 4441–4449.
27. Kilch, T., Alansary, D., Peglow, M., Dörr, K., Rychkov, G., Rieger, H., Peinelt, C. and Niemeyer, B.A. (2013) Mutations of the Ca^{2+}-sensing stromal interaction molecule STIM1 regulate Ca^{2+} influx by altered oligomerization of STIM1 and by destabilization of the Ca^{2+} channel Orai1. J. Biol. Chem., 288, 1653–1664.
28. Gwack, Y., Srikanth, S., Feske, S., Cruz-Guilloty, F., Oh-hora, M., Neems, D.S., Hogan, P.G. and Rao, A. (2007) Biochemical and functional characterization of Orai proteins. J. Biol. Chem., 282, 16232–16243.
29. Zhou, Y., Ramachandran, S., Oh-Hora, M., Rao, A. and Hogan, P.G. (2010) Pore architecture of the ORAI1 store-operated calcium channel. Proc. Natl Acad. Sci. USA, 107, 4896–4901.
30. Muik, M., Frischauf, I., Derler, I., Fahrner, M., Bergsmann, J., Eder, P., Schindl, R., Hesch, C., Polzinger, B., Fritsch, R. et al. (2008) Dynamic coupling of the putative coiled-coil domain of ORAI1 with STIM1 mediates ORAI1 channel activation. J. Biol. Chem., 283, 8014–8022.
31. Zhang, S.L., Yeromin, A.V., Hu, J., Amcheslavsky, A., Zheng, H. and Cahalan, M.D. (2011) Mutations in Orai1 transmembrane segment 1 cause STIM1-independent activation of Orai1 channels at glycine 98 and channel closure at arginine 91. Proc. Natl Acad. Sci. USA, 108, 17838–17843.
32. McNally, B.A., Somasundaram, A., Yamashita, M. and Prakriya, M. (2012) Gated regulation of CRAC channel ion selectivity by STIM1. Nature, 482, 241–245.
33. Zheng, H., Zhou, M.-H., Hu, C., Kuo, E., Peng, X., Hu, J., Kuo, L. and Zhang, S.L. (2013) Differential roles of the C and N termini of Orai1 protein in interacting with stromal interaction molecule 1 (STIM1) for Ca^{2+} release-activated Ca^{2+} (CRAC) channel activation. J. Biol. Chem., 288, 11263–11272.
34. Wei-Lapierre, L., Carrell, E.M., Boncompagni, S., Protasi, F. and Dirksen, R.T. (2013) Orai1-dependent calcium entry promotes skeletal muscle growth and limits fatigue. Nat. Commun., 4, 2805.
35. Senderek, J., Müller, J.S., Dusl, M., Strom, T.M., Guergueltcheva, V., Diepolder, I., Laval, S.H., Maxwell, S., Cossins, J., Krause, S. et al. (2011) Hexosamine biosynthetic pathway mutations cause neuromuscular transmission defect. Am. J. Hum. Genet., 88, 162–172.
36. Belaya, K., Finlayson, S., Slater, C.R., Cossins, J., Liu, W.W., Maxwell, S., McGowan, S.J., Maslau, S., Twigg, S.R., Walls, T.J. et al. (2012) Mutations in DPAGT1 cause a limb-girdle congenital myasthenic syndrome with tubular aggregates. Am. J. Hum. Genet., 91, 193–201.
37. Kiviluoto, S., Decuypere, J.P., De Smedt, H., Missiaen, L., Parys, J.B. and Bultynck, G. (2011) STIM1 as a key regulator for Ca^{2+} homeostasis in skeletal-muscle development and function. Skelet. Muscle, 1, 16.
38. Kumar, R. and Thompson, J.R. (2011) The regulation of parathyroid hormone secretion and synthesis. J. Am. Soc. Nephrol., 22, 216–224.
39. Fukumoto, S., Namba, N., Ozono, K., Yamauchi, M., Sugimoto, T., Michigami, T., Tanaka, H., Inoue, D., Minagawa, M., Endo, I. and Matsumoto, T. (2008) Causes and differential diagnosis of hypocalcemia—recommendation proposed by expert panel supported by ministry of health, labour and welfare, Japan. Endocr. J., 55, 787–794.
40. Malicdan, M.C., Noguchi, S. and Nishino, I. (2009) Monitoring autophagy in muscle diseases. Methods Enzymol., 453, 379–396.
41. Li, H. and Durbin, R. (2009) Fast and accurate short read alignment with Burrows-Wheeler transform. Bioinformatics, 25, 1754–1760.
42. DePristo, M.A., Banks, E., Poplin, R., Garimella, K.V., Maguire, J.R., Hartl, C., Philippakis, A.A., Angel, G., Rivas, M.A., Hanna, M. et al. (2009) A framework for variation discovery and genotyping using next-generation DNA sequencing data. Nat. Genet., 43, 491–498.
43. Wang, K., Li, M. and Hakonarson, H. (2010) ANNOVAR: functional annotation of genetic variants from high-throughput sequencing data. Nucleic Acids Res., 38, e164.
44. Maniatis, T., Fritsch, E.F. and Sambrook, J. (1982) Molecular Cloning: A Laboratory Manual. Cold Spring Harbor Laboratory Press, Cold Spring Harbor, NY.
45. Ihara, Y., Urata, Y., Goto, S. and Kondo, T. (2006) Role of calreticulin in the sensitivity of myocardiac H9c2 cells to oxidative stress caused by hydrogen peroxide. Am. J. Physiol. Cell Physiol., 290, C208–C221.
46. Pan, Z., Zhao, X. and Brotto, M. (2012) Fluorescence-based measurement of store-operated calcium entry in live cells: from cultured cancer cell to skeletal muscle fiber. J. Vis. Exp., 13, e3415.

DAG1 mutations associated with asymptomatic hyperCKemia and hypoglycosylation of a-dystroglycan

Mingrui Dong, MD
Satoru Noguchi, PhD
Yukari Endo, MD
Yukiko K. Hayashi, MD, PhD
Shinobu Yoshida, MD, PhD
Ikuya Nonaka, MD, PhD
Ichizo Nishino, MD, PhD

Correspondence to Dr. Noguchi: noguchi@ncnp.go.jp

ABSTRACT

Objectives: To identify gene mutations in patients with dystroglycanopathy and prove pathogenicity of those mutations using an in vitro cell assay.

Methods: We performed whole-exome sequencing on 20 patients, who were previously diagnosed with dystroglycanopathy by immunohistochemistry and/or Western blot analysis. We also evaluated pathogenicity of identified mutations for phenotypic recovery in a DAG1-knockout haploid human cell line transfected with mutated DAG1 complementary DNA.

Results: Using exome sequencing, we identified compound heterozygous missense mutations in DAG1 in a patient with asymptomatic hyperCKemia and pathologically mild muscular dystrophy. Both mutations were in the N-terminal region of a-dystroglycan and affected its glycosylation. Mutated DAG1 complementary DNAs failed to rescue the phenotype in DAG1-knockout cells, suggesting that these are pathogenic mutations.

Conclusion: Novel mutations in DAG1 are associated with asymptomatic hyperCKemia with hypoglycosylation of a-dystroglycan. The combination of exome sequencing and a phenotype-rescue experiment on a gene-knockout haploid cell line represents a powerful tool for evaluation of these pathogenic mutations. Neurology® 2015;84:273–279

GLOSSARY

cDNA 5 complementary DNA; DAG1 5 dystroglycan 1 (dystrophin-associated glycoprotein 1); KO 5 knockout; WES 5 whole-exome sequencing.

Dystroglycan is a central component of the dystrophin–glycoprotein complex, which links the cytoskeleton and extracellular matrix through sarcolemma.[1,2] Dystroglycan has important roles in the development and maintenance of skeletal muscle, the CNS,[3] and other organs.[4–6] It is encoded by the DAG1 gene. The synthesized polypeptide is posttranslationally cleaved into 2 subunits, namely, a- and b-dystroglycan; then the former is highly glycosylated.[7,8] a-Dystroglycan is composed of 3 distinct domains: the N-terminal region, the mucin-like domain, and the C-terminal domain, at which the mucin-like domain is highly glycosylated by O-linked mannosyl-oligosaccharides and binds to ligands such as laminin and agrin by its sugar chains.[9,10] Reports show that the N-terminal region is required for functional glycosylation of the mucin-like domain by LARGE, an intracellular enzyme-substrate recognition motif necessary for initiation of specific glycosylation.[8,11]

Defects in glycosylation of a-dystroglycan lead to a subgroup of muscular dystrophies and brain and eye malformations, termed dystroglycanopathies.[12] There is a broad spectrum of severity in these diseases, ranging from Walker-Warburg syndrome, muscle-eye-brain disease, and Fukuyama congenital muscular dystrophy to the milder form of limb-girdle muscular dystrophy, such as LGMD2I.[13,14] Recent advances in DNA sequencing techniques facilitated identification of new causative genes in dystroglycanopathies[15–18]; to date, 18 causative genes have been identified. Among them, DAG1 mutations cause primary dystroglycanopathy in limb-girdle muscular dystrophy[19] and muscle-eye-brain disease.[20]

Supplemental data at Neurology.org

From the Department of Neuromuscular Research, National Institute of Neuroscience (M.D., S.N., Y.E., Y.K.H., I. Nonaka, I. Nishino) and Department of Clinical Development, Translational Medical Center (S.N., Y.E., Y.K.H., I. Nishino), NCNP, Tokyo, Japan; Department of Neurology (M.D.), China-Japan Friendship Hospital, Beijing, China; Department of Neurophysiology (Y.K.H.), Tokyo Medical University; and Department of Pediatrics (S.Y.), Omihachiman Community Medical Center, Shiga, Japan.

Go to Neurology.org for full disclosures. Funding information and disclosures deemed relevant by the authors, if any, are provided at the end of the article.

Herein, we report the case of a patient in whom dystroglycanopathy was caused by novel compound heterozygous missense mutations in DAG1 identified by whole-exome sequencing (WES) and we prove the pathogenicity of the mutations.

METHODS Standard protocol approvals, registrations, and patient consents. The ethics committee of the National Center of Neurology and Psychiatry approved this study. All patients gave written informed consent before study participation.

Subjects. To identify the cause of a-dystroglycanopathy, we selected a cohort of 20 unrelated individuals who were diagnosed with a-dystroglycanopathy by negative reactivity with an antibody for glycoepitope of a-dystroglycan (VIA4-1; Millipore, Billerica, MA) on a muscle biopsy and/or decreased VIA4-1 immunoreactivity and laminin binding ability as shown by Western blotting.[21] We immunostained muscle with antibodies for b-dystroglycan (43DAG1; Leica, Wetzlar, Germany), dystrophin (NCL-DYS1, Leica), merosin (4H8-2; Alexis, Lausen, Switzerland), and b-sarcoglycan (5B1, Leica), and conducted Western blotting using the core antibody for a-dystroglycan peptide, GT20ADG. We confirmed that all study patients did not have 3-kb retrotransposal insertion at FKTN.

Whole-exome sequencing. WES was performed as reported previously.[22] Briefly, after genomic DNA isolation from muscle specimens or peripheral blood lymphocytes using standard techniques, we performed exon capture according to the manufacturer's instructions (SureSelect Human All Exon kit V4, 50 Mb; Agilent, Santa Clara, CA), followed by paired-end 100-base massively parallel sequencing on an Illumina HiSeq1000 (Illumina, Inc., San Diego, CA). Then, we mapped and aligned to the human genome chromosomal sequence using the Burrows-Wheeler Aligner. We removed duplicate reads using Picard for downstream analysis and conducted local realignments around indels and regions for low base quality scores using the Genome Analysis Toolkit for recalibration. We identified single-nucleotide variants and small indels using the Genome Analysis Toolkit Unified Genotyper (version 1.6) and filtered according to the Broad Institute's best-practice guidelines. We used ANNOVAR to annotate genetic variations. Data filtering included the following conditions: (1) mutation effect—splicing, start lost, exon deletion, frame shift, stop gained or lost, nonsynonymous codon change, codon insertion or deletion; (2) variation frequency less than 0.01 in HapMap and in 1000 Genomes Project database; and (3) inheritance mode—homozygous mutations, hemizygous mutation, or more than 2 mutations in the same genes. We used Sanger sequencing to confirm mutations.

Validation for the pathogenicity of identified mutations. To examine the pathogenicity of identified mutations, we analyzed functional recovery of dystroglycans in DAG1-knockout (KO) haploid human cell line (HAP1) cells using transfection of lentivirus vectors, pLVSIN-IRES-ZsGreen (Clontech, Mountain View, CA), harboring wild-type or mutated human DAG1 complementary DNA (cDNA). Jae et al.[23] established the DAG1-KO HAP1 cell as reported previously. For the glycosylation in a-dystroglycan assay, we cultured HAP1 cells on laminin-coated glass-bottom dishes. Five days after lentivirus infection, we incubated live cells with IIH6-C4 antibody against glycoepitope of a-dystroglycan (Millipore) in medium and then visualized the cells with Alexa Fluor 568-labeled anti-mouse immunoglobulin M secondary antibody. We observed the cultured cells using a fluorescent microscope (BZ-9000; Keyence, Itasca, IL) with Z-axis scanning throughout whole cells to acquire green fluorescent protein and a-dystroglycan images together (7 images with 1-mm intervals) for full-focus images. After staining with 43DAG1 antibody and GM130 antibody (Cell Signaling Technology, Beverly, MA), we observed localization of b-dystroglycan in formalin-fixed HAP1 cells.

Biotinylation of cell-surface proteins on HAP1 cells. We labeled living HAP1 cells with the membrane-impermeable biotin reagent, Sulfo-NHS-LC-Biotin, according to manufacturer's instructions (Thermo Scientific, Waltham, MA) and then subjected streptavidin-purified proteins to Western blotting using standard techniques. We detected b-dystroglycans with 43DAG1 antibody.

RESULTS Identification of DAG1 mutation by WES. After analysis of a cohort of 20 unrelated patients with a-dystroglycanopathy, we identified one patient who harbored mutations in DAG1 genes. WES analysis summary is presented in table e-1 on the Neurology® Web site at Neurology.org. We identified 7 genes with homozygous mutations, 18 genes with compound heterozygous mutations, and 8 genes with hemizygous mutations in this patient (data not shown). Among them, we identified compound heterozygous mutations, c.220G.A (rs189360006) and c.331G.A (rs117209107) in DAG1, which are predicted to lead to missense mutations, p.Val74Ile and p.Asp111Asn, respectively. We did not find any other genes involved in the glycosylation pathway in the patient. We confirmed the 2 mutations in DAG1 by Sanger sequencing (figure 1A) and the compound heterozygosity by transcript analysis (data not shown). Residues at both mutated sites are located in the N-terminal region of a-dystroglycan and are highly conserved during evolution (figure 1, B and C). In silico analyses of mutation function demonstrated that p.Val74Ile and p.Asp111Asn, respectively, were predicted as damaging and tolerated by SIFT and probably damaging and benign in PolyPhen-2, and both mutations were predicted as disease-causing in MutationTaster. Other than DAG1 mutations, the compound heterozygous missense alterations were found in TTN and AHNAK genes among muscle-related genes.

Clinical phenotype and histologic features of muscle biopsy. This is a 7-year-old boy coming from a nonconsanguineous marriage who has compound heterozygous mutations in DAG1. He was born normally (length at birth, 51.5 cm; birth weight, 3,672 g) and demonstrated normal development milestones. At the age of 4 years and 7 months, he was 98 cm tall, weighed 17 kg, and had a head circumference of 50.8 cm. When he was 4 years

Figure 1 Compound heterozygous mutations in the DAG1 gene in the described patient

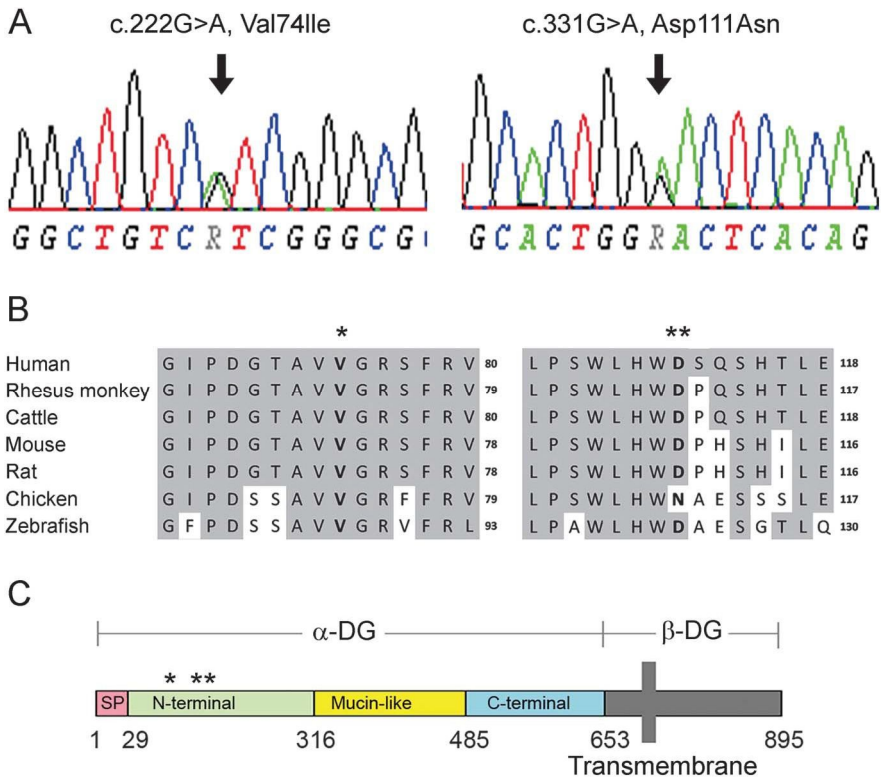

(A) Electropherograms around the mutation sites in DAG1 genes from Sanger sequencing. (B) Amino acid conservation in mutation sites among species. (C) Localization of mutation sites (* and **) in domain structures in DAG1 protein. DG 5 dystroglycan.

and 5 months, he became dehydrated in the wake of acute tonsillitis, and was diagnosed with hyperCKemia by chance. After recovery from dehydration, hyperCKemia continued (range, 1,855–6,512 IU/L; normal range, 45–287 IU/L). Physical examination showed no symptomatic muscle weakness but we observed calf pseudohypertrophy. Muscle CT imaging showed low intensity in the rectus femoris, semimembranosus, and gastrocnemius muscles. Brain CT images showed no morphologic abnormality.

Muscle histologic analysis showed muscular dystrophy–like appearance including a few regenerating fibers, internal nuclei, and mild endomysial fibrosis. Immunohistochemical analysis was positive for dystrophin, merosin, sarcoglycans, and b-dystroglycan, but negative for glycoepitope of a-dystroglycan (figure 2). Results of Western blotting and the laminin overlay assay of muscle proteins corroborated the reduction in glycosylation of a-dystroglycan (figure 2); in contrast, we detected strong immunoreactivity to GT20ADG at lower molecular mass. b-Dystroglycan was normal.

Pathogenesis is proven by rescue of DAG1-KO HAP1 cells by the wild-type and mutant DAG1 gene. To prove the pathogenicity of the 2 missense mutations harbored by this patient, we transfected lentivirus vectors with wild-type or mutated DAG1 cDNAs (p.Val74Ile and p.Asp111Asn) into DAG1-KO HAP1 cells, which showed defects in reactivity for the anti-a-dystroglycan antibody, IIH6 (figure 3A). DAG1-KO HAP1 cells were rescued by introduction of wild-type cDNA showing recovery of strong IIH6 immunoreactivity similar to that of wild-type HAP1 cells (figure 3A). On the contrary, cDNAs with p.Val74Ile and p.Asp111Asn mutations failed to rescue (figure 3A).

We also analyzed mutated b-dystroglycan transport to the cell surface in HAP1 cells. DAG1-KO cells were negative for b-dystroglycan staining (figure 3B). Introduction of wild-type and mutated DAG1 cDNAs into DAG1-KO cells resulted in recovery of b-dystroglycan staining at the cell surface (in red) but not in the Golgi apparatus (GM130, blue), suggesting that processing and transport of dystroglycan was not affected by the mutations. Cell-surface biotin-labeling experiments in DAG1-KO cells transfected with wild-type and mutated DAG1 cDNAs also showed recovery of b-dystroglycan in the biotinylated protein fraction (figure 3C). These results demonstrate that these 2 mutations are pathogenic and impair glycosylation of a-dystroglycan, but not dystroglycan expression.

Figure 2 Hypoglycosylation of a-dystroglycan in the described patient

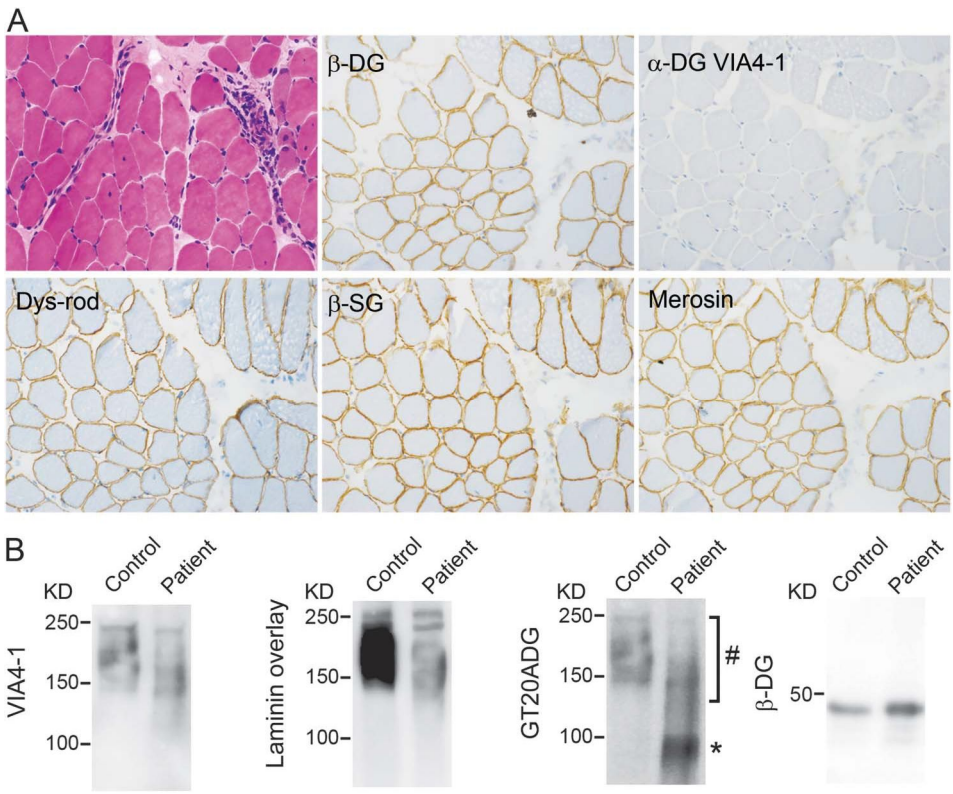

(A, top) Histology and immunostaining of skeletal muscle from the patient. Muscle histology showed muscular dystrophy–like appearance including a few regenerating fibers, internal nuclei, and mild endomysial fibrosis. (A, bottom) Muscle stained positive for antibodies to dystrophin (Dys-rod), merosin, b-sarcoglycan (b-SG), and b-dystroglycan (b-DG), but negative for glycoepitope antibody to a-dystroglycan (a-DG VIA4-1). (B) Western blotting with VIA4-1 antibody and the laminin overlay assay of muscle proteins showing reduced glycosylation of a-dystroglycan; in contrast, strong immunoreactivity to GT20ADG for core peptide was detected at lower molecular mass (*). After Western blotting with VIA4-1 antibody, the same membrane was used for GT20ADG. The bands labeled with # were the VIA4-1 antibody-reactive bands. b-Dystroglycan staining was normal.

DISCUSSION Herein, we report on a patient with dystroglycanopathy, who has compound heterozygous mutations in DAG1. This patient had asymptomatic hyperCKemia with mild muscular dystrophy and deficiency in laminin-binding glycosylation in a-dystroglycan. Although the patient could be presymptomatic for muscle weakness or intellectual disability, the clinical phenotype is much milder compared with a previous report of a patient who had limb-girdle–type muscular dystrophy accompanied by mild cognitive impairment.[19] Our finding expands the clinical and pathologic spectrum of dystroglycanopathy associated with DAG1 mutation from a muscle-eye-brain disease–like phenotype and mild limb-girdle muscular dystrophy[19,20] to asymptomatic hyperCKemia. Myopathic asymptomatic hyperCKemia has been reported in secondary dystroglycanopathies, with mutations in FKRP and FKTN genes.[24–26] By WES, we also identified 2 missense alterations in each of the TTN and AHNAK genes, which have been known to be expressed in skeletal muscles. Both alterations in TTN were predicted as probably damaging in PolyPhen-2 or disease-causing in MutationTaster in silico functional analyses. These alterations in TTN were not localized in the exons in which the mutations have been identified in other muscle diseases, such as hereditary myopathy with early respiratory failure, cardiomyopathy, or tibial muscular dystrophy. AHNAK missense alterations were predicted as probably damaging and benign in PolyPhen-2 or polymorphism in MutationTaster. Functional experiments for the mutated proteins would be required for final conclusion of their pathogenicities.

Although one could argue whether the c.220G.A and c.331G.A variants previously annotated in the dbSNP131, 1000 Genomes, and HapMap databases can be the candidate pathogenic mutations, we still presume they are pathogenic because we did not find any other strong candidate gene for dystroglycanopathy in this patient. Because it is known that the 3-kb retrotransposal insertion in FKTN with a frequency of 1/88 allele is associated with a high prevalence of Fukuyama congenital muscular dystrophy in Japan,[27]

Figure 3 Mutant DAG1 observed in patients does not rescue hypoglycosylation of a-dystroglycan in DAG1-KO cells

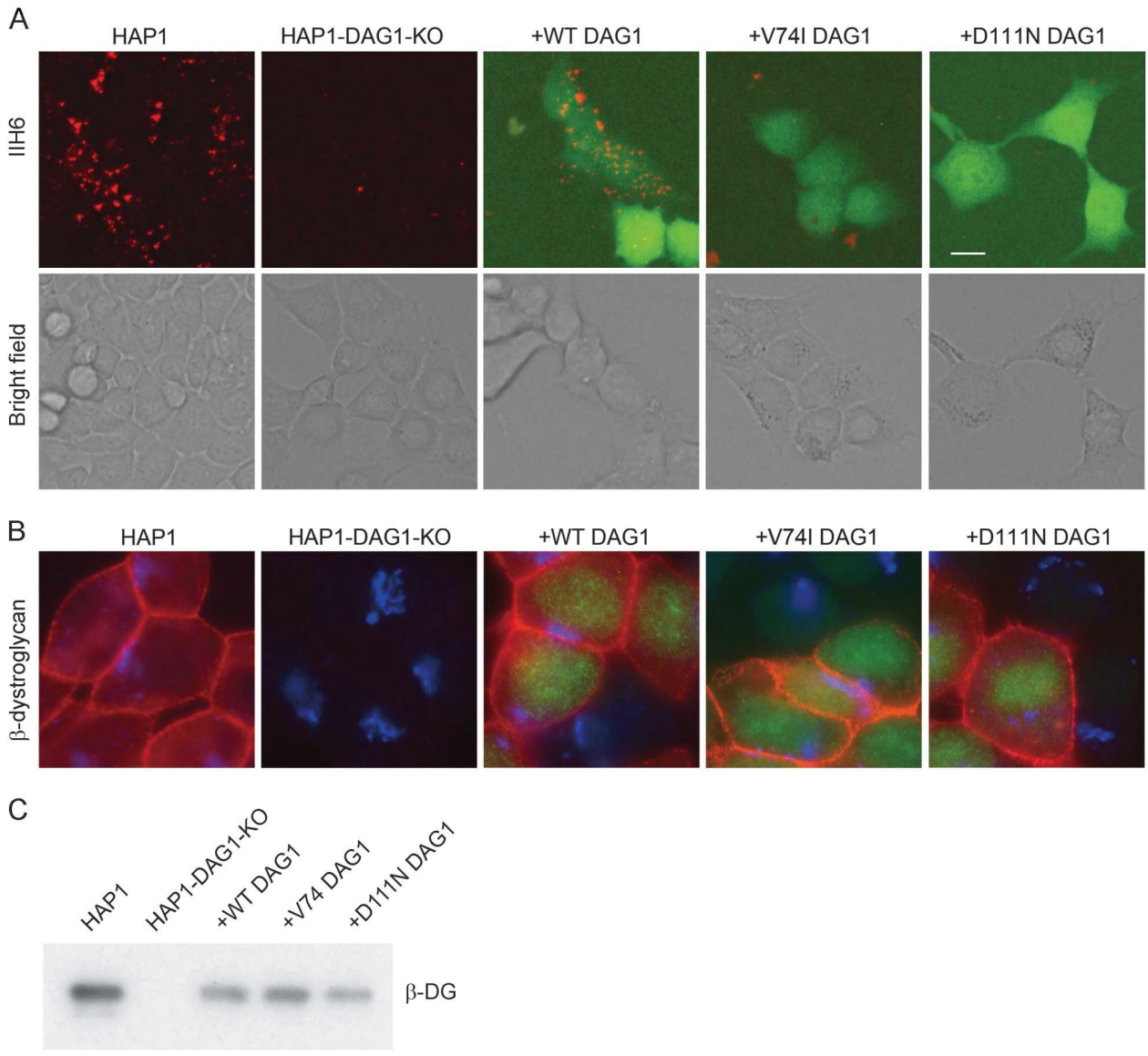

(A) IIH6-4C2 staining of wild-type HAP1 cells (in red), DAG1-knockout cells (HAP1-DAG1-KO), and DAG1-KO cells transfected with wild-type (1WT-DAG1), Val74Ile-mutated (1V74I DAG1), and Asp111Asn-mutated DAG1 (1D111N DAG1). Transfected cells are positive for ZsGreen expression (in green). (B, C) Recovery of b-dystroglycan on cell surface in DAG1-KO cells by transfection with wild-type (1WT-DAG1), p.Val74Ile-mutated (1V74I DAG1), and p.Asp111Asn-mutated DAG1 (1D111N DAG1). HAP1, wild-type haploid cells; HAP1-DAG1-KO, DAG1-KO HAP1 cells. (B) Immunostaining of b-dystroglycan (red) and Golgi protein, GM130 (blue). (C) Western blot analysis of cell-surface biotin-labeled fraction. Scale bar denotes 20 mm. b-DG 5 b-dystroglycan.

it is logical to suspect a mutation with a variation frequency of more than 0.01. Because the c.331G.A mutation has a variation frequency of 0.005 in all populations in 1000 Genomes and a higher frequency (0.028) in the Japanese population in the Human Genetic Variation Database, there is a possibility that a higher incidence of potential dystroglycanopathy caused by p.Asp111Asn substitution exists in the Japanese population. However, in other populations, the frequency has not been known.

As reported, hypoglycosylation levels of a-dystroglycan do not consistently correlate with clinical severity.[28] Our patient should be classified as having a primary dystroglycanopathy with mutations in DAG1; he had typical hypoglycosylation of a-dystroglycan in terms of low molecular mass of the protein, positive reactivity to anti-core peptide antibody, and decreased binding to lam- inin, but he showed a milder phenotype. The level of hypoglycosylation of a-dystroglycan is not necessarily predictive of phenotypic severity in dystroglycanopathy.

Our results suggest that the missense mutation of p.Val74Ile or p.Asp111Asn in the N-terminal region of a-dystroglycan does not influence expression of the dystroglycan, but it does cause a defect in

posttranslational modification. Similarly, Hara et al.[19] reported a missense mutation (p.The192Met) in the N-terminal region, which is also associated with hypoglycosylation of a-dystroglycan but with normal b-dystroglycan localization. LARGE catalyzes the extension of specific disaccharide structures [23GlcAa124Xylb12] on a phosphorylated O-mannosyl glycan in the mucin-like domain, which is required for laminin binding, within the Golgi apparatus.[29] The N-terminal region in a-dystroglycan serves as a recognition site for LARGE[8]; of note, Hara et al. demonstrated that the p.The192Met mutation in DAG1 impairs interaction between a-dystroglycan and LARGE. This N-terminal region is predicted to have L-shaped modular architecture and comprises 2 autonomous domains; domain 1 contains residues 28–168 in murine a-dystroglycan and belongs to the I-set domain of the immunoglobulin superfamily, and domain 2 contains residues 180–303 with a ribosomal RNA-binding protein fold.[30] Both mutated residues, Val74 and Asp111, are present in domain 1 and are neighbors of Gly75 and Gln113 (corresponding to Gly73 and His111in murine dystroglycan); each of these is predicted to be aligned on the interaction between domain 1 and 2, and the trimer interface of domain 1, respectively, in the crystal structure of the N-terminal region of murine a-dystroglycan. Both mutations may affect higher-order structural formation of the N-terminal region of a-dystroglycan. Another possibility is that the mutations may impair direct interaction of the N-terminal globular region of a-dystroglycan with extracellular matrix molecules, as suggested by Hall et al.[31] Remarkable secondary structure and hydrophobic character changes of the mutated fragment are reported to lead to weaker interaction of this domain with laminin.[32]

Previously, Willer et al.[15] have demonstrated the rescuing experiments using patients' fibroblasts in dystroglycanopathy for evaluation of the pathogenicity of gene mutations. In this study, we used gene-modified HAP1 cells because the patient's cells were not available. The phenotypic rescue experiments described here, using DAG1-KO HAP1 cells with lentivirus-mediated expression of mutated cDNA, enabled rapid and easy evaluation of the pathogenicity of the mutations. This is a simple method based on the recovery of the function of a-dystroglycan. Theoretically, this method can be applied to evaluate any of the mutations in all known causative genes as well as mutations in novel candidate genes for dystroglycanopathies without requiring enzymatic activity measurement, as long as the specific gene-KO HAP1 cells are available. This method would be applicable by any researcher for confirming the data from WES for each causative mutation in any disease, if the phenotypes of cells were characterized.

AUTHOR CONTRIBUTIONS

M.D. conducted acquisition, analysis and interpretation of data, and drafted and edited the manuscript. S.N. supervised all aspects of this study including study design, data interpretation, and drafted and edited the manuscript. Y.E. made WES pipeline and analyzed the data. Y.K.H. selected patients and performed WES. S.Y. collected clinical information of the patient. I. Nonaka and I. Nishino supervised manuscript preparation and edited the manuscript.

ACKNOWLEDGMENT

The authors thank Nozomi Matsuyama, Megumu Ogawa, Kanako Goto, and Asako Kaminaga for technical support, Thijn R. Brummelkamp for supplying HAP1 cells, and Kevin P. Campbell for supplying GT20ADG antibody.

STUDY FUNDING

This study was partially supported by Intramural Research Grant (25-5, 26-8) for Neurological and Psychiatric Disorders of NCNP (to S.N., I. Nishino); Research on Applying Health Technology from the Ministry of Health, Labour and Welfare (to I. Nishino).

DISCLOSURE

M. Dong reports no disclosures relevant to the manuscript. S. Noguchi serves as an editor of Acta Neuropathologica Communications and received research support from the Ministry of Health, Labour and Welfare. Y. Endo reports no disclosures relevant to the manuscript. Y. Hayashi received research support from the Ministry of Health, Labour and Welfare. S. Yoshida and I. Nonaka report no disclosures relevant to the manuscript. I. Nishino serves as an associate editor of Neuromuscular Disorders and Neurology and Clinical Neuroscience, serves on the speakers bureau of Genzyme and Kitano Hospital, serves as a consultant of Novartis Pharma, and received research support from Genzyme and the Ministry of Health, Labour and Welfare. Go to Neurology.org for full disclosures.

Received May 31, 2014. Accepted in final form September 29, 2014.

REFERENCES

1. Ibraghimov-Beskrovnaya O, Ervasti JM, Leveille CJ, Slaughter CA, Sernett SW, Campbell KP. Primary structure of dystrophin-associated glycoproteins linking dystro- phin to the extracellular matrix. Nature 1992;355: 696–702.
2. Michele DE, Barresi R, Kanagawa M, et al. Post-translational disruption of dystroglycan-ligand interactions in congenital muscular dystrophies. Nature 2002;418:417– 422.
3. Moore SA, Saito F, Chen J, et al. Deletion of brain dystroglycan recapitulates aspects of congenital muscular dys- trophy. Nature 2002;418:422–425.
4. Saito F, Moore SA, Barresi R, et al. Unique role of dystroglycan in peripheral nerve myelination, nodal structure, and sodium channel stabilization. Neuron 2003;38: 747–758.
5. Durbeej M, Talts JF, Henry MD, Yurchenco PD, Campbell KP, Ekblom P. Dystroglycan binding to laminin alpha1LG4 module influences epithelial morphogenesis of salivary gland and lung in vitro. Differentiation 2001;69:121–134.
6. Matsumura K, Chiba A, Yamada H, et al. A role of dystroglycan in schwannoma cell adhesion to laminin. J Biol Chem 1997;272:13904–13910.

7. Noguchi S, Wakabayashi E, Imamura M, Yoshida M, Ozawa E. Formation of sarcoglycan complex with differ- entiation in cultured myocyte. Eur J Biochem 2000;267: 640–648.
8. Kanagawa M, Saito F, Kunz S, et al. Molecular recognition by LARGE is essential for expression of functional dystroglycan. Cell 2004;117:953–964.
9. Brancaccio A, Schulthess T, Gesemann M, Engel J. Electron microscopic evidence for a mucin-like region in chick muscle alpha-dystroglycan. FEBS Lett 1995;368: 139–142.
10. Chiba A, Matsumura K, Yamada H, et al. Structures of sialylated O-linked oligosaccharides of bovine peripheral nerve alpha-dystroglycan: the role of a novel O-mannosyl-type oligosaccharide in the binding of alpha-dystroglycan with laminin. J Biol Chem 1997; 272:2156–2162.
11. Hara Y, Kanagawa M, Kunz S, et al. Like-acetylglucosa- minyltransferase (LARGE)-dependent modification of dystroglycan at Thr-317/319 is required for laminin bind- ing and arenavirus infection. Proc Natl Acad Sci USA 2011;108:17426–17431.
12. Muntoni F, Brockington M, Brown SC. Glycosylation eases muscular dystrophy. Nat Med 2004;10:676–677.
13. Brown SC, Torelli S, Brockington M. Abnormalities in alpha-dystroglycan expression in MDC1C and LGMD2I muscular dystrophies. Am J Pathol 2004;164:727–737.
14. Mendell JR, Boué DR, Martin PT. The congenital muscular dystrophies: recent advances and molecular insights. Pediatr Dev Pathol 2006;9:427–443.
15. Willer T, Lee H, Lommel M, et al. ISPD loss-of-function mutations disrupt dystroglycan O-mannosylation and cause Walker-Warburg syndrome. Nat Genet 2012;44: 575–580.
16. Roscioli T, Kamsteeg EJ, Buysse K, et al. Mutations in ISPD cause Walker-Warburg syndrome and defective glycosylation of a-dystroglycan. Nat Genet 2012;44: 581–585.
17. Manzini MC, Tambunan DE, Hill RS, et al. Exome sequencing and functional validation in zebrafish identify GTDC2 mutations as a cause of Walker-Warburg syndrome. Am J Hum Genet 2012;91:541–547.
18. Carss KJ, Stevens E, Foley AR, et al. Mutations in GDP-mannose pyrophosphorylase B cause congenital and limb-girdle muscular dystrophies associated with hypoglycosylation of a-dystroglycan. Am J Hum Genet 2013; 93:29–41.
19. Hara Y, Balci-Hayta B, Yoshida-Moriguchi T, et al. A dystroglycan mutation associated with limb-girdle muscular dystrophy. N Engl J Med 2011;364:939–946.
20. Geis T, Marquard K, Rödl T. Homozygous dystroglycan mutation associated with a novel muscle-eye-brain disease- like phenotype with multicystic leucodystrophy. Neuro- genetics 2013;14:205–213.
21. Hayashi YK, Ogawa M, Tagawa K, et al. Selective defi- ciency of alpha-dystroglycan in Fukuyama-type congenital muscular dystrophy. Neurology 2001;57:115–121.
22. Saitsu H, Nishimura T, Muramatsu K, et al. De novo mutations in the autophagy gene WDR45 cause static encephalopathy of childhood with neurodegeneration in adulthood. Nat Genet 2013;45:445–449.
23. Jae LT, Raaben M, Riemersma M, et al. Deciphering the glycosylome of dystroglycanopathies using haploid screens for lassa virus entry. Science 2013;340:479–483.
24. de Paula F, Vieira N, Starling A, et al. Asymptomatic carriers for homozygous novel mutations in the FKRP gene: the other end of the spectrum. Eur J Hum Genet 2003;11:923–930.
25. Fernandez C, de Paula AM, Figarella-Branger D, et al. Diagnostic evaluation of clinically normal subjects with chronic hyperCKemia. Neurology 2006;66:1585–1587.
26. Fiorillo C, Moro F, Astrea G, et al. Novel mutations in the fukutin gene in a boy with asymptomatic hyperCKemia. Neuromuscul Disord 2013;23:1010–1015.
27. Colombo R, Bignamini AA, Carobene A, et al. Age and origin of the FCMD 3'-untranslated-region retrotransposal insertion mutation causing Fukuyama-type congenital muscular dystrophy in the Japanese population. Hum Genet 2000;107:559–567.
28. Jimenez-Mallebrera C, Torelli S, Feng L, et al. A comparative study of alpha-dystroglycan glycosylation in dystro- glycanopathies suggests that the hypoglycosylation of alpha-dystroglycan does not consistently correlate with clinical severity. Brain Pathol 2009;19:596–611.
29. Yoshida-Moriguchi T, Yu L, Stalnaker SH, et al. O-mannosyl phosphorylation of alpha-dystroglycan is required for laminin binding. Science 2010;327:88–92.
30. Bozic D, Sciandra F, Lamba D, Brancaccio A. The structure of the N-terminal region of murine skeletal muscle alpha-dystroglycan discloses a modular architecture. J Biol Chem 2004;279:44812–44816.
31. Hall H, Bozic D, Michel K, Hubbell JA. N-terminal alpha-dystroglycan binds to different extracellular matrix molecules expressed in regenerating peripheral nerves in a protein-mediated manner and promotes neurite extension of PC12 cells. Mol Cell Neurosci 2003;24:1062–1073.
32. Bhattacharya S, Das A, Ghosh S, Dasgupta R, Bagchi A. Hypoglycosylation of dystroglycan due to T192M mutation: a molecular insight behind the fact. Gene 2014;537: 108–114.

RESEARCH PAPER

Mutation profile of the GNE gene in Japanese patients with distal myopathy with rimmed vacuoles (GNE myopathy)

Anna Cho,[1] Yukiko K Hayashi,[1,2,3] Kazunari Monma,[1] Yasushi Oya,[4] Satoru Noguchi,[1] Ikuya Nonaka,[1] Ichizo Nishino[1,2]

► Additional material is published online only. To view please visit the journal online (http://dx.doi.org/10.1136/jnnp-2013-305587).

[1]Department of Neuromuscular Research, National Institute of Neuroscience, National Center of Neurology and Psychiatry, Tokyo, Japan
[2]Department of Clinical Development, Translational Medical Center, National Center of Neurology and Psychiatry, Tokyo, Japan
[3]Department of Neurophysiology, Tokyo Medical University, Tokyo, Japan
[4]Department of Neurology, National Center Hospital, National Center of Neurology and Psychiatry, Tokyo, Japan

Correspondence to Professor Yukiko K Hayashi, Department of Neurophysiology, Tokyo Medical University, 6-1-1 Shinjuku, Shinjuku, Tokyo 160-8402, Japan; yhayashi@tokyo-med.ac.jp

Received 4 June 2013
Revised 21 August 2013
Accepted 22 August 2013
Published Online First 11 September 2013

► http://dx.doi.org/10.1136/jnnp-2013-306414

To cite: Cho A, Hayashi YK, Monma K, et al. J Neurol Neurosurg Psychiatry 2014;85:912–915.

ABSTRACT

Background GNE myopathy (also called distal myopathy with rimmed vacuoles or hereditary inclusion body myopathy) is an autosomal recessive myopathy characterised by skeletal muscle atrophy and weakness that preferentially involve the distal muscles. It is caused by mutations in the gene encoding a key enzyme in sialic acid biosynthesis, UDP-N-acetylglucosamine 2-epimerase/N-acetylmannosamine kinase (GNE).

Methods We analysed the GNE gene in 212 Japanese GNE myopathy patients. A retrospective medical record review was carried out to explore genotype–phenotype correlation.

Results Sixty-three different mutations including 25 novel mutations were identified: 50 missense mutations, 2 nonsense mutations, 1 insertion, 4 deletions, 5 intronic mutations and 1 single exon deletion. The most frequent mutation in the Japanese population is c.1714G>C (p.Val572Leu), which accounts for 48.3% of total alleles. Homozygosity for this mutation results in more severe phenotypes with earlier onset and faster progression of the disease. In contrast, the second most common mutation, c.527A>T (p.Asp176Val), seems to be a mild mutation as the onset of the disease is much later in the compound heterozygotes with this mutation and c.1714G>C than the patients homozygous for c.1714G>C. Although the allele frequency is 22.4%, there are only three homozygotes for c.527A>T, raising a possibility that a significant number of c.527A>T homozygotes may not develop an apparent disease.

Conclusions Here, we report the mutation profile of the GNE gene in 212 Japanese GNE myopathy patients, which is the largest single-ethnic cohort for this ultra-orphan disease. We confirmed the clinical difference between mutation groups. However, we should note that the statistical summary cannot predict clinical course of every patient.

INTRODUCTION

GNE myopathy, which is also known as distal myopathy with rimmed vacuoles,[1] quadriceps sparing myopathy[2] or hereditary inclusion body myopathy (hIBM),[3] is an autosomal recessive myopathy characterised by skeletal muscle atrophy and weakness that preferentially involve the distal muscles such as the tibialis anterior. It is a progressive disease, whereby the symptoms of muscle weakness start to affect the patient from the second or third decade of life, and most of the patients become wheelchair-bound between twenties and sixties.[4] The characteristic histopathological features in muscle biopsy include muscle fibre atrophy with the presence of rimmed vacuoles and intracellular congophilic deposits.[4 5] GNE myopathy is caused by mutations in the gene encoding a key enzyme in sialic acid biosynthesis, UDP-N-acetylglucosamine 2-epimerase/N-acetylmannosamine kinase (GNE).[6–8] Genetically confirmed GNE myopathy was initially recognised in Iranian Jews and Japanese,[7 9] but later appeared to be widely distributed throughout the world. More than 100 mutations in the GNE gene have been described up to date.

During the last decade, there has been extensive experimental work to elucidate the pathogenesis and to develop therapeutic strategies of GNE myopathy.[6 10–12] Better knowledge on the basis of those research achievements have currently enabled us to enter the era of clinical trial for human patients. At this moment, the identification of new GNE myopathy patients with precise genetic diagnosis and the expansion of global spectrum of GNE mutations are timely and important. Here, we report the molecular profile of Japanese GNE myopathy patients with a brief discussion of genotype–phenotype correlations.

METHODS

Patients

Two hundred and twelve patients from 201 unrelated Japanese families were included in this study. There were 117 female and 95 male patients. All cases were genetically confirmed as GNE myopathy. A retrospective medical record review was carried out to explore genotype–phenotype correlation. Informed consent was obtained for the collection of clinical data and extraction of DNA to perform mutation analysis.

Genetic analysis

DNA was extracted from peripheral blood leukocytes or skeletal muscle tissue. We used the previously described sequencing method to describe mutations at cDNA level.[7] All exons and splice regions of the GNE gene were sequenced. NM_005476.5 was used as a reference sequence. We screened 100 alleles from normal Japanese individuals to determine the significance of novel variations.

Pathological analysis

To evaluate histopathological phenotype according to genotype, we analysed muscle biopsies from two

most common genotype groups in Japanese population. Each of the three age-matched and biopsy site-matched samples from c.1714G>C homozygous group and c.1714G>C/c.527A>T compound heterozygous group was compared. Muscle samples were taken from biceps brachii and frozen with isopentane cooled in liquid nitrogen. Serial frozen sections of 10 μm were stained using a set of histochemical methods including haematoxylin-eosin and modified Gomori trichrome.

Statistical analysis

Statistics were calculated using GraphPad Prism 5 software (GraphPad Software, La Jolla, California, USA). Between-group comparison for clinical data was performed using one-way analysis of variance with Dunnett's post-test. All values are expressed as means±SD. We performed two-sided tests with a $p<0.05$ level of significance.

Table 1 Allele frequency for GNE mutations in 212 Japanese GNE myopathy patients

	Allele frequency
Mutation type	
Missense	402 (94.8%)
Nonsense	3 (0.7%)
Insertion	1 (0.2%)
Small deletion	4 (0.9%)
Single exon deletion	2 (0.5%)
Intron	12 (2.8%)
Three most common mutations	
c.1765G>C (p.Val572Leu)	205 (48.3%)
c.578A>T (p.Asp176Val)	95 (22.4%)
c.38G>C (p.Cys13Ser)	15 (3.5%)
Total alleles	424

RESULTS

Mutation profile

We identified homozygous or compound heterozygous GNE mutations in all 212 patients (see online supplement 1). In total, 63 different mutations were found including 50 missense mutations, 2 nonsense mutations, 1 insertion, 4 deletions, 5 intronic mutations and 1 single exon deletion (figure 1). Twenty-five novel mutations were identified including 17 missense mutations, 4 small deletions, 3 intronic mutations and 1 single exon deletion (figure 1, see online supplement).

Twenty-one mutations were found to be shared between two or more unrelated families. The three mutations occurring most frequently in the Japanese population were c.1714G>C (p.Val572Leu), c.527A>T (p.Asp176Val) and c.38G>C (p.Cys13Ser); these comprised 48.3%, 22.4% and 3.5%, respectively, of the total number of alleles examined (table 1).

Genotype–phenotype correlations

The mean age of genetic analysis was 41.6±14.1 years (n=212), and the mean age of symptom onset based on the data available was 28.4±10.2 years (n=195). The earliest onset age was 10 and the latest was 61 years old in our cohort. Thirty-six among 154 patients (23.4%) were full-time wheelchair users at the point of genetic diagnosis with the average age at loss of ambulation being 36.8±11.3 years (n=36). The youngest wheelchair-bound age was 19, and the oldest ambulant age was 78. To investigate genotype–phenotype correlations in the major GNE mutations of Japanese population, we compared the age at symptom onset and loss of ambulation between the patients groups carrying either of the two most frequent mutations, c.1714G>C and c.527A>T (table 2). As with a previous report,[13] homozygous c.1714G>C mutations resulted in earlier symptom onset (23.9±7.1 years, $p<0.01$) and the majority of full-time wheelchair users were in this group. On the other hand, c.1714G>C/c.527A>T compound heterozygous patients first developed symptoms at a later age (37.6±12.6 years, $p<0.01$), and there were no wheelchair-bound patients at the time of genetic analysis in this group. Only three homozygous c.527A>T mutation patients were identified, and their average onset age (32.3±5.7 years) was also higher among total patients (28.4±10.2 years). All three patients were ambulant until the last follow-up visits (29, 40 and 44 years).

Among 212 cases, 80 patients underwent muscle biopsies. Overall pathological findings in our series were compatible with GNE myopathy. The characteristic rimmed vacuoles were observed in the majority (76/80, 95.0%) of the cases. Through the analysis of muscle biopsies from age-matched and biopsy site-matched samples, we found that the histopathological phenotypes were in line with these genotype–phenotype correlations (figure 2). Homozygous c.1714G>C mutations have led to much more advanced pathological changes with severe myofibre atrophy and increased numbers of rimmed vacuoles. Marked adipose tissue replacement was appreciated in a case with reflecting very advanced stage of muscle degeneration.

DISCUSSION

As shown in figure 1, mutations were located throughout the whole open reading frame of the GNE gene. The majority (94.8%, 402/424 alleles) of the mutations in our series were missense mutations (table 1), and there were no homozygous null mutations. These results are in accordance with previous reports[7 9] signifying that total loss of GNE function might be

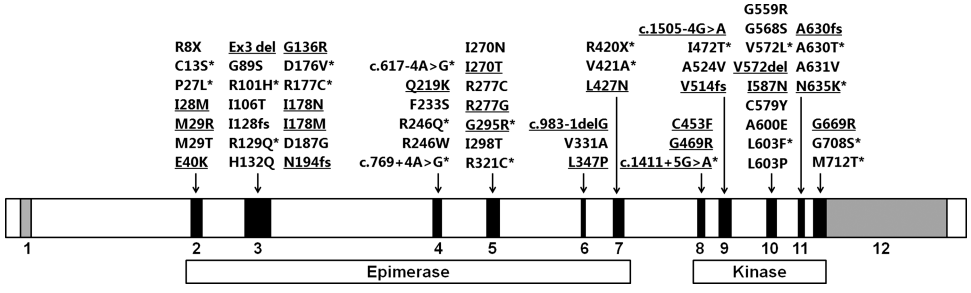

Figure 1 Mutation spectrum of GNE in the Japanese population. The mutations are located throughout the whole open reading frame. Twenty-five novel mutations are underlined, and 21 shared mutations are indicated with asterisks.

Table 2 Comparison of clinical course between two most frequent GNE mutations in Japanese population

Mutations	Age at exam (years)		Age at onset (years)		Age at WB (years)		Ambulant
c.1714G>C/c.1714G>C	38.6±13.4	(n=71)	23.9±7.1	(n=65)**	35.4±10.6	(n=28)	n=22
c.1714G>C/other	32.3±13.2	(n=25)	21.9±6.8	(n=22)*	37.0±8.6	(n=4)	n=16
c.1714G>C/c.527A>T	48.9±14.1	(n=38)	37.6±12.6	(n=35)**		(n=0)	n=29
c.527A>T/c.527A>T	37.7±7.7	(n=3)	32.3±5.7	(n=3)		(n=0)	n=3
c.527A>T/other	41.3±11.1	(n=51)	30.6±8.0	(n=46)		(n=2)	n=33
other/other	49.8±14.7	(n=24)	28.8±9.5	(n=24)		(n=2)	n=16
Total	41.6±14.1	(n=212)	28.4±10.2	(n=195)	36.8±11.3	(n=36)	n=118

Dunnett's multiple comparison test (control: total patients) *p<0.05, **p<0.01.
Other: a mutation other than c.1714G>C and c.527A>T; WB, wheelchair-bound.

lethal in human beings. The embryonic lethality of null mutation in GNE had also been proved in the mouse model.[14] Only three of total 212 patients carried a nonsense mutation; clinical data were available for two of them. Interestingly, one patient with compound heterozygous c.22C>T (p.Arg8X)/c.1714G>C (p.Val572Leu) mutations developed his first symptoms at the age of 15, while the other patient with c.1258C>T (p.Arg420X)/c.527A>T (p.Asp176Val) mutations developed her symptoms much later, at the age of 45. The similar difference was also observed in the phenotypes of patients with frame-shift mutations. A patient carrying c.383insT (p.I128fs) and c.1714G>C (p.Val572Leu) mutations developed his first symptom at the age of 13, whereas another two patients with c.1541-4del4 (p.Val514fs)/c.527A>T (p.Asp176Val) and c.581delA (p.N194fs)/c.527A>T (p.Asp176Val) mutations had later symptom onset, at the age of 30 and 32 years, respectively. This clinical variation can be explained as it reflects alternative missense mutations, because the two patients with very early onset shared the same missense mutation c.1714G>C, while the patients with the milder phenotype shared c.527A>T.

Among five intronic mutations identified in our series, c.617−4A>G and c.769 + 4A>G were previously reported as pathological mutations.[7 15] Three novel variants were located at splice junction of exon 6 (c.983−1delG), exon 8 (c.1411+5G>A) and exon 9 (c.1505−4G>A), raising the high possibility of relevant exons skipping. These variants were not detected in 200 alleles from normal Japanese individuals and also in the single nucleotide polymorphism (SNP) database.

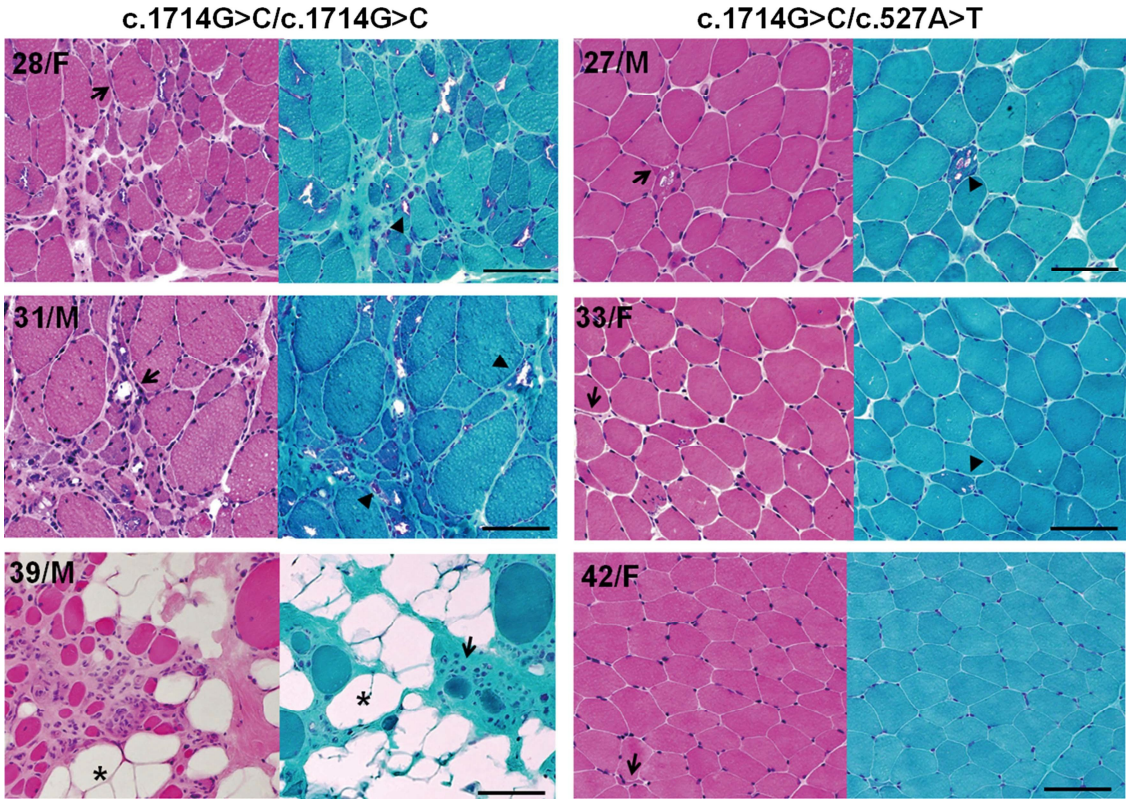

Figure 2 Comparison of muscle pathology between patients with homozygous c.1714G>C (p.Val572Leu) and with compound heterozygous c.1714G>C (p.Val572Leu)/c.527A>T (p.Asp176Val) mutations. Homozygous c.1714G>C (p.Val572Leu) mutations have led to much more advanced histopathological changes compared with compound heterozygous c.1714G>C (p.Val572Leu)/c.527A>T (p.Asp176Val) mutations. Haematoxylin-eosin (left) and modified Gomori trichrome (right) stains of muscle sections from age (c.1714G>C/c.1714G>C: 28, 31 and 39 years, c.1714G>C/c.527A>T: 27, 33 and 42 years) and biopsy site (biceps brachii muscles) matched samples. Bar=100μm; triangles: rimmed vacuoles; arrows: atrophic fibres; asterisks: adipose tissue.

As there are ethnic differences in GNE mutation frequencies,[9 16–19] establishing the mutation spectrum and defining predominant mutations in a certain population may be helpful for the diagnosis. Three most common mutations in the Japanese population and their allele frequencies (table 1) were in agreement with previous data.[7 13] The allele frequencies of top two mutations (c.1714G>C and c.527A>T) comprise more than two-third of the total number of alleles suggesting that founder effects are involved in the relatively higher incidence of GNE myopathy in Japan.

Although most of patients showed characteristic pathological features, the existence of exceptional cases with atypical biopsy findings implies that GNE myopathy cannot be totally excluded from the absence of rimmed vacuoles in muscle biopsies. On the other hand, we found 94 patients who were pathologically or clinically suspected but not had mutations in GNE. Several cases of VCP myopathy mutations in (VCP), myofibrillar myopathy mutations in (DES) and reducing body myopathy (FHL1) were later identified in this group, suggesting these diseases should be included as differential diagnosis of GNE myopathy.[20]

In terms of genotype–phenotype correlations, we confirmed that homozygosity for c.1714G>C (p.Val572Leu) mutation resulted in more severe phenotypes in clinical and histopathological aspects. In contrast, the second most common mutation, c.527A>T (p.Asp176Val), seems to be a mild mutation as the onset of the disease is much later in the compound heterozygotes with this mutation and c.1714G>C. Several evidences further strengthened the link between the more severe phenotype and c.1714G>C, and between the milder phenotype and c.527A>T. Compound heterozygosity for c.1714G>C and non-c.527A>T mutations resulted in earlier symptom onset (22.9±6.8 years, $p<0.05$) compared with the average onset age of the total group, whereas c.527A>T, both presented as homozygous and as compound heterozygous mutations, lead to slower disease progression (table 2). In addition, only three patients carrying this second most common mutation c.527A>T in homozygous mode were identified, which is much fewer than the number expected from high allele frequency (22.4%), raising a possibility that considerable number of c.527A>T homozygotes may not even develop a disease. In fact, we ever identified an asymptomatic c.527A>T homozygote at age 60 years.[7] Now he is at age 71 years and still healthy. Overall, these results indicate that different mutations lead to different spectra of severity. However, this is a result of a statistical summary that cannot predict clinical course of each individual patient.

Here, we presented the molecular bases of 212 Japanese GNE myopathy patients with 25 novel GNE mutations. Based on the current status of knowledge, sialic acid supplementation may lead to considerable changes in the natural course of GNE myopathy within near future. The ongoing identification of GNE mutations and further studies regarding the clinicopathological features of each mutation will provide better understanding of GNE myopathy and lead to accelerated development of treatment for this disease.

Acknowledgements The authors thank Kanako Goto and Yuriko Kure for their invaluable technical support and assistant in genetic analysis.

Contributors AC had full access to all of the data in the study and wrote the manuscript; YKH supervised all aspects of this study including study design, data interpretation and manuscript preparation; KM and YO participated in collecting and analysing all the clinical and genetic data; SN, I Nonaka and I Nishino were involved in data analysis and interpretation and also supervised manuscript preparation.

Funding This study was supported partly by Intramural Research Grant 23-4, 23-5, 22-5 for Neurological and Psychiatric Disorders of NCNP; partly by Research on Intractable Diseases, Comprehensive Research on Disability Health and Welfare, and Applying Health Technology from the Ministry of Health Labour and Welfare; and partly by JSPS KAKENHI Grant Number of 23390236.

Competing interests None.

Ethics approval This study was approved by the ethics committee of National Center of Neurology and Psychiatry.

Provenance and peer review Not commissioned; externally peer reviewed.

REFERENCES

1 Nonaka I, Sunohara N, Ishiura S, et al. Familial distal myopathy with rimmed vacuole and lamellar (myeloid) body formation. J Neurol Sci 1981;51:141–55.
2 Argov Z, Yarom R. "Rimmed vacuole myopathy" sparing the quadriceps. A unique disorder in Iranian Jews. J Neurol Sci 1984;64:33–43.
3 Askanas V, Engel WK. New advances in the understanding of sporadic inclusion-body myositis and hereditary inclusion-body myopathies. Curr Opin Rheumatol 1995;7:486–96.
4 Nonaka I, Noguchi S, Nishino I. Distal myopathy with rimmed vacuoles and hereditary inclusion body myopathy. Curr Neurol Neurosci Rep 2005;5:61–5.
5 Nishino I, Malicdan MC, Murayama K, et al. Molecular pathomechanism of distal myopathy with rimmed vacuoles. Acta Myol 2005;24:80–3.
6 Eisenberg I, Avidan N, Potikha T, et al. The UDP-N-acetylglucosamine 2-epimerase/N-acetylmannosamine kinase gene is mutated in recessive hereditary inclusion body myopathy. Nat Genet 2001;29:83–7.
7 Nishino I, Noguchi S, Murayama K, et al. Distal myopathy with rimmed vacuoles is allelic to hereditary inclusion body myopathy. Neurology 2002;59:1689–93.
8 Keppler OT, Hinderlich S, Langner J, et al. UDP-GlcNAc 2-epimerase: a regulator of cell surface sialylation. Science 1999;284:1372–6.
9 Eisenberg I, Grabov-Nardini G, Hochner H, et al. Mutations spectrum of GNE in hereditary inclusion body myopathy sparing the quadriceps. Hum Mutat 2003;21:99.
10 Noguchi S, Keira Y, Murayama K, et al. Reduction of UDP-N-acetylglucosamine 2-epimerase/N-acetylmannosamine kinase activity and sialylation in distal myopathy with rimmed vacuoles. J Biol Chem 2004;279:11402–7.
11 Malicdan MC, Noguchi S, Nonaka I, et al. A Gne knockout mouse expressing human GNE D176V mutation develops features similar to distal myopathy with rimmed vacuoles or hereditary inclusion body myopathy. Hum Mol Genet 2007;16:2669–82.
12 Malicdan MC, Noguchi S, Hayashi YK, et al. Prophylactic treatment with sialic acid metabolites precludes the development of the myopathic phenotype in the DMRV-hIBM mouse model. Nat Med 2009;15:690–5.
13 Mori-Yoshimura M, Monma K, Suzuki N, et al. Heterozygous UDP-GlcNAc 2-epimerase and N-acetylmannosamine kinase domain mutations in the GNE gene result in a less severe GNE myopathy phenotype compared to homozygous N-acetylmannosamine kinase domain mutations. J Neurol Sci 2012;318:100–5.
14 Schwarzkopf M, Knobeloch KP, Rohde E, et al. Sialylation is essential for early development in mice. Proc Natl Acad Sci USA 2002;99:5267–70.
15 Ikeda-Sakai Y, Manabe Y, Fujii D, et al. Novel Mutations of the GNE gene in distal myopathy with rimmed vacuoles presenting with very slow progression. Case Rep Neurol 2012;4:120–5.
16 Li H, Chen Q, Liu F, et al. Clinical and molecular genetic analysis in Chinese patients with distal myopathy with rimmed vacuoles. J Hum Genet 2011;56:335–8.
17 Liewluck T, Pho-Iam T, Limwongse C, et al. Mutation analysis of the GNE gene in distal myopathy with rimmed vacuoles (DMRV) patients in Thailand. Muscle Nerve 2006;34:775–8.
18 Kim BJ, Ki CS, Kim JW, et al. Mutation analysis of the GNE gene in Korean patients with distal myopathy with rimmed vacuoles. J Hum Genet 2006;51:137–40.
19 Broccolini A, Ricci E, Cassandrini D, et al. Novel GNE mutations in Italian families with autosomal recessive hereditary inclusion-body myopathy. Hum Mutat 2004;23:632.
20 Shi Z, Hayashi YK, Mitsuhashi S, et al. Characterization of the Asian myopathy patients with VCP mutations. Eur J Neurol 2012;19:501–9.

JNNP

Mutation profile of the *GNE* gene in Japanese patients with distal myopathy with rimmed vacuoles (GNE myopathy)

Anna Cho, Yukiko K Hayashi, Kazunari Monma, et al.

J Neurol Neurosurg Psychiatry 2014 85: 914-917 originally published online September 11, 2013
doi: 10.1136/jnnp-2013-305587

Available online at www.sciencedirect.com

ScienceDirect

Neuromuscular Disorders 24 (2014) 642–647

www.elsevier.com/locate/nmd

Case report

Deep sequencing detects very-low-grade somatic mosaicism in the unaffected mother of siblings with nemaline myopathy

Satoko Miyatake[a,1], Eriko Koshimizu[a,1], Yukiko K. Hayashi[b,c], Kazushi Miya[d], Masaaki Shiina[e], Mitsuko Nakashima[a], Yoshinori Tsurusaki[a], Noriko Miyake[a], Hirotomo Saitsu[a], Kazuhiro Ogata[e], Ichizo Nishino[b], Naomichi Matsumoto[a,⇑]

[a] Department of Human Genetics, Yokohama City University Graduate School of Medicine, Yokohama, Japan
[b] Department of Neuromuscular Research, National Institute of Neuroscience, National Center of Neurology and Psychiatry, Tokyo, Japan
[c] Department of Neurophysiology, Tokyo Medical University, Tokyo, Japan
[d] Department of Pediatrics, Faculty of Medicine, University of Toyama, Toyama, Japan
[e] Department of Biochemistry, Yokohama City University Graduate School of Medicine, Yokohama, Japan

Received 12 December 2013; received in revised form 1 April 2014; accepted 11 April 2014

Abstract

When an expected mutation in a particular disease-causing gene is not identified in a suspected carrier, it is usually assumed to be due to germline mosaicism. We report here very-low-grade somatic mosaicism in ACTA1 in an unaffected mother of two siblings affected with a neonatal form of nemaline myopathy. The mosaicism was detected by deep resequencing using a next-generation sequencer. We identified a novel heterozygous mutation in ACTA1, c.448A>G (p.Thr150Ala), in the affected siblings. Three-dimensional structural modeling suggested that this mutation may affect polymerization and/or actin's interactions with other proteins. In this family, we expected autosomal dominant inheritance with either parent demonstrating germline or somatic mosaicism. Sanger sequencing identified no mutation. However, further deep resequencing of this mutation on a next-generation sequencer identified very-low-grade somatic mosaicism in the mother: 0.4%, 1.1%, and 8.3% in the saliva, blood leukocytes, and nails, respectively. Our study demonstrates the possibility of very-low-grade somatic mosaicism in suspected carriers, rather than germline mosaicism.

Keywords: Nemaline myopathy; ACTA1; Deep resequencing; Next-generation sequencer; Low-grade somatic mosaicism

1. Introduction

Nemaline myopathy is a common form of congenital myopathy characterized clinically by general hypotonia and muscle weakness, and pathologically by the presence of nemaline bodies within the myofibers [1,2]. ACTA1 is one of the nine known genes associated with nemaline myopathy [3].

Sometimes in the clinic, an expected mutation is not identified in a suspected carrier. This is usually assumed to be because of germline mosaicism, in which mosaicism occurs in the carrier's germline only. Here we report, for the first time, very-low-grade somatic mosaicism detected by deep resequencing using a next-generation sequencer (NGS) in an unaffected mother of two affected siblings.

⇑ Corresponding author. Address: Department of Human Genetics, Yokohama City University Graduate School of Medicine, 3-9 Fukuura, Kanazawa-ku, Yokohama 236-0004, Japan, Tel.: +81 45 787 2604; fax: +81 45 786 5219.
E-mail address: naomat@yokohama-cu.ac.jp (N. Matsumoto).
[1] These authors contributed equally.

http://dx.doi.org/10.1016/j.nmd.2014.04.002
0960-8966/

2. Case report

2.1. The proband

The proband was a boy who was 6 years old at the time of the study. He was the first child of healthy nonconsanguineous Japanese parents. He had an affected sister (Fig. 1a). He was born by cesarean section at 40 weeks of gestation after an uneventful pregnancy. He was admitted to a neonatal intensive care unit immediately after birth because of asphyxia with loss of spontaneous respiration and general hypotonia. His birth weight was 2640 g, height 48 cm, and occipitofrontal head circumference 33 cm. His Apgar scores were 1 and 4 at 1 and 5 min, respectively. He quickly recovered with ventilatory support. Laboratory tests showed normal findings except mildly elevated creatine kinase (653 IU/L). When he was discharged at age 2 months, general hypotonia remained with absent deep tendon reflexes. Antigravity movements were not observed. Arthrogryposis and mild cardiomegaly were noted. Ultrasound cardiography revealed mild dilatation and dyskinesia of the left ventricle. At 7 months, he was given a tracheostomy, and home ventilation therapy was introduced because of aspiration pneumonia (Supplementary Fig. 1a). Tube-feeding was also started because of poor swallowing. At 9 months, a muscle biopsy was performed. On a modified Gomori trichrome stain, nearly all the muscle fibers contained nemaline rods. Intranuclear rods were also scattered (Fig. 1b). On staining for ATPases, type 1 fiber atrophy and predominance were seen. Immunolabeling of a muscle biopsy from the patient with a-actinin showed intensely stained rod bodies (Fig. 1c). Co-staining with a-actinin, lamin A (as a marker of the nuclear envelope), and DAPI clearly revealed intranuclear rods (Fig. 1c). His condition was diagnosed as nemaline myopathy. He could sit unassisted at age 2 years, move on his hip at age 3, and walk with assistance at age 5. He showed normal intellectual ability. At 5 years, his cardiac function was re-evaluated by ultrasound cardiography. Mild left ventricular dilatation and dyskinesia remained.

2.2. The affected sister

The proband's only sibling, a sister 3 years younger, was also affected (Fig. 1a). She was born by cesarean section at 38 weeks of gestation after an uneventful pregnancy. She was similarly admitted to a neonatal intensive care unit immediately after birth because of hypoventilation and hypotonia. Her birth weight was 2620 g, height 48.5 cm, and occipitofrontal head circumference 36.5 cm. Her Apgar scores were 4 and 6 at 1 and 5 min, respectively. Serum creatine kinase was 190 IU/L, which was within the normal range. She recovered with ventilatory support, but needed continuous oxygen therapy. She had difficulty thriving and tube-feeding was introduced. Her cardiac function was normal without cardiomegaly. General hypotonia remained. After she was discharged at age 2 months, frequent aspiration pneumonia occurred. She started to use nocturnal noninvasive positive pressure ventilation at the age of 22 months. At age 2 years, she was given a tracheostomy and was controlled under nocturnal ventilation after respiratory syncytial virus infection following respiratory failure (Supplementary Fig. 1a). Because of her clinical presentation, she was also suggested to have congenital (nemaline) myopathy. At present, she shows antigravity movement of the extremities although she has not acquired head control and cannot roll over.

2.3. Genetic and three-dimensional structural analysis

First we checked for ACTA1 (NM_001100.3) mutation in the proband's DNA, considering the presence of intranuclear rods. We identified a novel heterozygous missense mutation, c.448A>G (p.Thr150Ala), by Sanger sequencing. Because autosomal recessive inheritance was possible from the family tree, we performed whole-exome sequencing of the proband, affected sister, and their parents to identify a further genetic cause. Genomic DNA obtained from blood leukocytes was captured using a SureSelect^{XT} Human All Exon 50 Mb Kit (Agilent Technologies, Santa Clara, CA) and sequenced on a HiSeq2000 (Illumina, San Diego, CA) with 101-bp paired-end reads, as previously described [4]. The mean depth of coverage was 123x to 143x. We selected rare protein-altering and splice-site variants after filtering against dbSNP135 and 408 in-house control exomes. Among the rare variant calls, we first screened for genes known to cause nemaline myopathies, namely ACTA1 (MIM 102610) [3], TPM3 (MIM 191030) [5], NEB (MIM 161650) [6], TPM2 (MIM 190990) [7], TNNT1 (MIM 191041) [8], CFL2 (MIM 601443) [9], KBTBD13 (MIM 613727) [10], KLHL40 (MIM 615340) [11], and KLHL41 (MIM 607701) [12]. We identified only the novel heterozygous missense mutation c.448A>G (p.Thr150Ala) in ACTA1 in both the affected brother and sister, which we confirmed by Sanger sequencing. Copy number analysis by eXome Hidden Markov Model (XHMM) [13] using next-generation sequencing (NGS) data revealed that there were no copy number changes within the ACTA1 locus (Supplementary Fig. 1b). This mutation was not identified in either of the parents, after testing DNA obtained from their saliva, hair, nails, and blood by Sanger sequencing (Fig. 2a). This mutation, which alters the evolutionarily well-conserved Thr150 to Ala (Fig. 2b), was not present in the NHLBI Exome Sequencing Project (ESP6500). Two of three web-based prediction programs suggested that this mutation is pathogenic (PolyPhen-2: benign; SIFT: deleterious; MutationTaster: disease-causing). We also searched for any rare variants that were compatible with an autosomal recessive inheritance model, such as a homozygous mutation or compound heterozygous

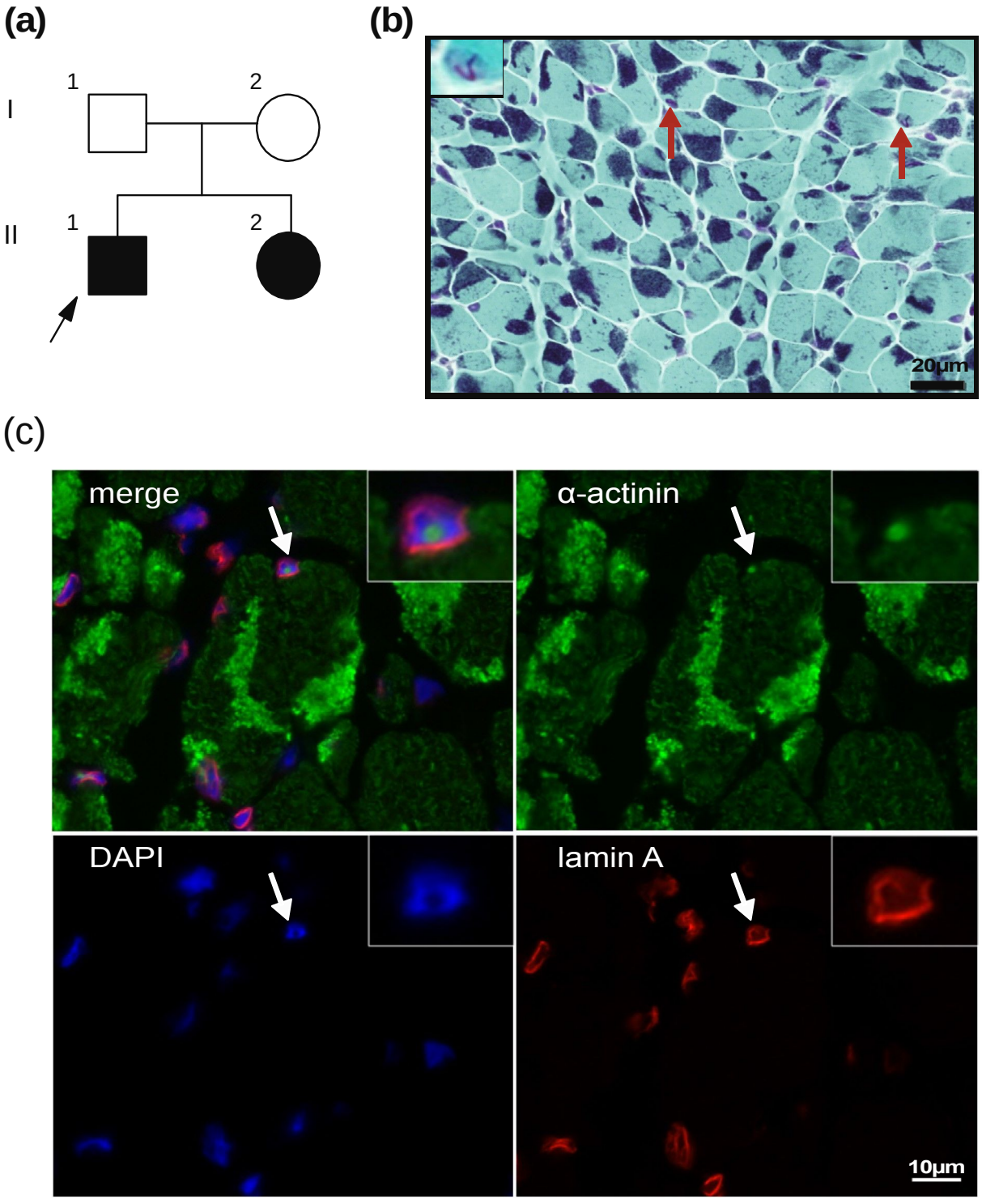

Fig. 1. (a) Family pedigree. (b) Light microscopic images of the muscle of the proband at age 9 months. With a modified Gomori trichrome stain, nearly all the muscle fibers can be seen to contain nemaline rods. Intranuclear rods (arrows, and upper-left window) are also scattered in some nuclei. Bar = 20 lm. (c) Immunohistochemical analysis of a muscle biopsy using anti-a-actinin (EA-53; Sigma, St. Louis, MO) (green) and anti-lamin A (red) antibodies [19]. Nuclei were stained with DAPI (blue). Nemaline rods were strongly stained by anti-a-actinin. An intranuclear rod was also seen (arrows, and higher-magnification inset boxes). Scale bar = 10 lm.

mutation, but no candidate mutations were identified (data not shown).

To explore the effect of the ACTA1 p.Thr150Ala mutation, we mapped the mutation onto reported crystal structures. Thr150 is located near the polymerization/interaction interfaces between actin monomers (Fig. 2c) and between actin and its interacting proteins (Fig. 2d, Supplementary Fig. 1c). Thus, p.Thr150Ala may

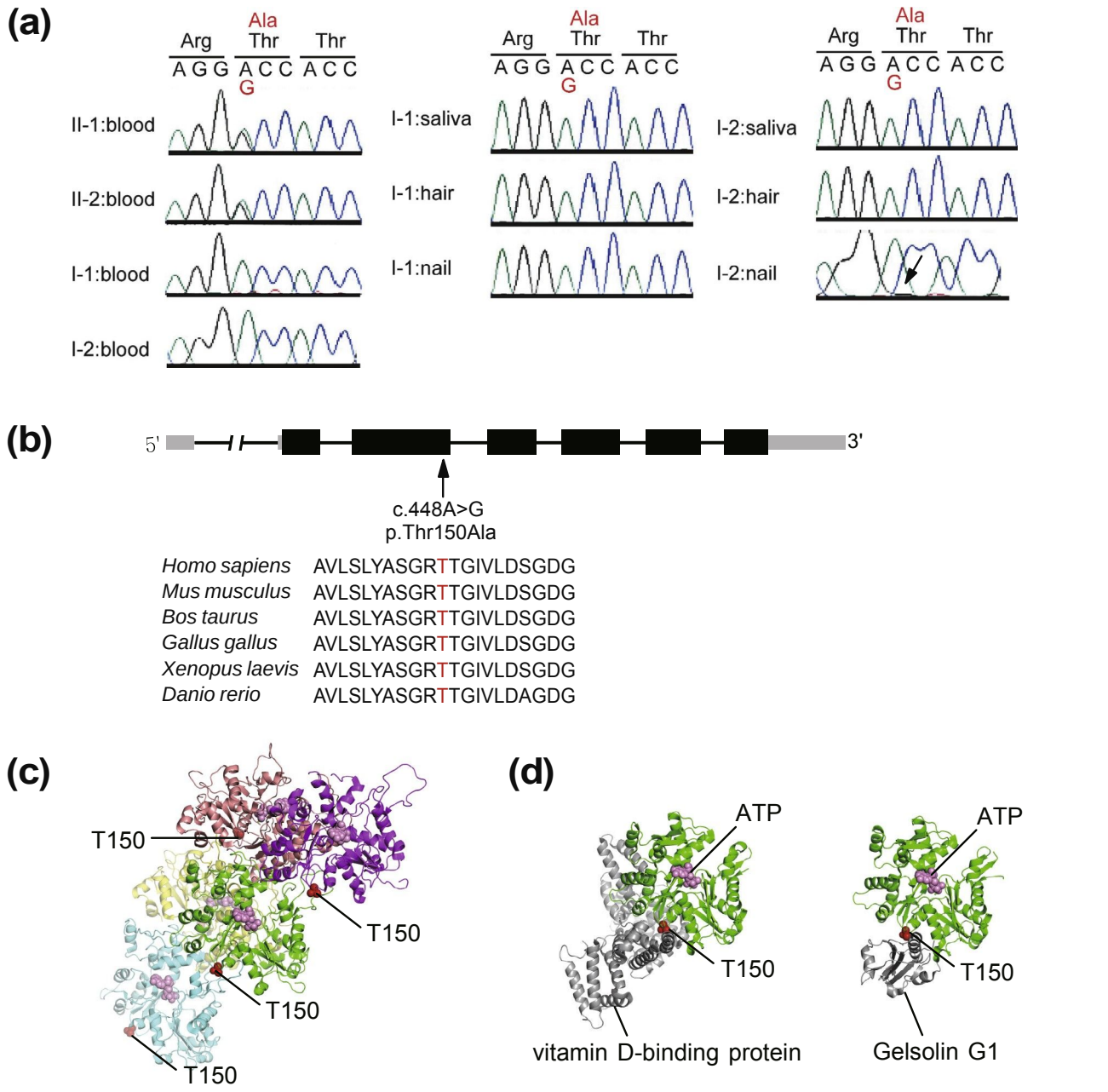

Fig. 2. (a) Sanger sequencing of the c.448A>G mutation using DNA from the affected siblings and the parents obtained from blood (left), and DNA from the father (middle) and mother (right) obtained from saliva, hair, and nails. The heterozygous mutation was identified in the affected siblings but not in any of the parental samples. No clear peak for the G allele was observed in the mother's nail DNA sample (arrow). (b) Schematic representation of ACTA1. The light gray bars represent untranslated regions and the black bars represent coding exons. Exon 1 is a non-coding exon. The c.448A>G mutation changes the well-conserved amino acid Thr150 (red) into Ala. (c, d) Structural implications of the p.Thr150Ala mutation in ACTA1. Structures of bare F-actin filaments determined by electron microscopy (Protein Data Bank (PDB) code 4A7N) (c) and G-actins in complex with vitamin D-binding protein (PDB code 1KXP) or gelsolin G1 (PDB code 1EQY) (d) are shown. The actin molecules are color-coded to discriminate each monomer in the F-actin filaments or are colored green in the G-actin complexes. Thr150 and ATP molecules are shown as red and pink space-filling spheres, respectively.

affect polymerization and/or the interactions of actin with other proteins.

We expected autosomal dominant inheritance from either parent. To test this, we performed deep resequencing for this mutation using an Illumina MiSeq platform. We used DNAs from the blood of the affected siblings, and from the saliva, nails, hair, and blood of their parents. The total read depth at c.448A in ACTA1 was 131495x to 425933x. Very-low-grade somatic mosaicism was confirmed in the mother: 0.4%, 1.1%, and 8.3% in saliva, blood, and nails, respectively (all beyond 0.1% of the background level) (Table 1).

We used allele-specific PCR to confirm the presence of the mutation in the mother. The primer sequences and

Table 1
Deep resequencing of c.448A>G in ACTA1 in various samples from each individual.

Individual	Tissue	Total depth (x)	Disease status	Wild-type allele (x)	Mutant allele (x)	% of wild-type allele	% of mutant allele
II-1 (Proband)	Blood	380016	Affected	192510	186808	50.7	49.2
II-2 (Sister)	Blood	425933	Affected	215496	209612	50.6	49.2
I-1 (Father)	Blood	261948	Unaffected	260897	355	99.6	0.1
I-2 (Mother)	Blood	364850	Unaffected	360030	4103	98.7	1.1
I-1 (Father)	Saliva	245895	Unaffected	245130	299	99.7	0.1
I-1 (Father)	Hair	190636	Unaffected	189929	253	99.6	0.1
I-1 (Father)	Nail	325282	Unaffected	324198	381	99.7	0.1
I-2 (Mother)	Saliva	239339	Unaffected	237872	999	99.4	0.4
I-2 (Mother)	Hair	324289	Unaffected	323120	400	99.6	0.1
I-2 (Mother)	Nail	131495	Unaffected	120210	10956	91.4	8.3

PCR conditions are available upon request. Both the wild-type and mutant alleles were amplified in the proband and the affected sister at a similar level. Both alleles could also be amplified in the mother, but the wild-type allele was amplified at a much greater level than the mutant allele. The wild-type allele only was amplified in the father (Supplementary Fig. 2a). Sanger sequencing of these amplicons confirmed the mutation in the proband, sister, and mother (Supplementary Fig. 2b).

There are various conventional methods to detect somatic mosaicism: Sanger sequencing to detect a small variant peak compared with the wild-type peak, high-resolution melting (HRM) analysis to detect an aberrant melting pattern, allele-specific PCR to amplify only the mutant allele, and pyrosequencing and SNaPshot analysis for quantitative variant detection [14]. We explored whether our very-low-grade somatic mosaicism could be detected by HRM, because this has been suggested to be one of the more sensitive methods [15]. We performed HRM analysis as previously described [16] using DNAs from normal controls, the affected siblings, the father (all DNA derived from blood), and the mother (DNA derived from the nails, which showed the highest rate of mosaicism (8.3%). The melting curves of both affected siblings were aberrant and were called mutant, but those of the father and mother were called normal (Supplementary Fig. 2c). In other words, this technique could not detect the 8.3% mosaicism.

3. Discussion

Here, we report very-low-grade somatic mosaicism in the unaffected mother of siblings with nemaline myopathy, identified by deep resequencing using NGS. Our study is significant in two ways. First, we demonstrate the possibility of very-low-grade somatic mosaicism in a suspected carrier, rather than germline mosaicism; this is likely to be a very rare event. Second, we present another example of the clinical application of NGS.

The novel heterozygous mutation c.448A>G (p.Thr150Ala) in ACTA1 is likely to be responsible for the nemaline myopathy in this pedigree based on four lines of evidence: the mutation is not registered in the ESP6500 database, the substituted amino acid is well conserved, two previously reported mutations also involve residue 150 (Thr150Asn, Thr150Ser) [17,18], and three-dimensional structural modeling suggests an impact on polymerization and/or the interactions of actin with other proteins. Interestingly, the mutation exists within a region where most of the mutations identified in patients with intranuclear rod myopathy, a variant of nemaline myopathy associated with ACTA1, are located [18].

The majority of reported ACTA1 mutations are de novo heterozygous mutations in sporadic cases. This is likely to be due to the severity of nemaline myopathy with ACTA1 mutation. However, autosomal dominant inheritance has been observed in a few situations: a pedigree with a relatively mild phenotype or incomplete penetrance, or parental somatic/germline mosaicism [2,18]. To date, there have been three reported cases of somatic mosaicism of ACTA1 in one parent of a severely affected patient [18].

In our study, allele-specific PCR, despite being non-quantitative, was sufficiently sensitive to detect mosaicism in blood leukocytes from the mother (mosaic rate 1.1%). Thus, this method is worth trying to confirm a suspected low-grade mosaicism. In contrast, as we were unable to detect 8.3% mosaicism using HRM, NGS should be the first choice for detecting very-low-grade somatic mosaicism that other methods might miss. A recent paper has described using NGS to detect somatic BRAF mutations down to 2% allele frequency, demonstrating the increased sensitivity of this method compared with HRM (limit 6.6% allele frequency), pyrosequencing (limit 5% allele frequency), and Sanger sequencing (limit 6.6% allele frequency) [15].

In our family, the mother does not seem to have any neurological problems in her daily activities, although she has not been clinically examined and no muscle imaging studies or biopsies have been undertaken.

The proband had mild left ventricular dilatation with dyskinesia without a hypertrophic phenotype. In the literature, cardiomegaly appears to be a rare complication. Patients with ACTA1 mutation usually have hypertrophic cardiomegaly [18,19].

In conclusion, we used NGS to confirm very-low-grade somatic mosaicism in the mother. Using conventional methods, the mother might have been judged to have germline mosaicism. Clinically, our data on the rate of

somatic mosaicism could be used to estimate the recurrence risk, although prenatal diagnosis would be required to provide certainty.

Acknowledgments

We thank all the participants for their cooperation in this research. We also thank Ms. K. Takabe and Mr. T. Miyama, from the Department of Human Genetics, Yokohama City University Graduate School of Medicine, for their technical assistance. This work was supported by grants from the Ministry of Health, Labour and Welfare of Japan (N. Miyake, N. Matsumoto), a Grant-in-Aid for Scientific Research (A) from the Japan Society for the Promotion of Science (N. Matsumoto), a Grant-in-Aid for Scientific Research (B) from the Japan Society for the Promotion of Science (N. Miyake, H.S.), a Grant-in-Aid for Young Scientists (B) (E.K.), a research grant from the Yokohama Foundation for Advancement of Medical Science (S.M.), the Takeda Science Foundation (N. Miyake, H.S., N. Matsumoto), the Fund for the Creation of Innovation Centers for Advanced Interdisciplinary Research Areas Program in the Project for Developing Innovation Systems (N. Matsumoto), the Strategic Research Program for Brain Sciences (E.K., N. Matsumoto), a Grant-in-Aid for Scientific Research on Innovative Areas (Transcription Cycle) from the Ministry of Education, Culture, Sports, Science, and Technology of Japan (N. Miyake, N. Matsumoto), a Grant-in-Aid for Research on Intractable Diseases, Comprehensive Research on Disability, Health and Welfare (Y.K.H., I.N.), a Grant-in-Aid for Applying Health Technology (Y.K.H., I.N.) from the Ministry of Health, Labour and Welfare, Japan, and an Intramural Research Grant 23-5 for Neurological and Psychiatric Disorders of NCNP (I.N.).

Appendix A. Supplementary data

Supplementary data associated with this article can be found, in the online version, at http://dx.doi.org/10.1016/j.nmd.2014.04.002.

References

[1] Nance JR, Dowling JJ, Gibbs EM, Bonnemann CG. Congenital myopathies: an update. Curr Neurol Neurosci Rep 2012;12:165–74.
[2] Romero NB, Sandaradura SA, Clarke NF. Recent advances in nemaline myopathy. Curr Opin Neurol 2013;26:519–26.
[3] Nowak KJ, Wattanasirichaigoon D, Goebel HH, et al. Mutations in the skeletal muscle alpha-actin gene in patients with actin myopathy and nemaline myopathy. Nat Genet 1999;23:208–12.
[4] Nakamura K, Kodera H, Akita T, et al. De novo mutations in GNAO1, encoding a galphao subunit of heterotrimeric g proteins, cause epileptic encephalopathy. Am J Hum Genet 2013;93: 496–505.
[5] Laing NG, Wilton SD, Akkari PA, et al. A mutation in the alpha tropomyosin gene TPM3 associated with autosomal dominant nemaline myopathy. Nat Genet 1995;9:75–9.
[6] Pelin K, Hilpela P, Donner K, et al. Mutations in the nebulin gene associated with autosomal recessive nemaline myopathy. Proc Natl Acad Sci USA 1999;96:2305–10.
[7] Donner K, Ollikainen M, Ridanpaa M, et al. Mutations in the beta-tropomyosin (TPM2) gene – a rare cause of nemaline myopathy. Neuromuscul Disord 2002;12:151–8.
[8] Johnston JJ, Kelley RI, Crawford TO, et al. A novel nemaline myopathy in the Amish caused by a mutation in troponin T1. Am J Hum Genet 2000;67:814–21.
[9] Agrawal PB, Greenleaf RS, Tomczak KK, et al. Nemaline myopathy with minicores caused by mutation of the CFL2 gene encoding the skeletal muscle actin-binding protein, cofilin-2. Am J Hum Genet 2007;80:162–7.
[10] Sambuughin N, Yau KS, Olive M, et al. Dominant mutations in KBTBD13, a member of the BTB/Kelch family, cause nemaline myopathy with cores. Am J Hum Genet 2010;87:842–7.
[11] Ravenscroft G, Miyatake S, Lehtokari VL, et al. Mutations in KLHL40 are a frequent cause of severe autosomal-recessive nemaline myopathy. Am J Hum Genet 2013;93:6–18.
[12] Gupta VA, Ravenscroft G, Shaheen R, et al. Identification of KLHL41 mutations implicates BTB-Kelch-mediated ubiquitination as an alternate pathway to myofibrillar disruption in nemaline myopathy. Am J Hum Genet 2013;93:1108–17.
[13] Fromer M, Moran JL, Chambert K, et al. Discovery and statistical genotyping of copy-number variation from whole-exome sequencing depth. Am J Hum Genet 2012;91:597–607.
[14] Tasca G, Fattori F, Ricci E, et al. Somatic mosaicism in TPM2-related myopathy with nemaline rods and cap structures. Acta Neuropathol 2013;125:169–71.
[15] Ihle MA, Fassunke J, Konig K, et al. Comparison of high resolution melting analysis, pyrosequencing, next generation sequencing and immunohistochemistry to conventional Sanger sequencing for the detection of p. V600E and non-p.V600E BRAF mutations. BMC Cancer 2014;14:13.
[16] Miyatake S, Miyake N, Touho H, et al. Homozygous c.14576G>A variant of RNF213 predicts early-onset and severe form of moyamoya disease. Neurology 2012;78:803–10.
[17] Sparrow JC, Nowak KJ, Durling HJ, et al. Muscle disease caused by mutations in the skeletal muscle alpha-actin gene (ACTA1). Neuromuscul Disord: NMD 2003;13:519–31.
[18] Laing NG, Dye DE, Wallgren-Pettersson C, et al. Mutations and polymorphisms of the skeletal muscle alpha-actin gene (ACTA1). Hum Mutat 2009;30:1267–77.
[19] Nowak KJ, Ravenscroft G, Laing NG. Skeletal muscle alpha-actin diseases (actinopathies): pathology and mechanisms. Acta Neuropathol 2013;125:19–32.